Subsurface Exploration

New Haven Harbor, New Haven, CT

Contract No. W912DS22D0017

Combined Geophysical and Geotechnical Report of Explorations

Final Report

February 5th, 2025

Submitted to:

Coastal Partners &

USACE New England District

Submitted by:

Gahagan & Bryant Associates, Inc.

9008-P Yellow Brick Road

Baltimore, MD 21237

(410) 682-5595

Report Authorization and Distribution

Authored: J. Barker, S. Hiller, L. McHugh, L. Pugh

Approved: D. Urso

Date	Rev	Description
06-Nov-2024	0	Interim Sections Issued for Client Comment
12-Dec-2024	0	Draft Combined Report Issued for Client Comment
20-Jan-2025	1	Final Combined Report Issued for Client Approval
5-Jan-2025	2	Final Combined Report

1 Table of Contents

GBA ENGINEERS ★ SURVEYORS EST. 1974
S. T. HUDSON ENGINEERS, INC.
PROFESSIONAL ENGINEERS & CONSULTANTS

2 Figures

GBA ENGINEERS ★ SURVEYORS Est. 1974

S. T. HUDSON ENGINEERS, INC.
PROFESSIONAL ENGINEERS & CONSULTANTS

3 Tables

4 Abbreviation Table

CRP	Central Reference Point
FIPS	Federal Information Processing Standards
FMGT	Fledermaus Geocoder Toolbox
FWD	Forward
GNSS	Global Navigation Satellite System
GPS	Global Positioning System
HRG	High Resolution Geophysical
Hz	Hertz
m	Meter
MCS	High Resolution Multichannel Seismic
MCSR	Multichannel Seismic Refraction
LB	Lift Boat Vessel
MV	Motor Vessel
MBES	Multibeam Echosounder
NAD83 (2011)	North American Datum of 1983 (2011)
NAVD88	North American Vertical Datum of 1988
NOAA	National Oceanic and Atmospheric Administration
POSMV	Position and Orientation System for Marine Vessels
PPK	Post-Processed Kinematic
PPS	Pulse per Second
QAQC	Quality Assurance/Quality Control
QPS	Quality Positioning Services
RTK	Real-Time Kinematic
RV	Research Vessel
ms	Millisecond
SBET	Smoothed Best Estimates Trajectory
SBP	Sub-bottom Profiler
SEG-Y	Society of Exploration Geophysicists seismic file format
SPCS	State Plane Coordinate System
STBD	Starboard
SVS	Sound Velocity Sensor
SVP	Sound Velocity Profiler
USCS	Unified Soil Classification System
UDP	User Datagram Protocol
UTM	Universal Transverse Mercator
VRS	Virtual Reference Station

1 Executive Summary

In support of the U.S. Army Corps of Engineers (USACE) New Haven Harbor Deepening and Channel Improvement Project (Contract W912DS22D0017), CEC-CDM Smith, a Joint Venture dba Coastal Partners (Coastal Partners), retained Gahagan & Bryant Associates, Inc. (GBA) to perform a High-Resolution Geophysical (HRG) and Geotechnical Survey along the navigable channel (Entrance Channel, Lighthouse Point Reach, New Haven Reach) in New Haven, CT, with additional areas of interest outside of the channel.

Marine Geophysical Survey Objectives:

- Identify locations, engineering properties, and quantities of the various materials to be dredged.
- Delineate the volumes of rock/ledge materials that will require blasting versus those that can be removed by mechanical methods (e.g., glacial till, weathered and fractured rock).
- Recommend areas for marine drilling investigations.

Marine Geotechnical Drilling Investigation Objectives:

- Characterize sediment and collect bedrock cores for laboratory evaluation of density, strength, and other engineering properties of bedrock and sediment and characterize those materials that will require blasting versus those that can be removed by mechanical methods.
- Assess subsurface conditions for the design and construction of a Confined Aquatic Disposal (CAD) cell.

Data Acquisition: The acquisition plan, set in place by GBA and USACE, was executed onboard the R/V *Pricus* for the Geophysical Investigation, included 200 ft average line spacing within the main channel and 30 ft average line spacing within the Confined Aquatic Disposal (CAD) cell, and intersecting crosslines stationed estimated every 3,250 ft along the route. Data collected under the geophysical plan included multibeam echosounder (MBES) with backscatter (BSC), parametric sub-bottom profiler (SBP), 2D and 3D Multi-channel Seismic Reflection (MCS), and Multi-channel Seismic Refraction (MCSR). The following Geotechnical plan was performed aboard the LB *Vision*, which included twenty (20) borings collected within the harbor channel alignment with roughly 2,000 ft spacing or in areas of geophysical interest, ten (10) rock core borings in the rock area between channel stations 65+00 to 113+25, and six (6) borings completed in the CAD cell just east of Sandy Point Bar Dike within the Inner Harbor. The line spacing and geotechnical boring layout encompassed the maximum proposed limits provided in this task order by USACE NAE. The final authorized channel alignment may vary from what was completed during this investigation.

Water Depths: Seafloor depths found within the survey area ranged from -3.5 ft and -46.7 ft MLLW. The shoalest area was found within the CAD cell, closest to the existing dike. Due to the shallow nature of the CAD Cell survey site, certain areas were deemed inaccessible for data coverage of any towed sensors.

Subsurface Interpretation and Horizons: A total of 5 geologic units were identified and delineated throughout the survey areas. Within the existing channel alignment, 3 horizons suggested an acoustic interface between the known Organic Sediments (OS) and Marine Sand (MS) layers, as well as Top of Rock (TOR) within the design considerations along the main rock area of interest that were identified in the geotechnical study. Within the CAD cell, geotechnical borings identified the OS and MS horizons noted in the channel, and 2 geologically distinguished units of Glacio-Marine Silt (GM) and Glacio-Marine Sands (GS).

Gas: Seismic reflection data showed that a large amount of shallow, biogenic gas was found in the Inner Harbor from approximately station 110+00 through the northern terminus of the channel template. This gas did mask high frequency reflection data and made interpretations in the Inner Harbor difficult. If additional surveys in the Inner Harbor are necessary, this large amount of gas should be considered during planning of those efforts.

The following report describes in detail the field operations, data processing, and final interpretation of all geophysical and geotechnical data acquired for USACE by GBA and STHE. Results presented in this report are representative of conditions found in the survey site at the time of data acquisition.

Recommendations for Further Study:

Seismic data around station 200+00 strongly suggested that a solid rock body exists at a shallower depth than anticipated. Boring FD24-B-10 demonstrated that the rock is beyond -60 ft. It is recommended that any future endeavors removing material below -44 ft MLLW physically determine the depth of this rock body.

A linear feature discovered at station 217+00 should be re-surveyed at the time of any construction or bottom disturbing activities in the vicinity to ensure adequate avoidance.

No magnetometer data was collected during this survey. Determining the presence and location of any utilities or subsurface assets that cross or run along the channel were not part of this scope of work. Existing utilities, specifically the cross-sound cable, are known to be present within the area of work. The lack of identification of any utility does not imply additional utilities are not physically present. At minimum, a high-resolution magnetometer survey is recommended for identification of ferrous targets and utilities before any material removal begins.

2 Introduction

Gahagan & Bryant Associates, Inc. (GBA) was retained by CEC-CDM Smith, a Joint Venture dba Coastal Partners (Coastal Partners), to perform investigations as part of the New Haven Harbor Deepening and Channel Improvement project under Contract W912DS22D0017. The U.S. Army Corps of Engineers (USACE) New England District (NAE) required subsurface investigations, including marine geophysical surveys and geotechnical drilling investigations, focused on the Federal Navigation Project (FNP) in New Haven, CT, with additional areas of interest outside of the FNP (Figure 1). A copy of the project Performance Work Statement (PWS), USACE NAS approved Workplan, and Accident Prevention Plan, can be reviewed in Appendices K to M, respectively.

USACE NAE provided the following maximum channel improvement limits as a part of this task order, which can be reviewed in Appendix K. The maximum proposed width for the Outer Harbor entrance channel outer approach was 600 ft; the channel bend near the east breakwaters was 800 ft; the main ship channel and inner channel within the Inner Harbor was 500 ft; and Turning Basin was ~200 ft north. This investigation covered the maximum possible channel limits for the following design considerations. The final authorized channel alignment may vary from what is provided in this explorations report, based on our provided results.

The high-resolution geophysical (HRG) survey utilized a suite of sensors that included Multibeam Echosounder (MBES), Sub-bottom Profiler (SBP), 2D Multi-channel Seismic Reflection (MCS), and Seismic Refraction (MCSR), operated onboard the R/V *Pricus*. The nearshore survey was designed to provide information for planning of future geotechnical and engineering activities and consenting requirements (State, Federal, QMA, etc.). Therefore, the main objectives for the survey were identified as:

- Identify locations, engineering properties, and quantities of the various materials to be dredged.
- Delineate the volumes of rock/ledge materials that will require blasting versus those that can be removed by mechanical methods (e.g., glacial till, weathered and fractured rock).
- Recommend areas for marine drilling investigations.

The marine geotechnical drilling campaign utilized a Central Mine Equipment (CME) 55 drill rig with mud rotary drilling methods for soil data collection and NQ rock core wireline for rock core collection operated onboard the Lift Boat (LB) *Vision,* with M/V *Almar-31* providing drill crew daily transportation. Therefore, a list of main objectives for the subsurface investigation were identified as:

- Characterize sediment and collect bedrock cores for laboratory evaluation of density, strength, and other engineering properties of bedrock and sediment and characterize those materials that will require blasting versus those that can be removed by mechanical methods.
- Assess subsurface conditions for the design and construction of a Confined Aquatic Disposal (CAD) cell.

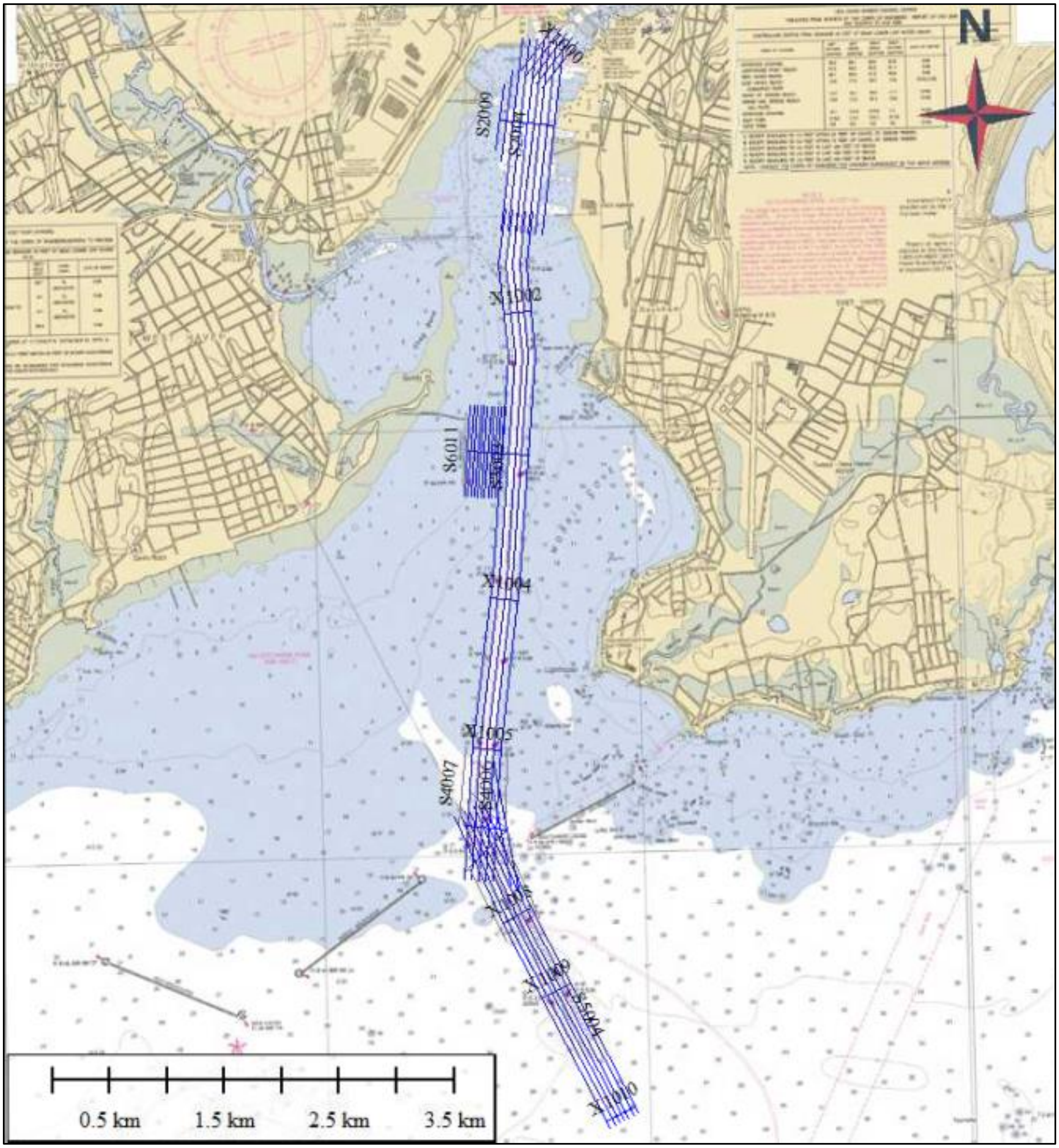

Figure 1. Survey Area Overview

2.1 Fieldwork Summary

Survey operations were undertaken on the R/V *Pricus* (HRG) and the LB *Vision* (Geotechnical).

For geophysical operations, the R/V *Pricus* HRG and MCS mobilization was completed between May 1st and May 4th, 2024. MCS field operations began on May 4th, 2024 and concluded on May 10th, 2024. Demobilization occurred and was completed on May 10th, 2024. The R/V *Pricus* MCSR mobilization was completed between May 11th and May 12th,

2024. MCSR field operations began on May 13th, 2024 and concluded on May 14th, 2024. Demobilization occurred and was completed on May 15th, 2024.

For geotechnical operations, the M/V *Almar-31* mobilization began on June 26th, 2024, and the LB *Vision* mobilization began on June 27th, 2024. Both vessels completed mobilization on June 29th, 2024. Geotechnical field operations began on June 30th, 2024 and concluded on August 31st, 2024. Demobilization for both vessels was completed between August 31st and September 3rd, 2024.

A total number of thirty-six (36) borings were collected within the project limits, twenty (20) soil borings were collected throughout the main channel alignment, six (6) borings were completed within the proposed CAD cell, and ten (10) rock core borings completed within the main area of interest for bedrock within the proposed dredge template within the elbow of the southern limits of the existing channel. Operational time accounted for approximately 60% of the total project time; weather conditions were unfavorable for approximately 10% of the duration of the project, and mobilization accounted for 10% of the total project time. Contractor downtime for the drill rig and vessel accounted for the remaining 20% of the total project time.

The tables below summarize the fieldwork operations from the R/V *Pricus* and LB *Vision,* as well as the support vessel M/V *Almar-31*:

- Table 1: Fieldwork schedule for all three vessels
- Table 2: Geophysical line summary (R/V Pricus)
- Table 3: Geotechnical sample summary (LB *Vision*)
- Table 4: Time summary analysis for all three vessels

Table 1. Fieldwork Schedule Summary

Fieldwork Summary – R/V *Pricus*	
Mobilization and Sea Trials (MCS)	May 1st – May 4th, 2024
Survey Operations (MCS)	May 4th – May 10th, 2024
Demobilization (MCS)	May 10th, 2024
Mobilization and Sea Trials (MCSR)	May 11th – May 12th, 2024
Survey Operations (MCSR)	May 13th – May 14th, 2024
Demobilization (MCSR)	May 15th, 2024
Fieldwork Summary – M/V *Almar-31*	
Mobilization and Sea Trials	June 26th – June 29th, 2024
Survey Operations	June 30th, 2024 – August 31st, 2024
Demobilization	August 31st – September 3rd, 2024
Fieldwork Summary – LB *Vision*	
Mobilization and Sea Trials	June 27th – June 29th, 2024
Survey Operations	June 30th, 2024 – August 31st, 2024
Demobilization	August 31st – September 3rd, 2024

Table 2. Geophysical Fieldwork Line Summary

R/V *Pricus* Line Summary	
Survey Line Type	**Total Data Collection (miles)**
MCS Area 1	48.8584
MCS Area 2	33.2744
MCSR	26.1225
Total	108.2553

Table 3. Geotechnical Sample Summary

Geotechnical Sample Summary		
Sample Type	**Vessel**	**Total Samples**
Soil Borings	LB Vision	20
CAD Cell Borings	LB Vision	6
Rock Core Borings	LB Vision	10

Table 4. Time Breakdown

TIME SUMMARY ANALYSIS – R/V *Pricus*		
Activity	**Hours**	**Percentage**
Mobilization	58:35	34.9
Demobilization	2:10	1.3
Operational time	84:36	50.3
Weather standby	8:27	5.0
Contractor time	14:12	8.5
Total	**168:00**	**100**
TIME SUMMARY ANALYSIS – LB *Vision*		
Activity	**Hours**	**Percentage**
Mobilization	48:00	5.7
Demobilization	36:00	4.3
Operational time	504:15	59.6
Weather standby	88:45	10.5
Other standby	0:00	0.0
Standby fisheries	0:00	0.0
Contractor time	106:15	12.5
Contractor time vessel	62:45	7.4
Total	**846:00**	**100**
TIME SUMMARY ANALYSIS – M/V *Almar-31*		
Activity	**Hours**	**Percentage**
Mobilization	48:00	5.7
Demobilization	36:00	4.3
Operational time	504:15	59.6
Weather standby	88:45	10.5
Other standby	0:00	0.0
Standby fisheries	0:00	0.0
Contractor time	106:15	12.5
Contractor time vessel	62:45	7.4
Total	**846:00**	**100**

2.2 Personnel

The following personnel played key roles throughout the life of the project (Table 5 and Table 6).

Table 5. Key Office Personnel

Personnel	Role
GBA Management	
Kevin Kremkau	Project Executive
William Jenkins	VP Marine Services
Dennis Urso	Senior Project Manager
Steven MacDonald	Geophysical Project Manager
Scott Hiller	Chief of Geosciences
Jonathan Barker	Geotechnical Project Manager
Lawrence Andrews	Lead Technical Advisor
Lauren McHugh	Data & Reporting Manager
Ben Cushing	Lead Engineer
Lindsay Pugh	Project Geologist
Loukas Rimanelli	Geologist
USACE Management	
Craig Martin	Project Manager
Gina Romano	Geologist
Stephen Potts	Geologist
Brendan Sprague	Engineer
CDM Smith Management	
Nathan Jones	Project Manager
Doug Aghjayan	Technical Lead
Luis Jimenez	Program Support
Debra Beck	Contracting
CEC Management	
Brett Borne	Project Manager
Michael Poff	Program Manager

Table 6. Key Field Personnel

Personnel	Role	Vessel
GBA		
Mark Carter	Party Chief	R/V *Pricus*
Carlos Miro	Survey Technician	R/V *Pricus*
Jordan Clemente	Survey Technician	R/V *Pricus*
Henrique Duarte	Seismic Technician	R/V *Pricus*
Theresa Bohm	Seismic Technician	R/V *Pricus*
Evgenii Vinogradov	Seismic Technician	R/V *Pricus*
Mihran Wartanian	Seismic Technician	R/V *Pricus*
Lisa Hill	Seismic Technician	R/V *Pricus*
Jamie Dozier	Air Source Operator	R/V *Pricus*
David Nielsen	Vessel Master	R/V *Pricus*
Jonathan Barker	Project Geologist	M/V *Almar-31,* LB *Vision*
Lindsay Pugh	Project Geologist	M/V *Almar-31,* LB *Vision*
Loukas Rimanelli	Geologist	M/V *Almar-31,* LB *Vision*
Ryan Cooper	Vessel Master	M/V *Almar-31*
Nick Culwell	Vessel Master	M/V *Almar-31*
Ryan Cooper	Vessel Master	M/V *Almar-31*
Carl Brubach	Vessel Master	M/V *Almar-31*
Paul Winchell	Vessel Master	M/V *Almar-31*
USACE		
Gina Romano	Project Geologist	R/V *Pricus,* M/V *Almar-31,* LB *Vision*

2.3 Geodetic Parameters

The horizontal reference system for the project was the North American Vertical Datum of 1983 (NAD83) – 2011, Geoid 18 in conterminous United States, projected to US State Plane Coordinate System (SPCS) Connecticut FIPS 600. Raw data were vertically referenced to the North American Vertical Datum of 1988 (NAVD88) and shifted in post-processing using NOAA's VDatum to Mean Lower Low Water (MLLW). The offset from NAVD88 to MLLW was 3.60 ft; therefore, the correction was added to NAVD88 to convert to MLLW. Horizontal and vertical units were US survey feet.

3 Field Operations Summary

3.1 Geophysical Operations

3.1.1 Vessel Summary

The R/V *Pricus* (Figure 2) was utilized for the geophysical scopes. The vessel specifications are shown below in Figure 3.

Figure 2. R/V *Pricus* – for reference only.

DIMENSIONS

LENGTH	40 ft	O.N.	1301746
BEAM	18 ft	MAX SPEED	19 kts
GROSS	24 GT	CRUISE SPEED:	16 kts
CERTIFICATIONS	USCG Oceanographic Research Vessel		

PROPULSION, MACHINERY & STEERING

MAIN ENGINES	(2) Cummins C-9	TOTAL HORSEPOWER	1,006 hp
PROPELLERS	(2) FPP, 5-Blade	PROPELLER DIAMETER	28 in
PRIMARY GENERATORS	(2) Northern Lights 20KW	TOTAL RATING	40 kw
RUDDER	Independent Steering	POWER GENERATION	240V/60 Hz/1(Φ)
GEAR	Twin Discs with Troll Valves		

CAPACITIES AND EQUIPMENT

FUEL CAPACITY	900 gal	AFT DECK AREA	15ft x 16ft
POTABLE WATER	50 gal	SURVEY WINCHES	(2) Hydraulic Slip Ring 300m/1000m
BLACK/GRAY WATER	50 gal	AFRAME	16 ft wide 13ft tall 2,000lb SWL
RANGE	700 km	TRANSDUCER MOUNTS	(2) Hydraulically deployed side poles
BURN @ CRUISE	30 gph	POSITIONING	POS MV Oceanmaster V5
BURN @ SURVEY	10 gph	COUNTING SHEAVES	24" Ocean Instruments (2)
CREW	2	MOB RECOVERY	Fiberlight Rescue Cradle
SCIENTIFIC PARTY	10	AFRAME, WINCH, POLE CONTROLS	Wireless Remote

Figure 3. R/V *Pricus* Specifications

3.1.2 Offsets

All equipment offsets were surveyed using a combination of conventional land survey techniques and ultra-high resolution 3D laser scanning. This was achieved by utilizing the R/V *Pricus* dimensional control vessel survey report, that determined the existing equipment mount offsets, using a combination of 3D laser scan point clouds and land surveying total station to build a field of points, to determine their offsets from a central reference point of the vessel. Any equipment installed that required a bracket, an offset measurement was noted and were readjusted accordingly to represent the accurate locations of the equipment's measure point or acoustic center. Afterwards, the output nodes were compared using two independent positional systems on board. These offsets for primary equipment and vessel nodes are shown in Table 7. The units are presented in meters to match how the offsets were surveyed in the field and post processing.

Table 7. Survey Sensor Offsets R/V *Pricus*

Survey Sensor Offsets (m)			
Description	**STBD (+)**	**FWD (+)**	**UP (+)**
CRP (POSMV)	0.000	0.000	0.000
Norbit MBES	2.888	2.812	-2.949
POSMV IMU	0.000	0.000	0.000
POS Primary Antenna	-1.218	1.789	3.249
POS Secondary Antenna	0.817	1.789	3.274
Innomar SBP	2.884	-1.022	-3.714
MCS Port Towpoint	-2.000	-4.132	0.300
MCS Stbd Towpoint	2.000	-4.132	0.300
Streamer 1 Towpoint	6.000	-4.132	0.300

Survey Sensor Offsets (m)			
Description	**STBD (+)**	**FWD (+)**	**UP (+)**
Streamer 2 Towpoint	2.500	-4.132	0.300
Streamer 3 Towpoint	0.000	-4.132	0.300
Streamer 4 Towpoint	-2.500	-4.132	0.300
Streamer 5 Towpoint	-6.000	-4.132	0.300
MCSR Towpoint	2.000	-4.132	0.300

3.1.3 Survey Equipment

The following survey equipment and software were used during operations onboard the R/V *Pricus* (Table 8); Table 9 lists the software that was used for processing and data QC.

Table 8. R/V *Pricus* Geophysical Survey Equipment

Equipment Type	Equipment Model
Primary Navigation, Motion, Heading (GPS)	Applanix POSMV OceanMaster, Supplemented with RTK Corrections
Secondary Navigation	Hemisphere A222 with Atlas H10 Corrections
Multibeam Echosounder (MBES)	Norbit Winghead i77h
Sub-bottom Profiler (SBP)	SES-2000 Medium-100 Innomar (Parametric)
Sound Velocity Probe (SVP)	AML Base X-3
Multichannel Seismic Reflection (MCS, 2D)	GeoSpark 1000X Pulsed Power Supplies 1x Geo-Sense Ultra-Light Weight Streamer, Single Element, 12 channels @ 1mgi
Multichannel Seismic Reflection (MCS, 3D)	GeoSpark 1000X Pulsed Power Supplies 5x Geo-Sense Ultra-Light Weight Streamer, Single Element, 12 channels @ 1mgi
Multichannel Seismic Refraction (MCSR, 2D)	Sercel Mini G-Source I Airgun (20cu in) with Teledyne HotShot Seismic Source Synchronization Box and 1x Geo-Sense Ultra-Light Weight Streamer, 72 Channels (24 channels at 1mgi, 48 channels at 2mgi)
Acquisition Software	QPS Qinsy 9.5.5 (Positioning, Vessel Navigation, MBES) Applanix POSView (GPS) Innomar SESWIN (SBP) GeoSuite Acquisition (MCS/MCSR)

Table 9. QA/QC Offline Software

Software Type	Software Make/Model
Data QAQC and Integration	Blue Marble Global Mapper 25.1 QPS Fledermaus 8.6.1
Post-Processed GNSS	Applanix POSPac MMS 9.0
MBES Data	QPS Qimera 2.6.2 (Bathymetry) + FMGT 7.11.0 (Backscatter)
SBP Data	RadExPro 2023.2 and CTI SonarWiz 7.07.07
MCS/MCSR	RadExPro 2023.2

3.1.3.1 Primary Positioning System

The vessels and survey sensors were positioned and motion-compensated using the Applanix POSMV OceanMaster that was close-couple with the Norbit multibeam sonar. This system operated as an inertial navigation unit and coupled two (2) antennas mounted on the roof of the vessel with the motion sensor to provide industry leading accuracy specifications (Figure 4). The system was supplemented with Real-Time Kinematic (RTK) corrections on the Virtual Reference Station (VRS) network for accurate positions at the time of survey. Post-Processed Kinematic (PPK) data was collected by logging the internal system files of the GNSS and motion data in a *.000 file format to enable post processing and two-way motion and position corrections.

PERFORMANCE SUMMARY (APPLANIX POS MV OCEANMASTER ACCURACY[1])

	DGNSS	FUGRO MARINESTAR[2]	IARTK	POSPac™ MMS PPP	POSPac MMS IAPPK	ACCURACY FOLLOWING 60 s GNSS OUTAGE	CENTERPOINT® RTX MARINE[8]
Position	0.5 - 2 m[2]	Horizontal: 10 cm 95% Vertical: 15 cm 95%	Horizontal: +/- (8 mm + 1 ppm x baseline length)[3] Vertical: +/- (15 mm + 1 ppm x baseline length)[3]	Horizontal: < 0.1 m Vertical: < 0.2 m	Horizontal: +/- (8 mm + 1 ppm x baseline length)[3] Vertical: +/- (15 mm + 1 ppm x baseline length)[3]	~ 6 m (DGPS) ~ 3 m (RTK) ~ 2 m (PPDGNSS) ~ 1 m (IAPPK)	Horizontal: 3 cm Vertical: 6 cm
Roll & Pitch[4]	0.02°	0.01°	0.01°	< 0.01°	0.008°	0.03°	0.01°
Heading[4]	0.01° with 4 m baseline 0.02° with 2 m baseline	0.01° with 4 m baseline 0.02° with 2 m baseline	0.01° with 4 m baseline 0.02° with 2 m baseline	0.01° with 4 m baseline 0.02° with 2 m baseline	0.01° with 4 m baseline 0.02° with 2 m baseline	1° per hour degradation (negligible for outages <60 s)	0.01° with 4 m baseline 0.02° with 2 m baseline
Heave TrueHeave	5 cm or 5%[5] 2 cm or 2%[6]	5 cm or 5%[5] 2 cm or 2%[6]	5 cm or 5%[5] 2 cm or 2%[6]	-	-	5 cm or 5%[5] 2 cm or 2%[6]	5 cm or 5%[5] 2 cm or 2%[6]

Figure 4. POSMV OceanMaster Accuracy Table

3.1.3.2 Secondary Positioning System

A Hemisphere A222 GNSS Smart Antenna was used as an accurate, redundant GNSS position system for the project. The A222 antenna received Atlas H10 GNSS Global Correction Services to operate with high-accuracy GNSS positions. The data was logged in Qinsy.

3.1.3.3 Multibeam Echosounder

The R/V *Pricus* was equipped with a variable frequency (200-700 kHz), Norbit Winghead i77h multibeam sonar (Figure 5). The sonar is capable of 1024 soundings per ping with a 0.5° across track and 0.9° along track resolution at a maximum ping rate of 60 kHz, done through a FM pulse type with configurable bandwidths and sweep direction (low-high/high-low). This also aids in the reduction of any acoustic interference with the SBP. A continuous logging surface Sound Velocity Sensor (SVS) was mounted in the sonar head and feeds data directly into the Norbit software for real time raytracing. A planned sonar frequency range of 350-390 kHz was used to minimize interference with other sensors, primarily the Innomar SBP. A continuous logging surface Sound Velocity Sensor (SVS) was mounted in the sonar head and fed data directly into the Norbit software for real-time raytracing. MBES data was monitored in real-time and recorded in Qinsy.

SWATH COVERAGE	5-210° FLEXIBLE SECTOR (SHALLOW WATER IHO SPECIAL ORDER >155°)
RANGE RESOLUTION	<10mm ACOUSTIC w. 80kHz BANDWIDTH
NUMBER OF BEAMS	256, 512, 1024 EA & ED
OPERATING FREQUENCY	NOMINAL FREQUENCY 400kHz (FREQUENCY AGILITY 200-700kHz)
DEPTH RANGE	0.2m to >400m*
PING RATE	UP TO 60Hz, ADAPTIVE
RESOLUTION (ACROSS X ALONG)	STANDARD: 0.5° X 0.9° @400kHz, 0.3° x 0.5° @700kHz
POSITION	HOR: ±(8mm +1ppm x DISTANCE FROM RTK STATION) VER: ±(15mm +1ppm x DISTANCE FROM RTK STATION) (ASSUMES 1m GNSS SEPARATION)
HEADING ACCURACY	0.02° WITH 2m ANTENNA SEPARATION 0.01° WITH 4m ANTENNA SEPERATION
PITCH/ROLL ACCURACY	0.008° RTK & PPK, 0.01° INDEP. OF ANTENNA SEPARATION
HEAVE ACCURACY	2 cm OR 2% (TRUEHEAVE™), 5 cm OR 5% (REAL TIME)
INTERFACE	ETHERNET
POWER CONSUMPTION	<90W (10-28VDC, 110-240VAC) TOTAL
DIMENSIONS	DIMENSIONS WITHOUT BRACKET H: 447mm/17.605", L: 296mm/11.657", W: 101.9mm/4.010"
WEIGHT	6.9kg (AIR) 3.8kg (WATER) EXCL. BRACKET 7.4kg (AIR) 4.0kg (WATER) INCL. BRACKET
CABLE LENGTH	STD 8m, OPTIONAL: 2m, 25m
OPERATING TEMP.	-4°C to +40°C (TOPSIDE -20°C to +55°C)
STORAGE TEMP.	-20°C to +60°C
ENVIRONMENTAL	TOPSIDE: IP67: DUST TIGHT, PROTECTED AGAINST THE EFFECT OF IMMERSION UP TO 1m WET-END (SONAR): 100m

OUTLINE DRAWING

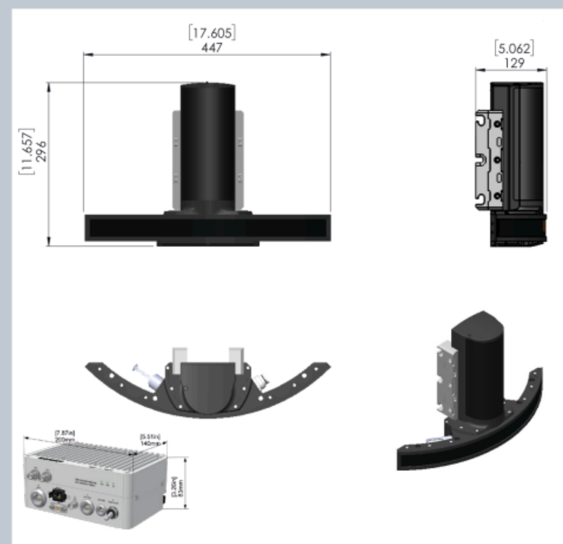

Sonar including bracket (bracket shown in grey)

Figure 5. Norbit Winghead i77h Technical Specifications

3.1.3.4 Sound Velocity Profiler

The AML Oceanographic Base X-3 sound velocity probe (SVP) was used to measure the speed of sound through the water column for all vessels by lowering the probe to the seabed through the water column and logging data internally (Figure 6).

Parameter	Range	Precision	Accuracy	Resolution	Response
Xchange™					
C•Xchange™	0 to 70 mS/cm	+/-0.003mS/cm	+/-0.01mS/cm	0.001mS/cm	25ms at 1m/s flow
SV•Xchange™	1375 to 1625 m/s	+/-0.006 m/s	+/-0.025 m/s	0.001 m/s	47 microseconds
P•Xchange™	up to 100 dBar	+/-0.03%FS	+/-0.05%FS	0.02%FS	10 milliseconds
T•Xchange™	-2 to 32°C	+/-0.003°C	+/-0.005°C	0.001°C	100 milliseconds
Turbidity•Xchange™	up to 3000 NTU	up to +/- 0.1NTU	up to +/- 1%NTU	up to 0.01NTU	<0.7s

Figure 6. AML Base X-3 Technical Specifications

3.1.3.5 Parametric Sub-Bottom Profiler

An SES-2000 Medium-100 Innomar Parametric sub-bottom profiler was used to acquire high-resolution full-waveform, 24-bit data (Figure 7). The system was installed on a separate pole mount from the multibeam. Position and motion compensation data were sent from the Applanix OceanMaster system to the sensor's acoustic center.

Bottom tracking was performed at the 100kHz (nominal) Primary Frequency and 6kHz (nominal) for the Secondary Frequency Range.

Water Depth Range	2 – 2,000 m below transducer
Sediment Penetration	up to 70 m (depending on sediment type and noise)
Sample / Range Resolution	<1 cm / up to 5 cm (depending on pulse settings)
Transmit Beam Width (-3dB)	c. 2° (±1°) for all frequencies / footprint c. 3.5% of water depth
Ping Rate	up to 40 Hz (pings/s), multi-ping mode available
Heave / Roll / Pitch Compensation	heave + roll (or pitch); depending on external sensor data
Primary Frequencies (PHF)	c. 100 kHz (frequency band 85 – 115 kHz)
PHF Source Level / Acoustic Power	>247 dB//µPa re 1m / c. 5.5 kW
Secondary Low Frequency (SLF)	centre frequency user selectable: 4, 5, 6, 8, 10, 12, 15 kHz
SLF Total Frequency Band	2 – 22 kHz
SLF Pulse Type	Ricker, CW, FM Chirp
Pulse Width	user selectable 0.07 – 1.0 ms (CW); 3.5 ms (chirp)
Data Acquisition and Recording	digital 24 bit / 96 kHz (SLF full waveform, PHF envelope)
Data File Format	Innomar "SES3" (24 bit), "SEGY" (via SESconvert)
External Sensor Interfaces	HRP (motion), GNSS position, depth (all RS232 / UDP), trigger (BNC)
Bottom Detection	internal (PHF and SLF data) or external depth
Depth Accuracy	(2 cm @ 100 kHz / 4 cm @ 10 kHz) + 0.02% of water depth
Remote Control / Survey Integration	KVM / basic functions via COM or Ethernet (UDP), NMEA
Topside Unit (Transceiver)	W 52 cm × D 40 cm × H 44 cm (19" / 9U) / weight c. 44 kg
Transducer	W 50 cm × D 50 cm × H 12 cm / weight c. 60 kg (incl. 30 m cable)
Transducer Depth Rating	Surface
Power Supply	100–240 V AC
Power Consumption	typ. 250 W, max. 400 W
Control / Data Storage PC	integrated PC (MS Windows 10/11 OS) with 10" TFT display

Figure 7. Innomar Medium Technical Specifications

3.1.3.6 Multi-channel Seismic Reflection (MCS)

The vessel was mobilized with a Multichannel Ultra High-Resolution Seismic (MCS) reflection system from GeoMarine Survey Systems. The source array for both the 2D and 3D consisted of two GeoSpark 1000X Pulsed Power Supplies (PPS) from Geo Marine Survey Systems (GMSS). The GeoSpark operated in combination with two Geo Source Sparkers towed at a depth of 0.5 m. The receiver arrays for the 3D consisted of five (5) Geo-Sense Ultra-Light Weight streamers with 12 channels each (single element) and 1 m group spacing interval. The total active length per streamer was 11 meters. For the 2D survey, 4 streamers were removed.

All data were recorded in the native format within the GeoSuite Acquisition program. A source hydrophone was towed below the MCS source where water depths allowed to record the shot signal for each shot point for deconvolution processing.

3.1.3.7 Multi-channel Seismic Refraction (MCSR)

The R/V Pricus was mobilized with a Multichannel Marine Seismic Refraction (MCSR) system from GeoMarine Survey Systems. The streamer and source were optimized to measure arrival times in the upper 60 ft below the seabed. Shot spacing allowed for a horizontal resolution of approximately 5 m along the sail line. A few cross lines were collected for calibration purposes, but the delivered data relied on data collected parallel with the channel. Refraction data provides P-wave velocity information along a depth profile.

The source array for the Refraction consisted of one Sercel Mini G-SOURCE airgun. The airgun operated in combination with one Teledyne HotShot Seismic Source Synchronizer. The receiver arrays for Refraction consisted of one Geo-Sense Ultra-Light Weight streamer with 72 channels each (single element) and variable group spacing interval. The first 24 channels were spaced at 1m and the following 48 channels spaced at 2m. The total active length of the refraction streamer was 120 m.

3.1.4 Navigation Suite Interfacing

Qinsy was used as the primary operating navigation software and output positioning system for geophysical sensors. The Innomar SBP positioning data strings originated from Qinsy by a serial output string from its output node. The node was fed by a combination of POSMV positioning and node offsets. Navigation for survey line tracking was RTK positioned and steered from the center of the vessel. Qinsy interfacing from the survey sensors was performed using serial and UDP connections, as listed below in Table 10.

Table 10. QPS Qinsy I/O – R/V *Pricus*

Navigation – I/O QPS Qinsy	Settings
Applanix POS, HRP, HDT	UDP
MBES	UDP
ZDA PPS	UDP
SBP – custom string	19200/8/n/1

The 2D and 3D MCS spread was positioned in real time using two DGNSS antennas MK4 located on each sparker source. The receivers were positioned in real time with a layback method and repositioned via a proprietary triangulation method using the direct arrival times of the seismic signal. The MCSR spread was positioned in real time using two DGNSS antennas, one MK4 located on the airgun source and one MK3 at the tail buoy. All seismic positioning was recorded in Qinsy for redundancy.

3.2 Geotechnical Operations

3.2.1 Survey Controls

Horizontal and vertical controls were referenced at benchmarks USCG LIS 2 and 846 5705 B, located at Long Island Sound USCG station facility and New Haven Power Plant Pier, respectively. Their elevations were obtained from the National Geodetic Survey (NGS) OPUS Shared Solutions control sheets, which can be reviewed in Appendix G.

Due to the complicated logistics of daily access to the USCG station and power plant pier for daily checks, a temporary benchmark, GBA.LONGWHARFBM, was established on July 4th, 2024 located south of the gate entrance to the floating dock at Long Wharf Pier (Figure 8). Many of the easily accessible NGS monuments within the area were either destroyed or were not horizontally and vertically accurate for the specifications required for this project.

Figure 8. Location of temporary benchmark GBA.LONGWHARFBM

The surveys conducted for this project utilized Mean Lower Low Water (MLLW) as the vertical datum. The MLLW to NAVD88 correction for this project was a static correction of 3.60 ft. This correction was published by NOAA for the benchmark at New Haven, Connecticut (Station ID 8465748, 05/12/2004). The vertical datum relationship between NAVD88 and MLLW is shown in Figure 9. The coordinates and elevations used are shown in Table 11 below.

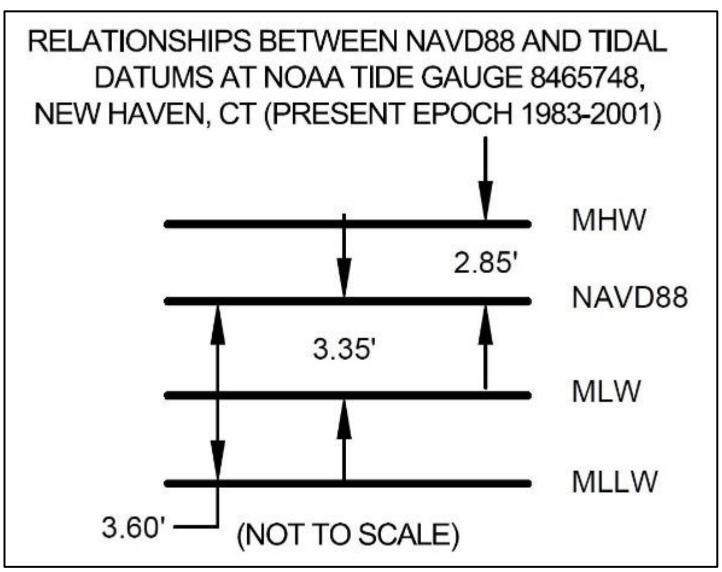

Figure 9. Project datum relationships

Table 11. Established Control Coordinates

Benchmark	Easting NAD83 (ft)	Northing NAD83 (ft)	Elev. NAVD88 (ft)
846 5705 B	956862.440	663951.828	9.649
USCG LIS 2	957656.254	659976.590	8.868
GBA.LONGWHARFBM	954322.666	667798.872	8.961

3.2.2 Vessel Summary

3.2.2.1 LB *Vision*

The LB *Vision*'s 70 ft drilling platform was the primary operating vessel utilized during the geotechnical investigation (Figure 10). The vessel capabilities include two moonpools which drill tooling could operate through and jack up capabilities, so the platform was not as affected by wind and wave action compared to a standard floating spud barge. The crew operating the vessel lived on board and worked 12 hours a day during drilling operations. No night operations were performed for the duration of the geotechnical investigation.

Figure 10. LB *Vision* on project site

3.2.2.2 M/V *Almar-31*

The M/V *Almar-31* was utilized on the project as the daily transport vessel for the onshore drilling crew and site inspector. The vessel is a custom-built highly versatile nearshore and intra-coastal survey vessel (Figure 11), specially built to be tailorable to provide rapid access to any port. With a cruising speed of 25 knots and shallow draft, the vessel can access a variety of survey areas.

Figure 11. M/V *Almar-31* off project site.

3.2.3 Offsets

All equipment offsets were surveyed using a combination of conventional land survey techniques. The offsets for primary equipment and vessel nodes are shown in Table 12.

Table 12. Geotechnical Survey Vessel Positioning Sensor Offsets

LB *Vision* Offsets (ft)		
Description	**STBD (+)**	**FWD (+)**
Hemisphere VR500	0.00	0.00
Moonpool (Aft)	5.00	29.85
Port Leg	-20.50	24.90
Starboard Leg	12.40	24.90
Stern Leg	-5.00	-26.80

3.2.4 Survey Equipment

The following survey equipment and software were used during operations onboard the LB *Vision* (Table 13); Table 14 lists the software that was used for data input and QC.

Table 13. Geotechnical Survey Equipment

Vessel	Equipment Type	Equipment Model
LB *Vision*	Primary Navigation & Heading	Hemisphere VR500
LB *Vision*	Primary Final Positioning	Leica GS18
LB *Vision*	Acquisition Software	QPS Qinsy 9.5.5 (Positioning, Vessel Navigation)

Table 14. QA/QC Software

Software Type	Software Make/Model
Digitizing Boring Data	Bentley gINT Professional, version 10.02.00.04

3.2.4.1 Positioning System and Tidal Corrections

The LB *Vision* was positioned using a Hemisphere VR500 antenna mounted on the railing of the vessel to provide industry leading accuracy specifications (Figure 12). The system received Atlas GNSS H10 global correction service with all data reported in QPS Qinsy.

Accuracy		
Positioning:	**RMS (67%)**	**2DRMS (95%)**
Autonomous, no SA: [2]	1.2 m	2.5 m
SBAS: [2]	0.25 m	0.5 m
Atlas: [2,6]	0.04 m	0.08 m
RTK: [1]	10 mm + 1 ppm	20 mm + 2 ppm
Heading (RMS):	<0.27°	
Pitch/Roll (RMS):	1°	
Heave (RMS):	30 cm (DGPS) [6],10 cm (RTK) [6]	

Figure 12. Hemisphere VR500 Antenna Accuracy Table

Once the LB *Vision* was positioned within 25 ft of the originally proposed location and the platform was deemed settled by the captain, the Leica GS18 would provide final horizontal and vertical positioning utilizing single baseline network RTK while collecting positions directly over the moonpool (Figure 4). The geologist on site performed periodic lead line measurements through a secondary moonpool to ensure the deck height had not settled any further for the duration of drilling activities while on location.

MEASUREMENT PERFORMANCE & ACCURACY[1]		
Time for initialisation		Typically 4 s
Real-time kinematic (Compliant to ISO17123-8 standard)	Single baseline Network RTK	Hz 8 mm + 1 ppm / V 15 mm + 1 ppm Hz 8 mm + 0.5 ppm / V 15 mm + 0.5 ppm
Real-time kinematic tilt compensated	Topographic points (not for static control points)	Additional Hz pole tip uncertainty typically less than 10 mm + 0.7 mm/° tilt
Post processing	Static (phase) with long observations Static and rapid static (phase)	Hz 3 mm + 0.1 ppm / V 3.5 mm + 0.4 ppm Hz 3 mm + 0.5 ppm / V 5 mm + 0.5 ppm
Code differential	DGPS / RTCM	Typically 25 cm

Figure 13. Leica GS18 Positioning System Accuracy Table

To determine the mudline elevation at each boring location, a lead line was lowered to the seafloor within the 4-inch casing, prior to being set into the subsurface, to reduce the influence of waves and current for the most accurate measurement. The NAVD88 elevation was corrected to MLLW by adding a static correction of 3.60 ft and checked against the elevation determined by the multibeam survey performed during the geophysical portion of this investigation and the most recent USACE bathymetric data collected in December 2023, prior to commencing drilling activities. Tide elevations were recorded from real-time tides from NOAA's New Haven, CT 8465705 tide gauge; however, because the LB *Vision* was lifted above the influence of the water line at high tide, the tidal cycle did not influence the determination of corrected sampling depths since the platform was stationary at its measured elevation.

3.2.4.2 CME-55

The drill rig on board the LB Vision was a track-mounted CME-55 with a 25 ft tower and custom-built Cummins diesel engine (Figure 14). The machinery was outfitted with two winch lines for lowering and raising tooling, along with a wireline winch line mounted to the side of the tower. Tooling racks were stored on the vessel platform and consisted of at least 100 ft of 3-inch diameter casing, 4-inch diameter casing, 5-inch diameter casing, and wireline core barrel casing for the advancement of NQ sized double-swivel core barrels for rock core collection. The drill rig consisted of 120 ft of NWJ rods for mud rotary sampling methods of the overburden material, with 4-inch and 3-inch clay bits and roller rock bits. A 140-lb automatic hammer with a 30-inch drop was used for all overburden split spoon samples.

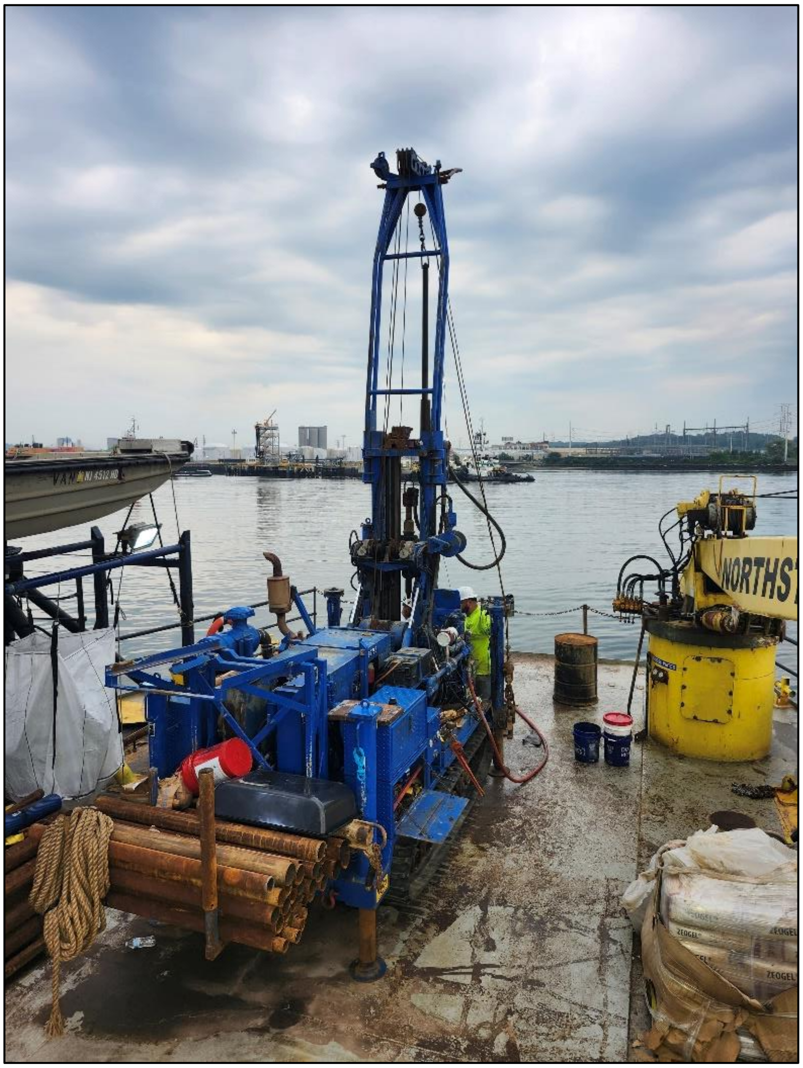

Figure 14. Drill Rig on LB *Vision*

3.2.5 Navigation Suite Interfacing

Qinsy was used as the primary operating navigation software and an output positioning system for the geotechnical survey. On the LB *Vision,* the positioning data strings originated from Qinsy by a serial output string from each respective output node. Navigation for geotechnical operations was network RTK positioned and steered from the center of the vessel. Qinsy interfacing was performed using serial connections, as listed below in Table 15.

Table 15. QPS Qinsy I/O

Navigation – I/O QPS Qinsy	Settings
Hemisphere VR500	38400/8/n/1

4 Geophysical Data Processing

Data processing was performed off site from the project location in a dedicated remote processing center in the Cherry Hill, NJ office. The Qinsy sounding grid was created for a high-resolution bathymetric surface coverage and was used for QC and coverage checks. Real time vessel tracks for individual survey sensors were checked on a nightly basis.

Data collected on the vessels were copied to external hard drives at the end of each survey day and were stored off site at the field staff accommodation. Data was partially uploaded overnight to the office for quality control analysis and verification. Weekly data drops of complete project data were conducted during the project with full, independent, data backups being brought to the Ocean View, NJ Office where they were then uploaded to the remote processing server in Cherry Hill, NJ.

Data processing QAQC was referenced to each sensor processing summary below. These checks included:

- Review QAQC Display Plots in POSPac for GNSS post-processing.
- Clean the MBES data to remove erroneous points. Check uncertainty and density surfaces.
- Review the SBP signal processing results to ensure data interpretability and signal penetration were within specifications and expectations.
- Review of MCS positioning (including source, receivers, and feather angles), source quality, and brute stacks for penetration and interpretability.
- Review of MCSR positioning (including source, receivers, and feather angles), source quality, and brute stacks for penetration and low frequency content.
- Positional Check (Horizontal and Vertical) of MBES vs. SBP vs. MCS, etc.

4.1 Post-Processed Kinematic (PPK) Processing

Post-processed Kinematic (PPK) records were recorded from the raw POSMV OceanMaster system in *.000 file format and were processed in POSPac Version 9.0 software. These data were output as *.SBET files and applied to the multibeam bathymetry for a better motion and positioning results product.

Before applying the SBET to any MBES datasets, the processor reviewed the Display Plots to QC the results. These plots included the Estimated Position Accuracies, PDOP (Position Dilution of Precision), Processing Mode, Lever Arm Figure of Merit, etc. Sample images for these plots are shown in Figure 15 to Figure 18.

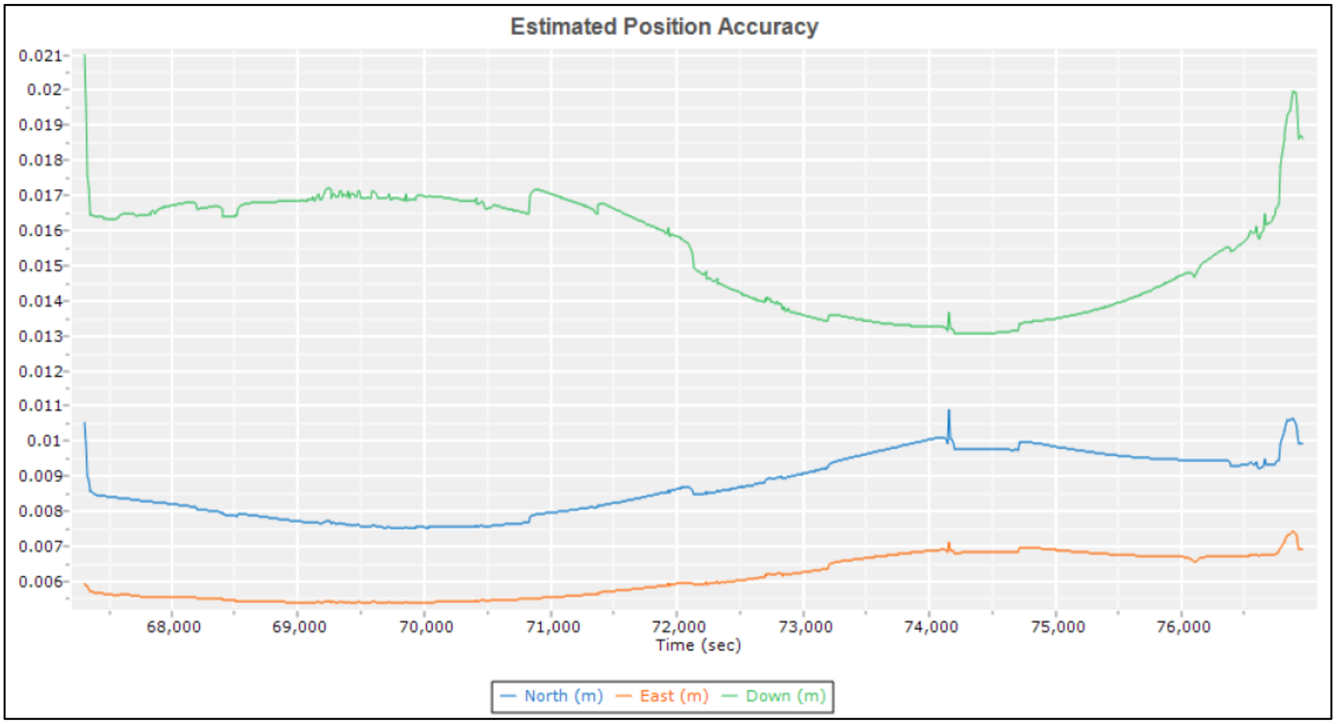

Figure 15. POSPac Smoothed Performance Metrics for JD126 with values below 3 cm

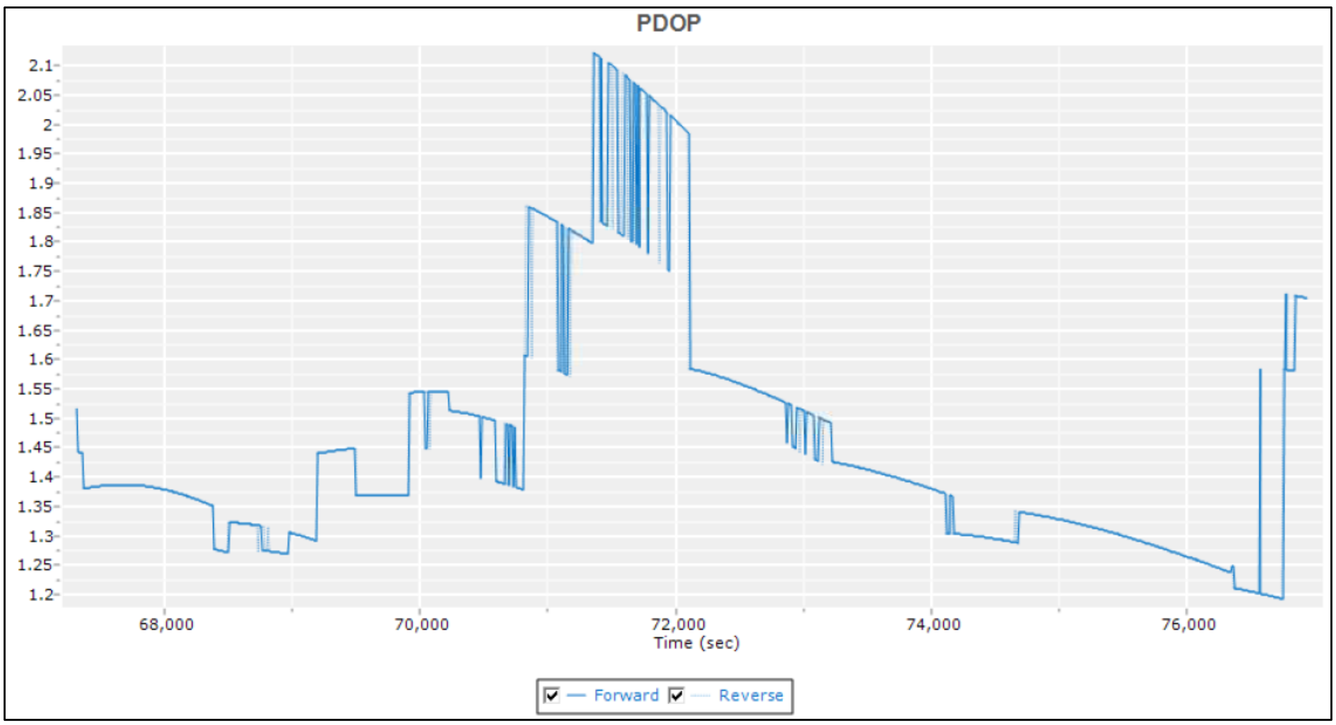

Figure 16. POSPac PDOP for JD126 with values below 3

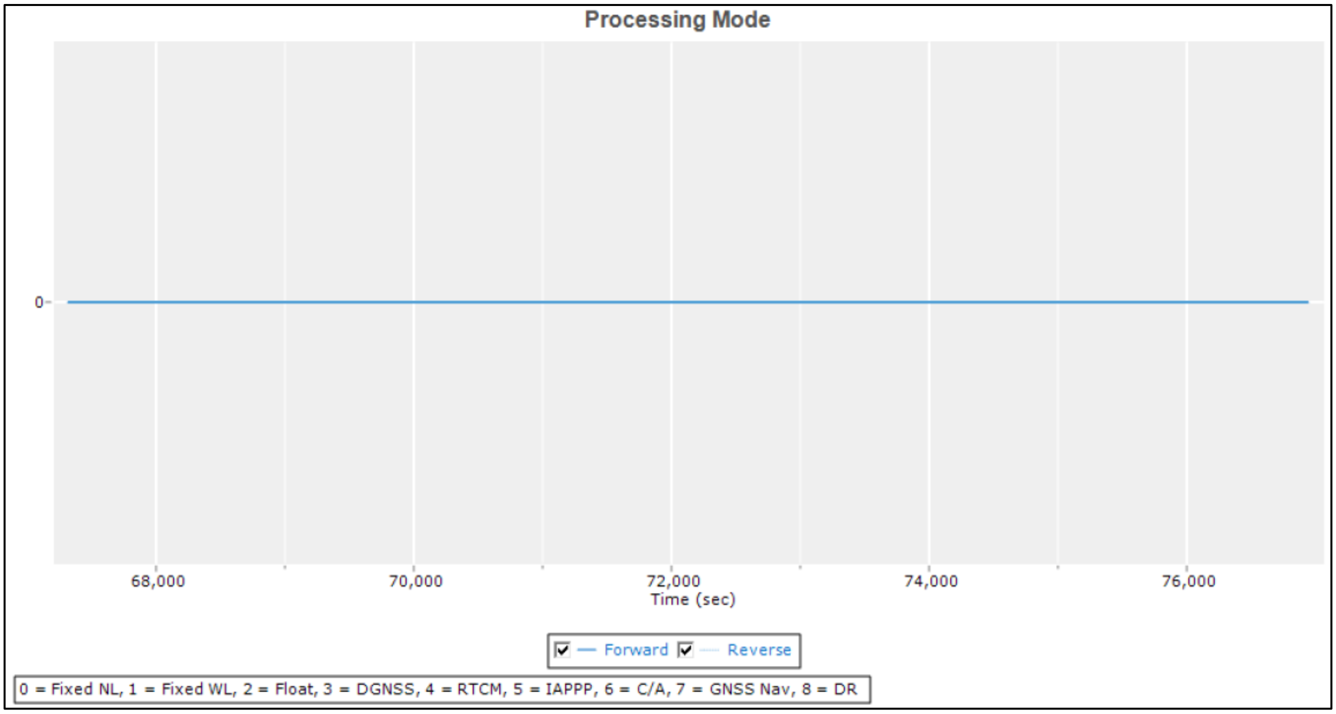

Figure 17. POSPac Processing Mode for JD126 with Fixed NL status (0, no loss of GPS corrections)

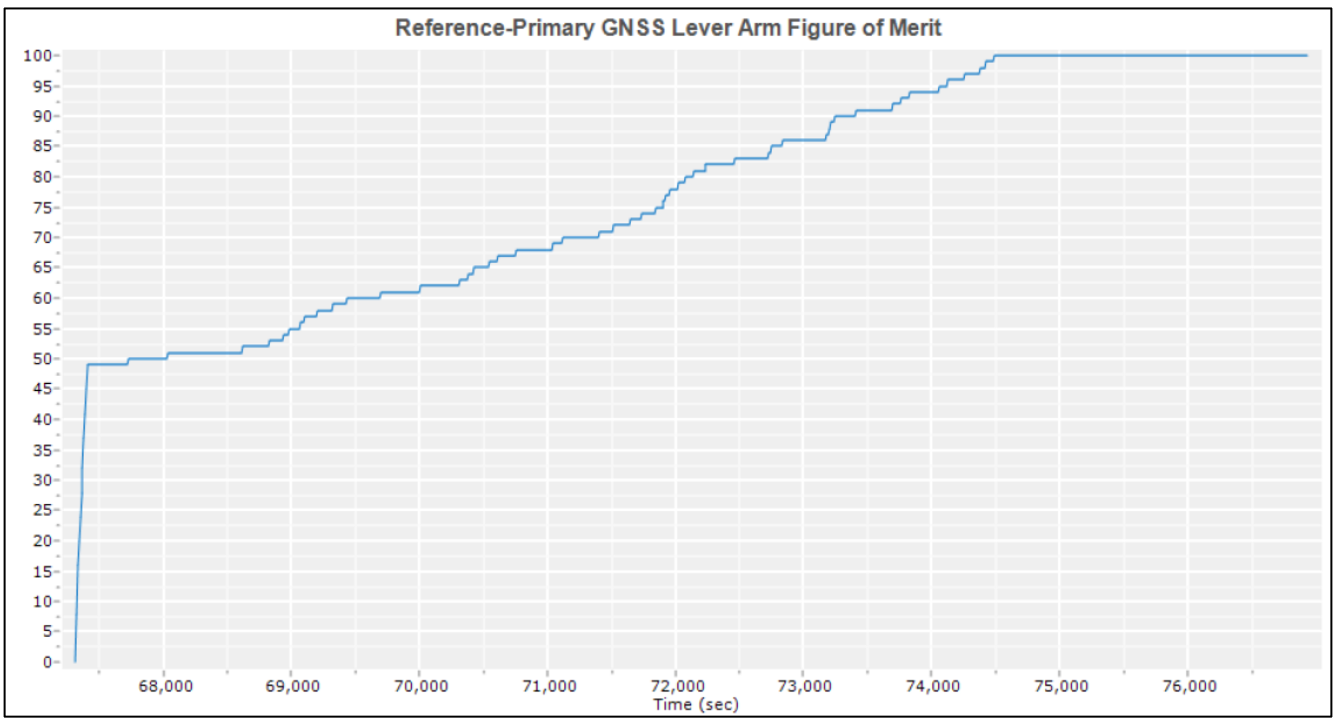

Figure 18. POSPac Figure of Merit for JD126 Installation Calibration Parameters (offsets) reaching 100%

GBA ENGINEERS ★ SURVEYORS Est. 1974

S. T. HUDSON ENGINEERS, INC.
PROFESSIONAL ENGINEERS & CONSULTANTS

4.2 Bathymetric Data Processing

Bathymetric records were imported and processed with QPS Qimera Version 2.6.2. Multibeam files were cleaned of noise and spurious data. The GPS tides, SBETs and sound velocity profiles were applied before being delivered as a final data set (Figure 19).

After all processing was completed, the surface was exported from Qimera and loaded in Global Mapper for final QAQC.

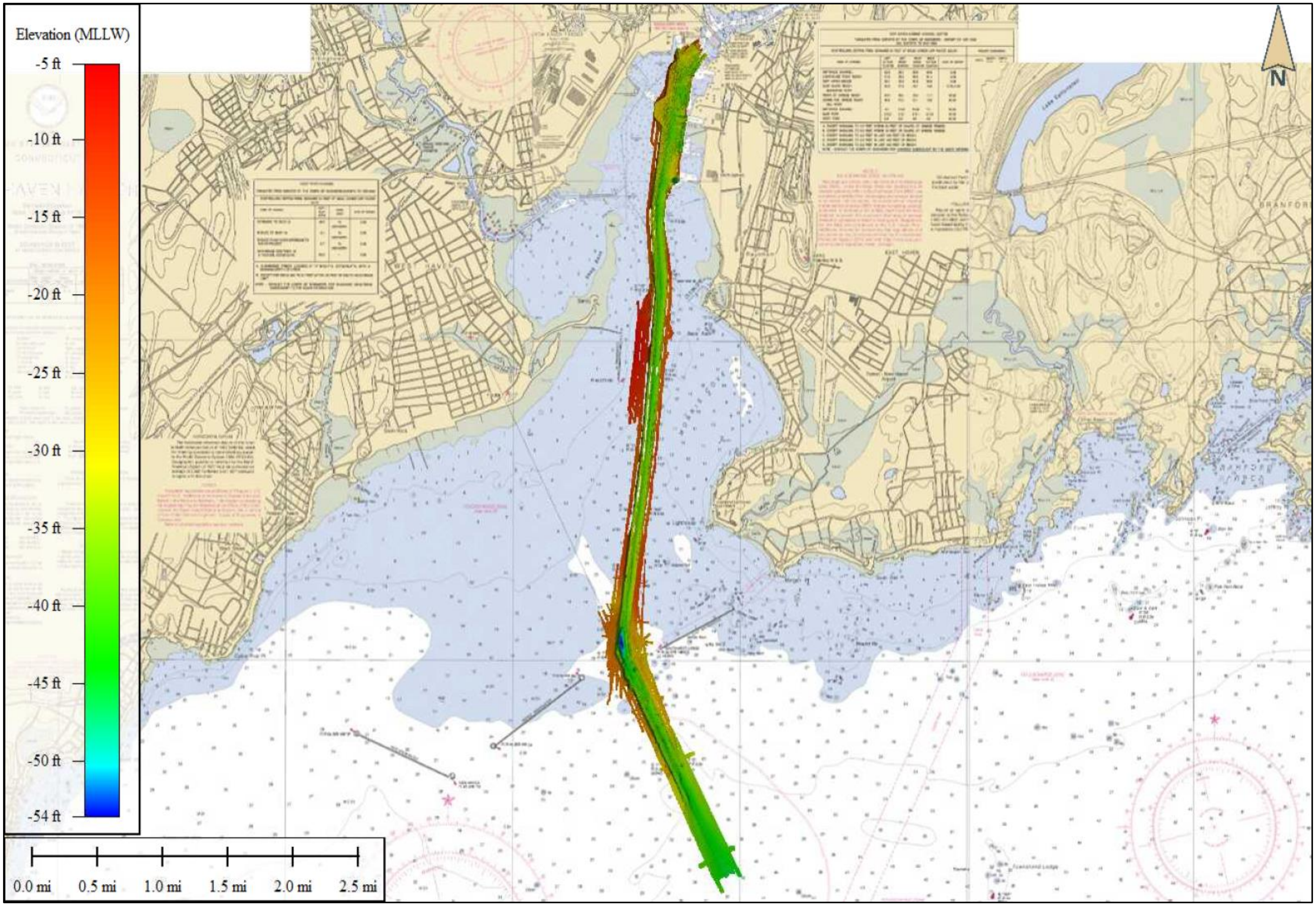

Figure 19. Final Bathymetric Surface showing distribution of elevations (feet) relative to MLLW

4.2.1 Acoustic Backscatter Processing

Backscatter collected concurrently with the multibeam bathymetry was imported and processed with QPS Fledermaus Geocoder Toolbox (FMGT) v 7.11.0.

The final processed MBES was used to export .GSF files for backscatter processing. The final MBES surface was loaded into the FMGT project to ensure proper geodesy and coverage with the backscatter mosaic. Once the .GSF files were loaded into the project and the initial mosaic had a beam pattern applied, the Cascading Normalization tool was used to optimize results and equalize gains across the entire dataset. Lines were ordered in the mosaic to minimize any remaining MBES noise or artifacts that could not be processed out of the backscatter. The final backscatter mosaic (Figure 20) was loaded into Global Mapper for final QAQC.

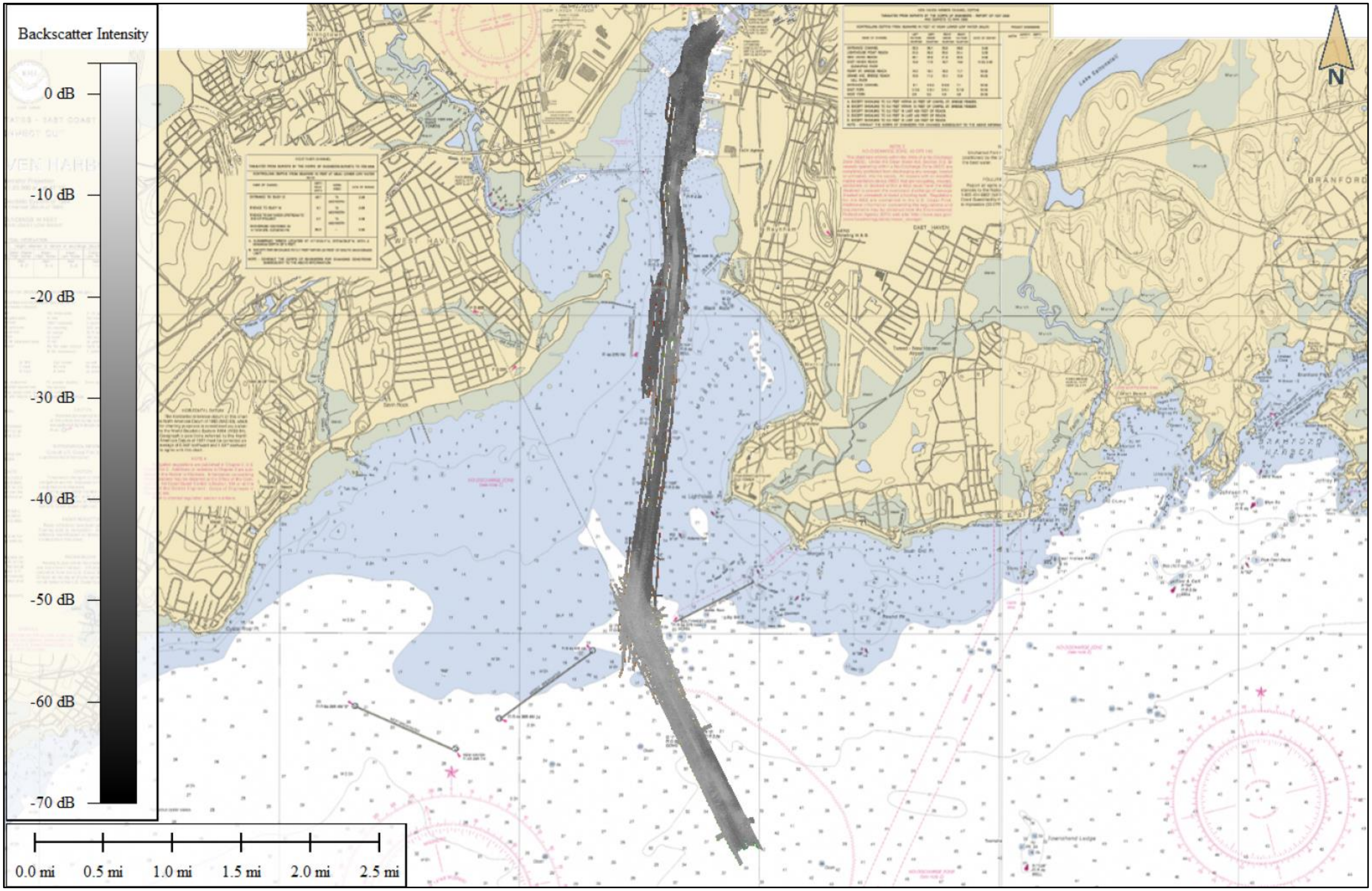

Figure 20. Backscatter Mosaic from FMGT; Scale showing intensity values in decibels (dB)

4.3 Sub-Bottom Sonar Processing

Sub-bottom data collected with the Innomar Medium-100 Parametric sub-bottom profiler were processed in RadExPro Build 2023.1 seismic processing software for all geometry assignments and signal processing. Final vertical referencing and draping to MBES bathymetry were accomplished in Chesapeake SonarWiz.

The raw data (Figure 21) were all treated with a variety of frequency and spatial filters to suppress the noise from a variety of sources and to improve the signal quality of the final profile used for geologic/geophysical correlations.

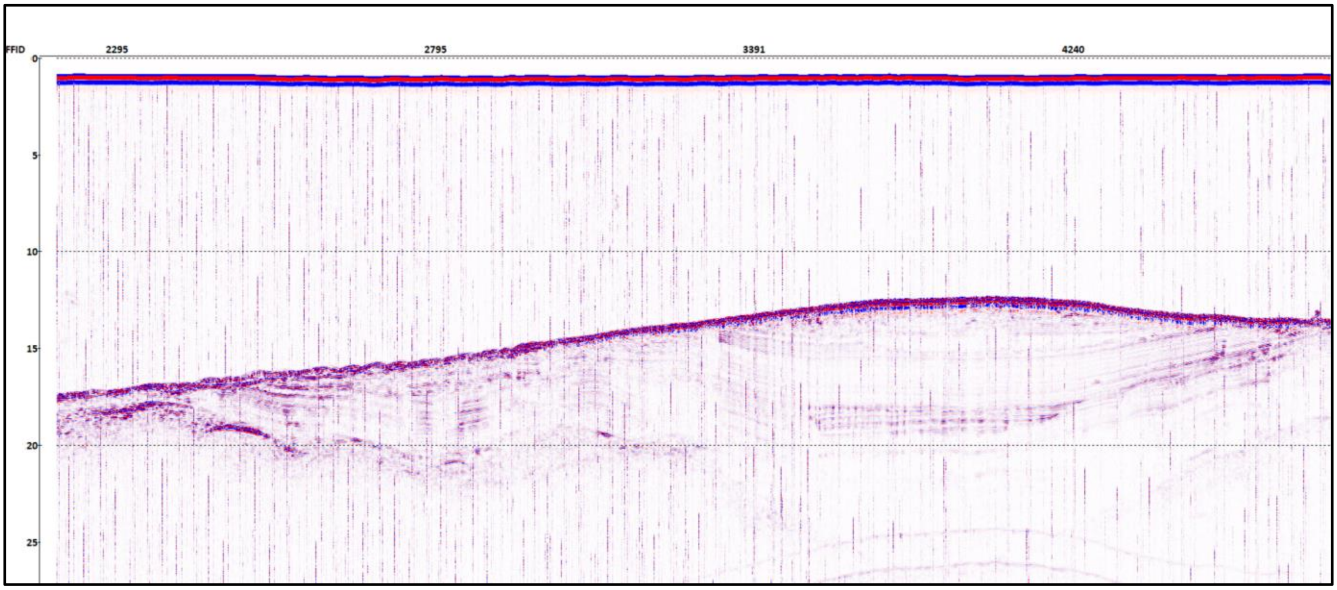

Figure 21. Raw Innomar Medium-100 data in two-way time (ms) and horizontal axis in trace numbers

All sub-bottom data were taken through a series of filters including but not limited to: DC gain removal, spherical divergence corrections, and band pass filtering. Based on the original quality of the data and ambient noise conditions on the specific acquisition lines, various additional filters were applied: source deconvolutions, burst removal, 2D-spatial filtering, and time-varying band pass (TVBP) filters (Figure 22).

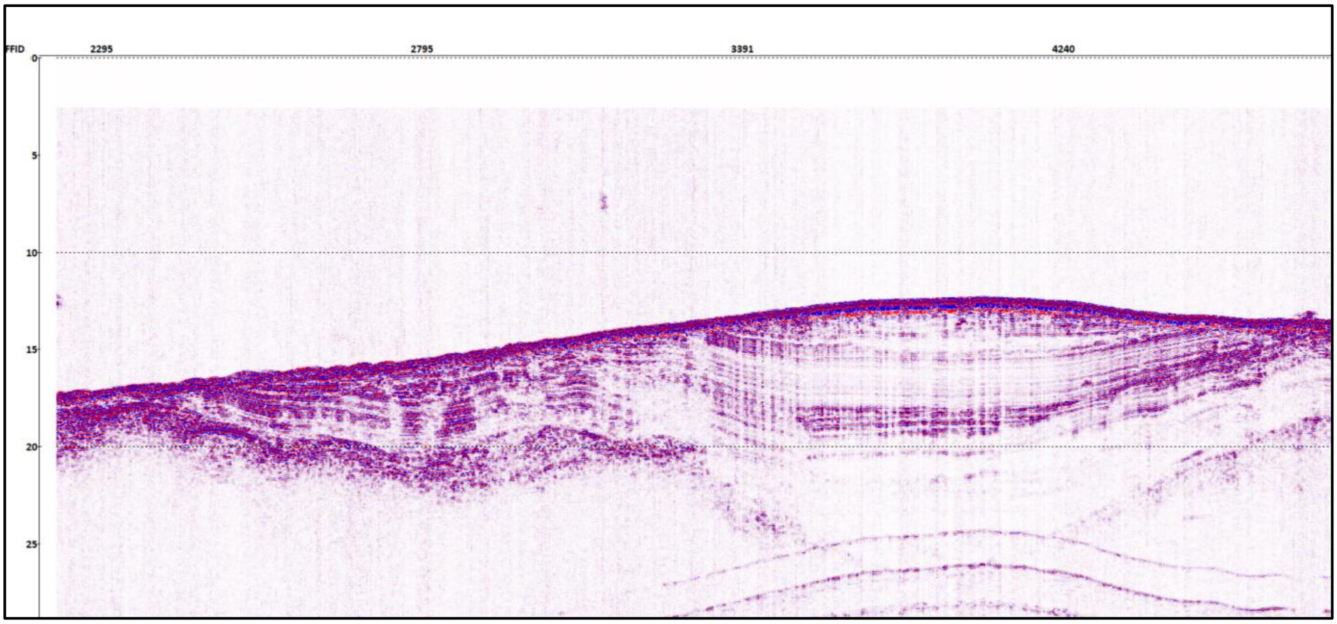

Figure 22. Processed Innomar Medium-100 data depicting the same profile as Figure 21

After the completion of signal processing, the data were exported to SEGY format and imported to SonarWiz for datum referencing and interpretation. Vertical adjustments were applied by draping the sub-bottom data onto the high resolution multibeam bathymetry collected in the channel.

Imaging quality was excellent in the outer harbor due to high relief bedrock geology, significant velocity contrasts, and high seismic Q (Figure 23). SBP imaging in the Inner Harbor was negatively affected by a high shallow gas content in much of the area. The gas was interpreted to be biogenic in origin and was expected due to the estuary setting (Figure 24).

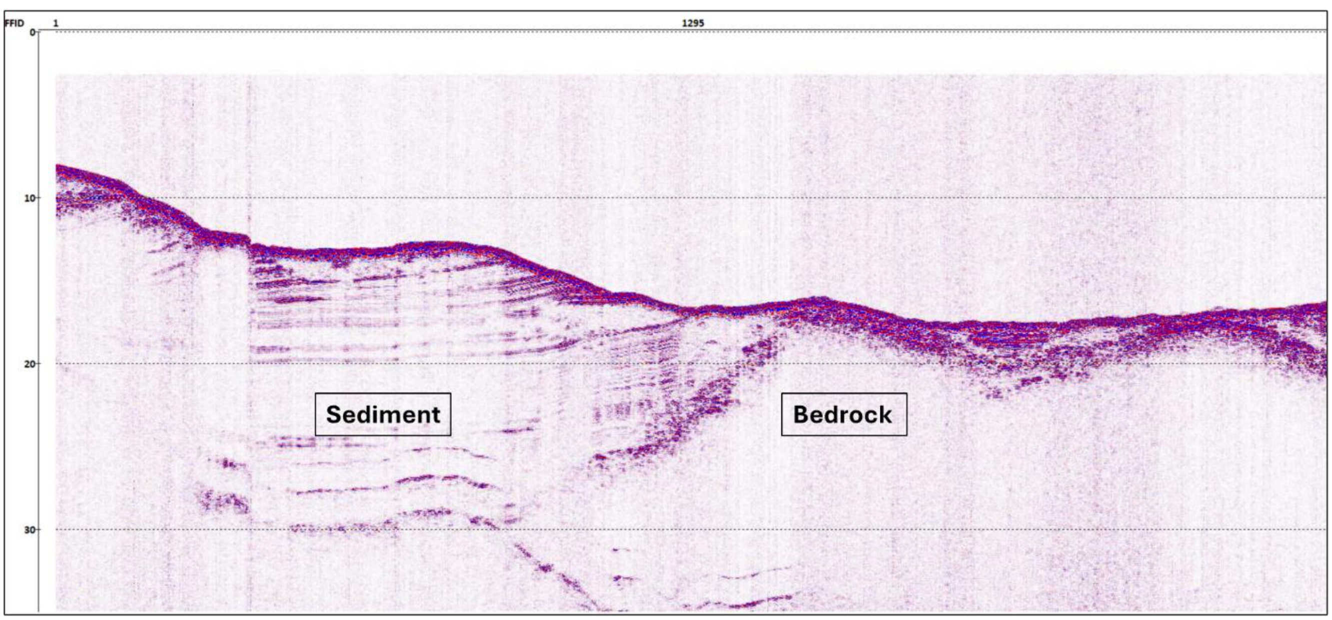

Figure 23. Processed seismic profile (TWT, ms) from the outer harbor depicting high resolution and interpretability

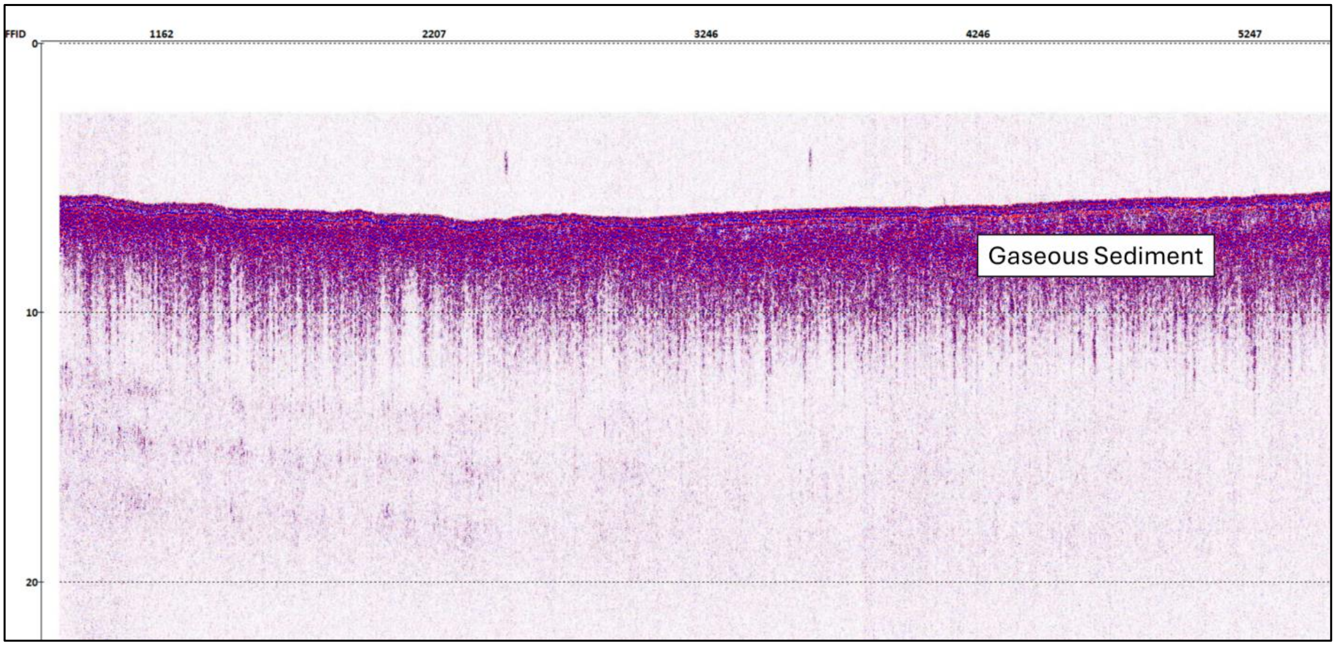

Figure 24. Processed SBP profile (TWT, ms) from the Inner Harbor with acoustic masking by shallow gas

4.4 Multi-channel Seismic Reflection (MCS)

Multi-channel seismic reflection data acquired throughout the project site were processed in RadExPro, Build 2023.1. Raw SEGY data files were loaded into RadExPro for initial quality control, geometry assignments, and signal processing (Figure 25). All seismic cross-section figures in this section have vertical units in two-way travel time (TWTT) in milliseconds (ms).

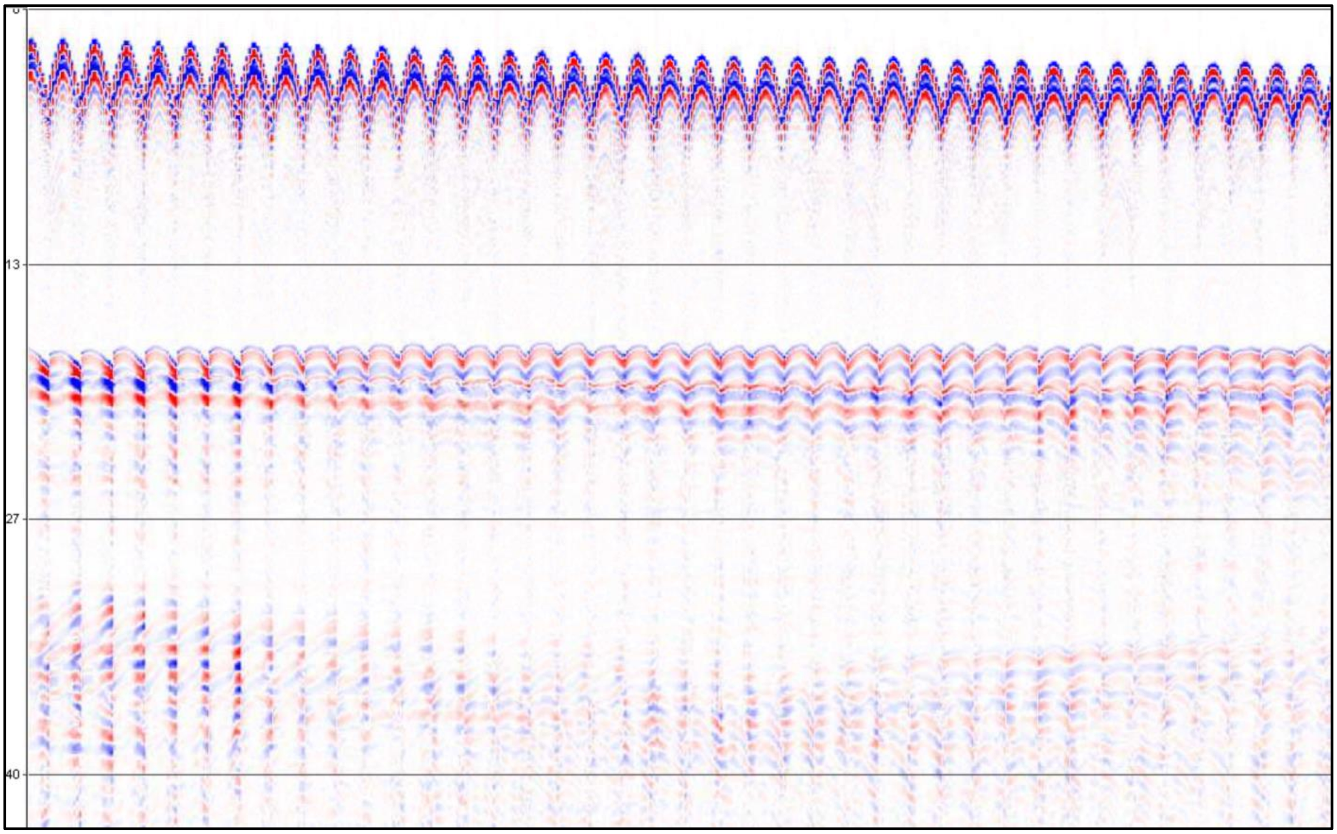

Figure 25. Raw 12-channel shot gathers (TWT, ms) acquired along line S5006

All 12 channels were used to construct a brute stack in the field to monitor coverage and data quality changes throughout the survey area (Figure 26). Initial data quality showed the ability to distinguish discrete sediment layers as well as a clear bedrock interface in some areas. A large amount of shallow gas, likely biogenic, obstructed the acoustic source in some areas of the Inner Harbor (Figure 27).

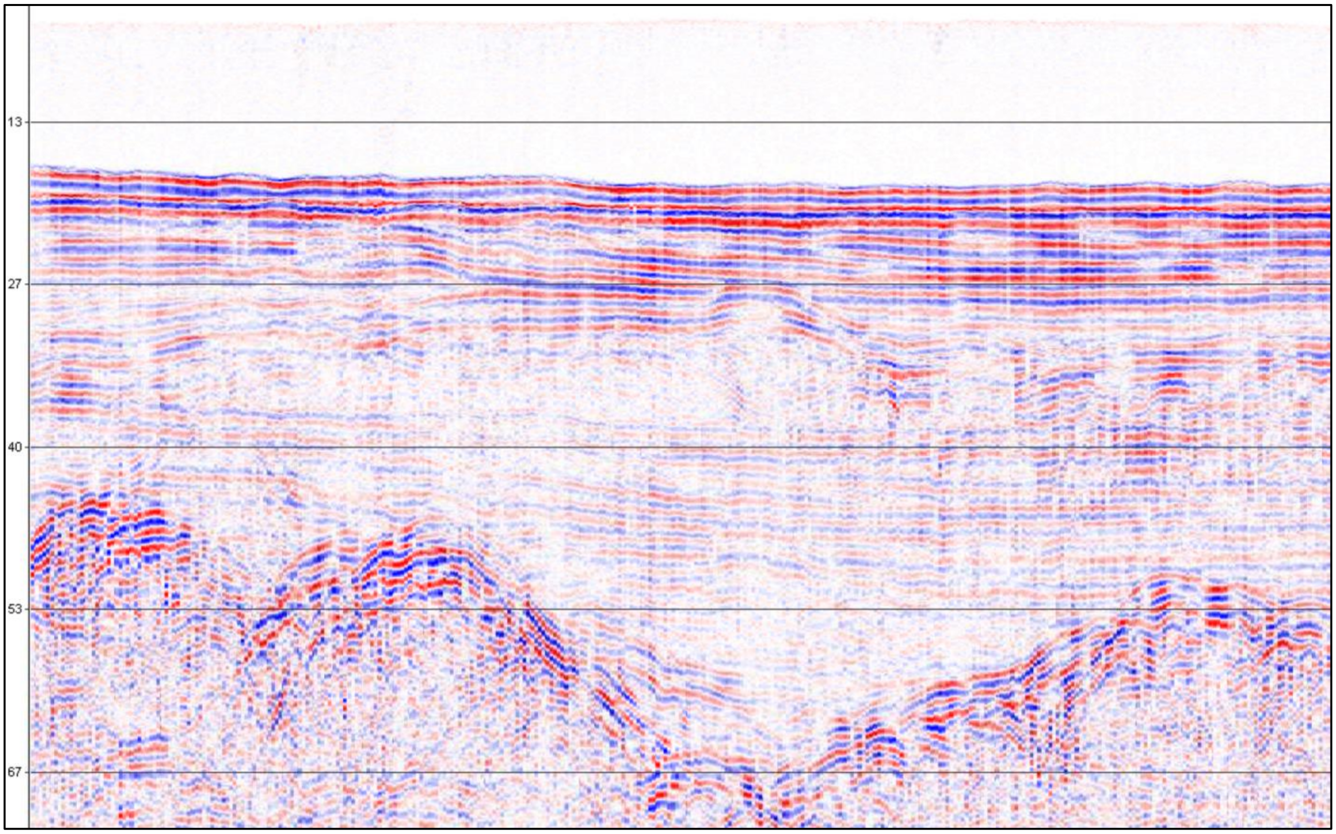

Figure 26. Brute Stack detail of Line S5006 (TWT, ms) as created during field acquisition

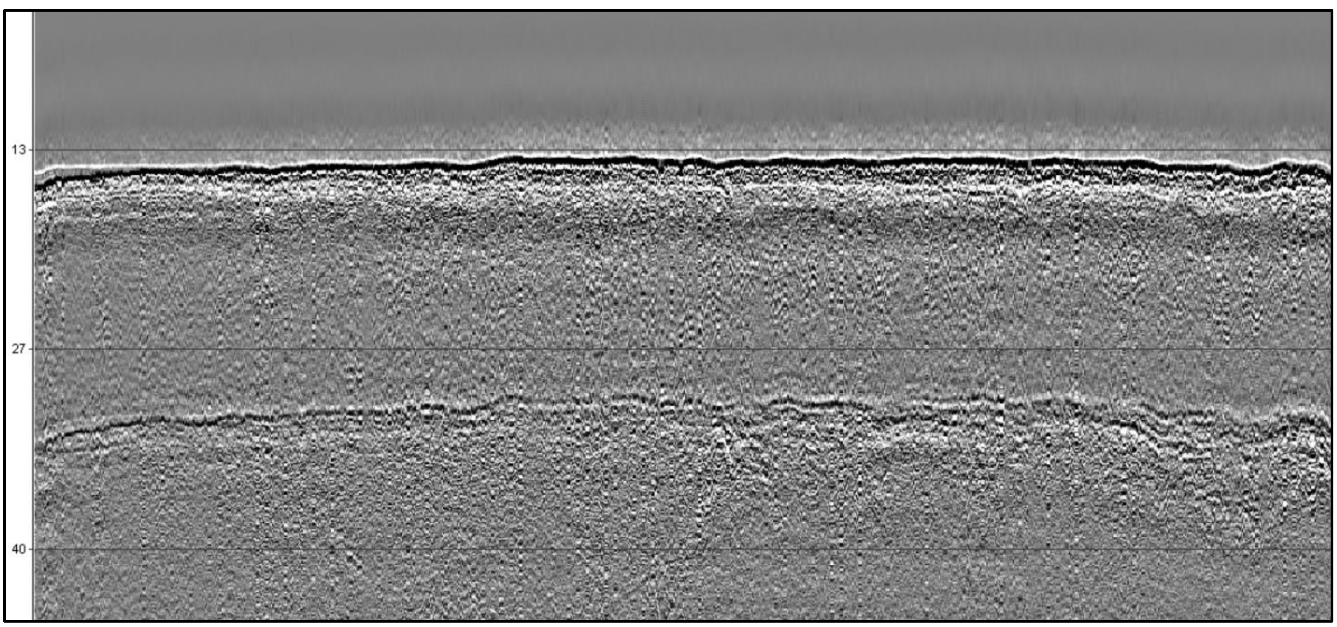

Figure 27. Processed MCS Profile of Line S3002 (TWT, ms) in the Inner Harbor depicted in grayscale to emphasize the gas sediment/noise

S. T. HUDSON ENGINEERS, INC.
PROFESSIONAL ENGINEERS & CONSULTANTS

In processing, pre-stack preparation included DC gain adjustments, source/receiver geometry adjustments, and noise suppression filters. Adjustments were made on a trace-by-trace basis for source vertical motion (heave) and streamer feather angle. Common depth point (CDP) bins were positioned along the adjusted track line.

A source deconvolution routine was performed on the data to increase the vertical resolution and overall energy content of the source pulse (Figure 28). Lines acquired as reference lines were used to model the source pulse using a custom impulse trace transformation. The compression of the source pulse sharpened the seabed and flattened the frequency response curve (normalizing both high and low frequency content) (Figure 29).

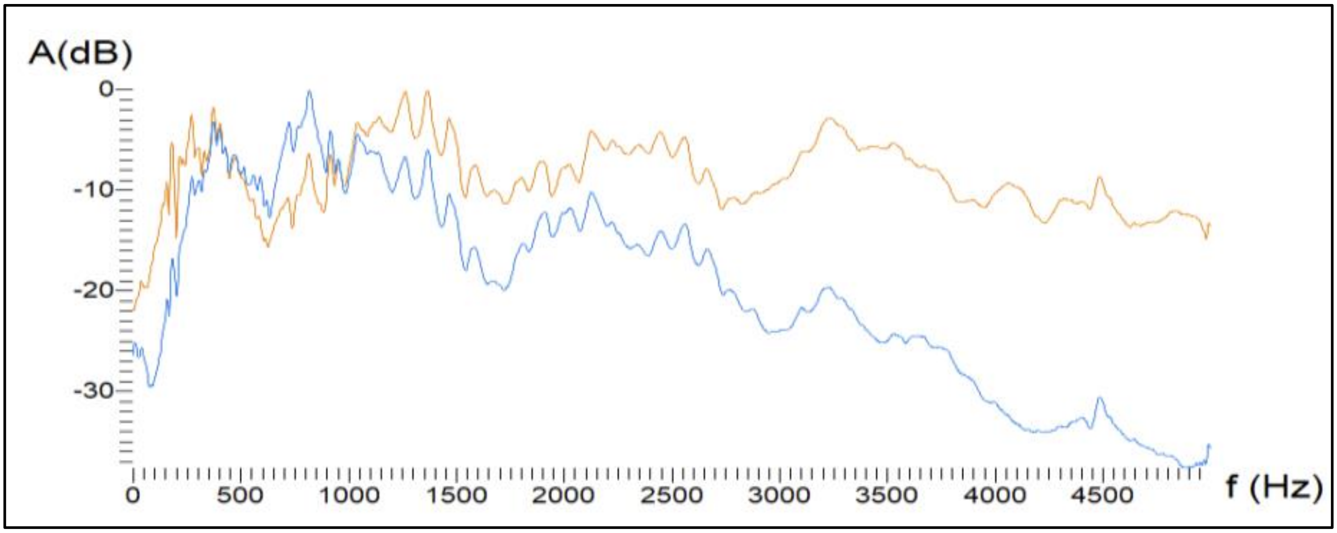

Figure 28. Frequency Response of Trace Data before (blue) and after (orange) Pre-stack Source Deconvolution

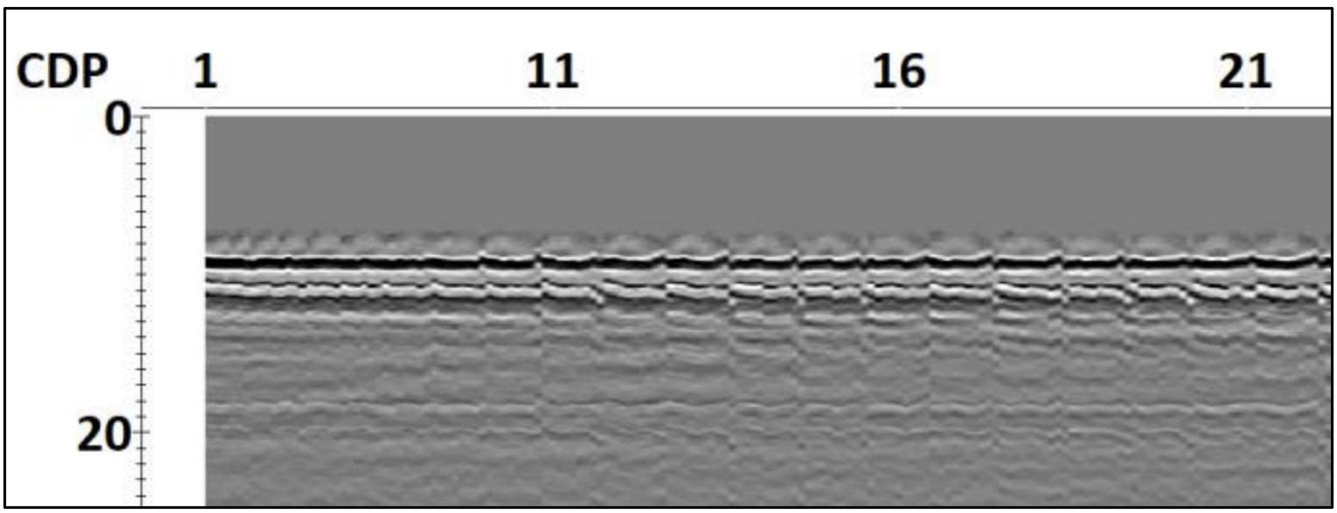

Figure 29. Pre-stack shot gather of geometrically corrected traces *before* deconvolution depicting thick seabed return

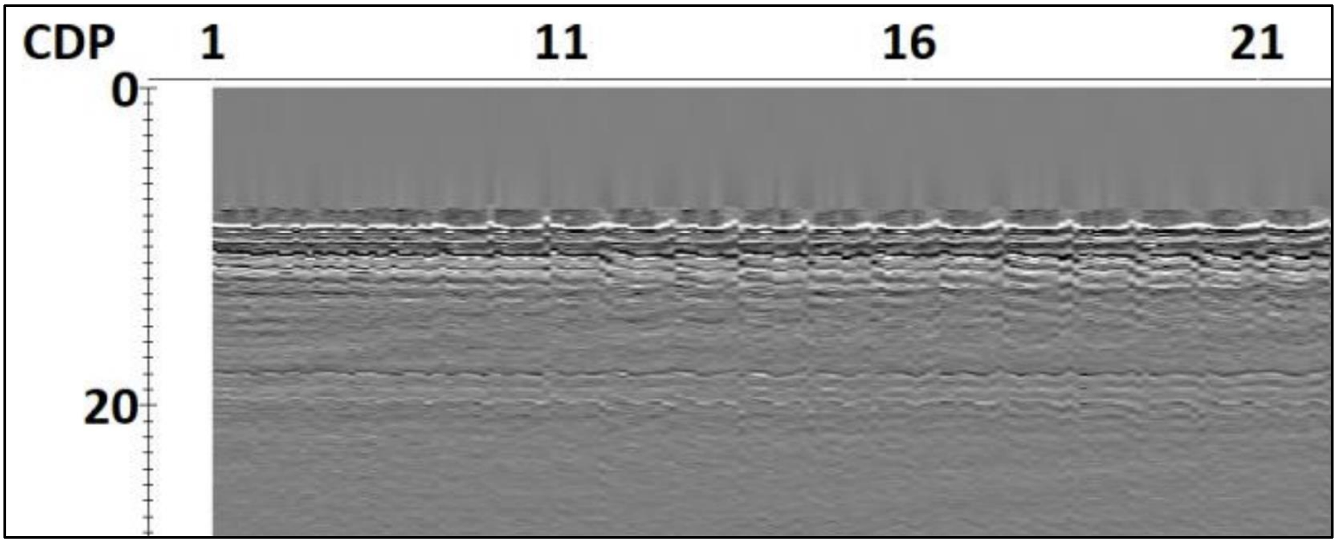

Figure 30. Pre-stack shot gather of geometrically corrected traces *after* deconvolution depicting sharp seabed return

Pre-stack de-ghosting was performed using a predictive wave filter. The receiver ghost wavelet was modeled after data collected in reference lines and used to subtract ghost related noise from the trace data. The receiver ghost was subtracted from the data in the pre-stack domain (Figure 30).

Velocity corrections were achieved through semblance analysis of the collected data. Two velocity models were constructed using super gathers and semblance analysis: RMS velocity vs. depth and a "layer cake" type interval velocity vs. depth. Due to the complexity of the underlying sediment and bedrock, the RMS model was chosen for migration and depth conversion. These velocity models were provided in SEGY format with the delivered data accompanying this report. The lines chosen to create these models are shown below in Table 16.

Table 16. 2D Seismic Reflection Velocity Modeling Results

Line	Minimum Velocity ft/sec	Maximum Velocity ft/sec	Range ft/sec
S3002	4,878	7,545	2,667
S3004	4,880	7,155	2,275
S5001	4,888	7,152	2,264
S5006	4,882	7,224	2,342
X1002	4,880	7,168	2,288
X1006	4,885	7,221	2,335
X1010	4,878	7,155	2,276

Post-stack processing included source deconvolutions, burst noise removal, surface related multiple elimination (SRME), 2D migration, trace-by-trace tidal datum corrections, and depth conversion. After all signal filtering, the final SEGY files were exported in their migrated format and imported into SonarWiz for analysis (Figure 31).

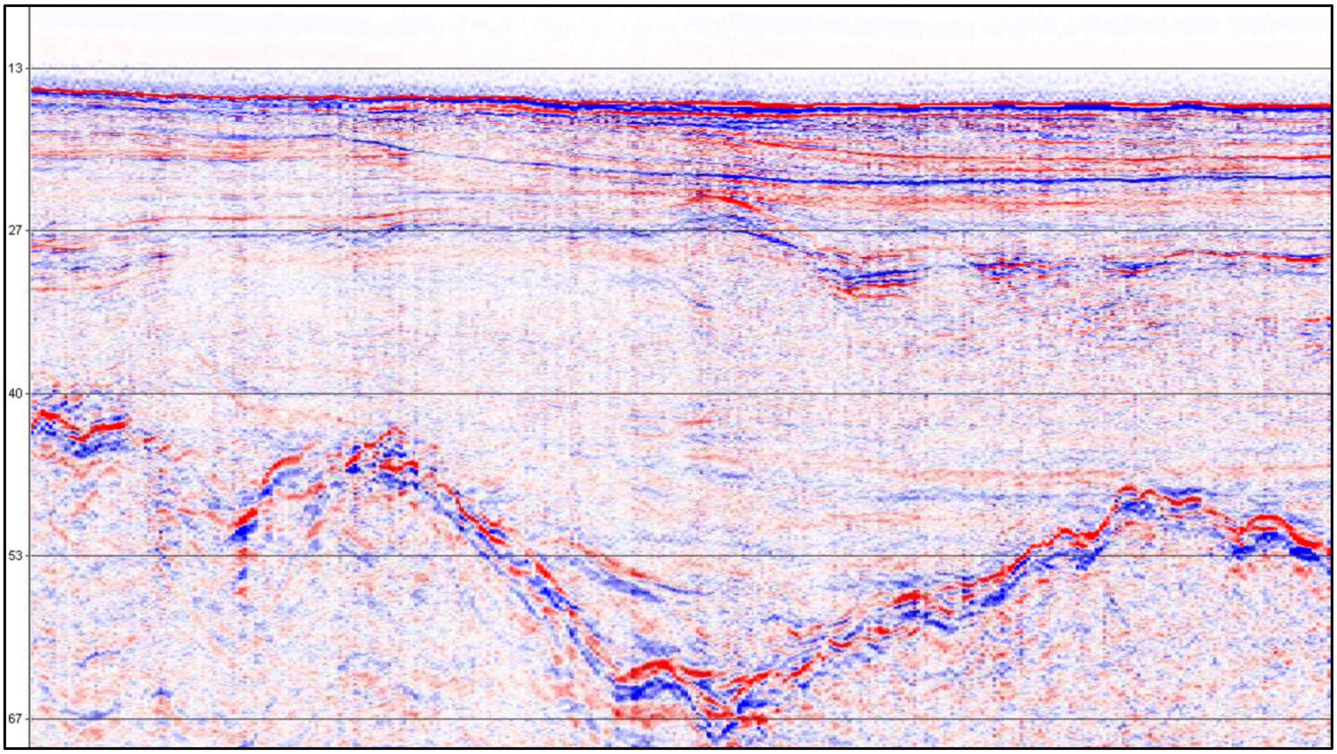

Figure 31. Seismic profile detail of Line S5006 after all data processing and migration

4.5 Multi-channel Seismic Refraction (MCSR)

Multi-channel seismic refraction was processed using a combination of RadExPro, Build 2023.1 and RAYFRACT refraction tomography software. Creating the P-wave velocity tomographic sections was an iterative process that involved using the data processed as reflection to understand where refractions may occur (Figure 32), and then examining the lines (usually starting with the last channel) for the presence of refracted wave energy. The shape and expected depth of bedrock is used to identify refracted energy in the shallow subsurface.

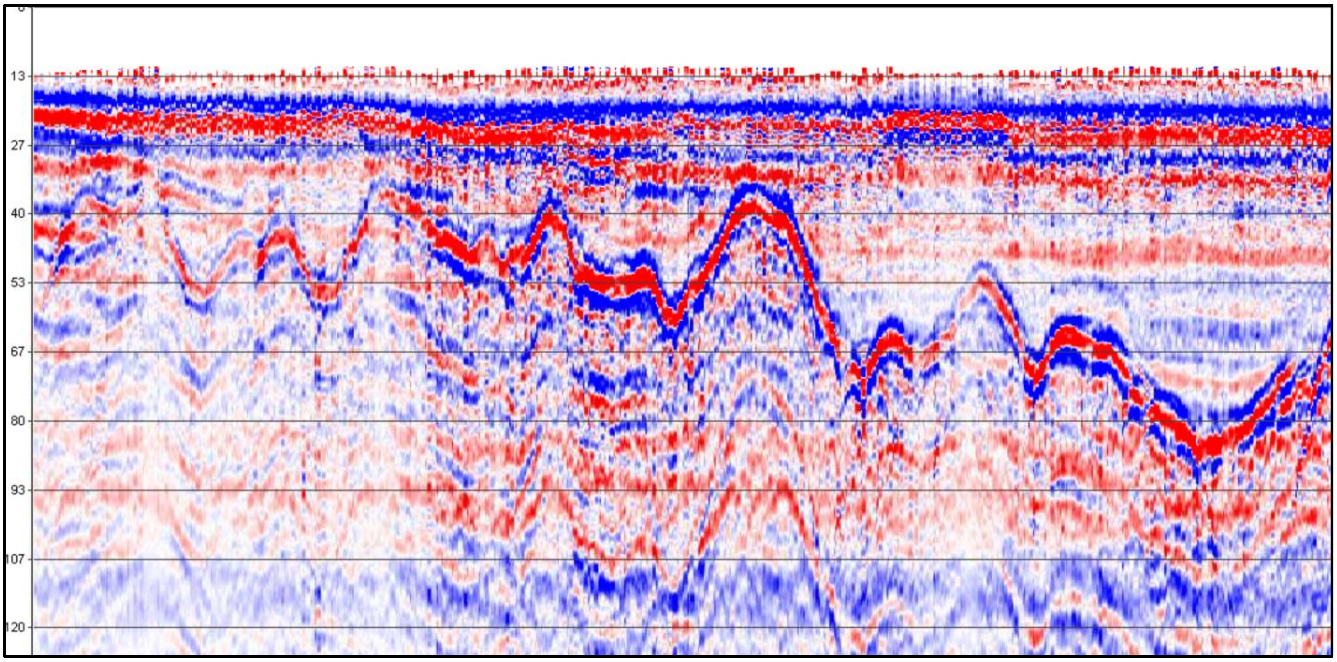

Figure 32. Brute stack of Refraction line R5003 (processed as reflection)

Initial processing in RadExPro included pre-stack demultiple in the channel domain and pre-stack source deconvolutions. This initial processing allowed for a clean record of each shot enabling the detection of refracted signals. In the image below, an example is shown of the full record from 6 shots, displaying all 72 channels of each shot (Figure 33).

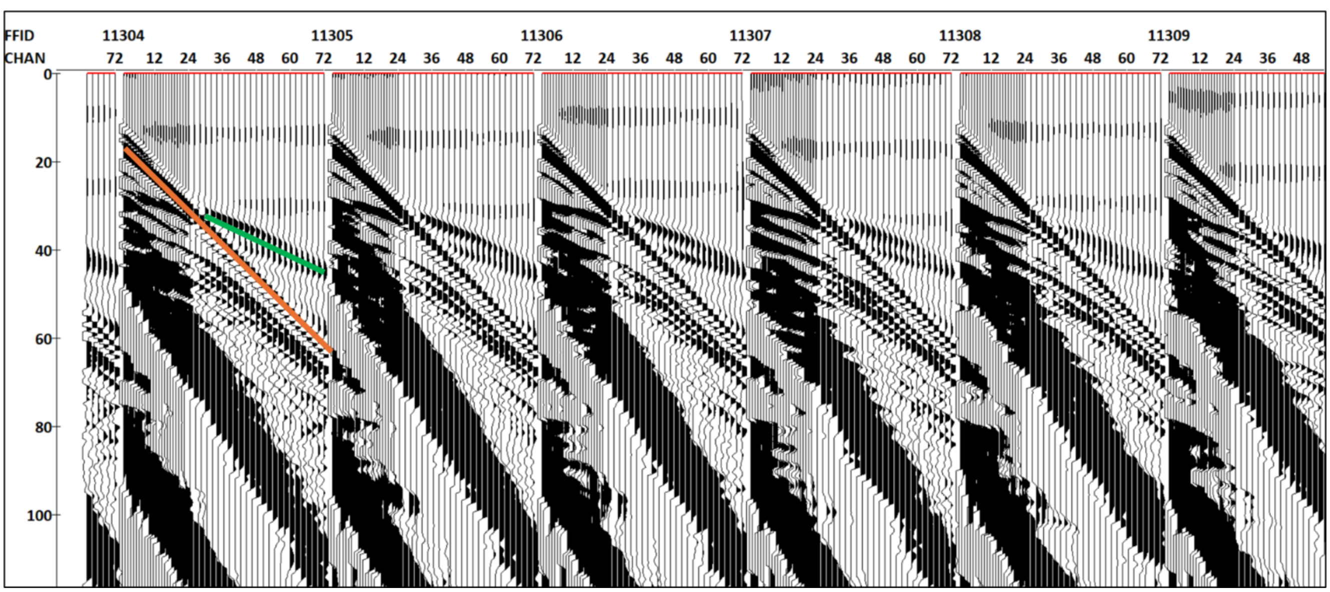

Figure 33. Raw shot-gather depicting 6 shots of the low frequency source.
The direct arrival (orange) and first refracted arrival (green) are shown on shot 11304.

Survey lines were meticulously screened for evidence of refracted energy by examining individual channels of minimally processed data. Velocity contrasts in the shallow subsurface were identified as substructure appearing above the natural seabed (Figure 34). Please note that this is an artifact used to detect the existence of velocity changes and not an actual indication of rock outcropping above the seafloor.

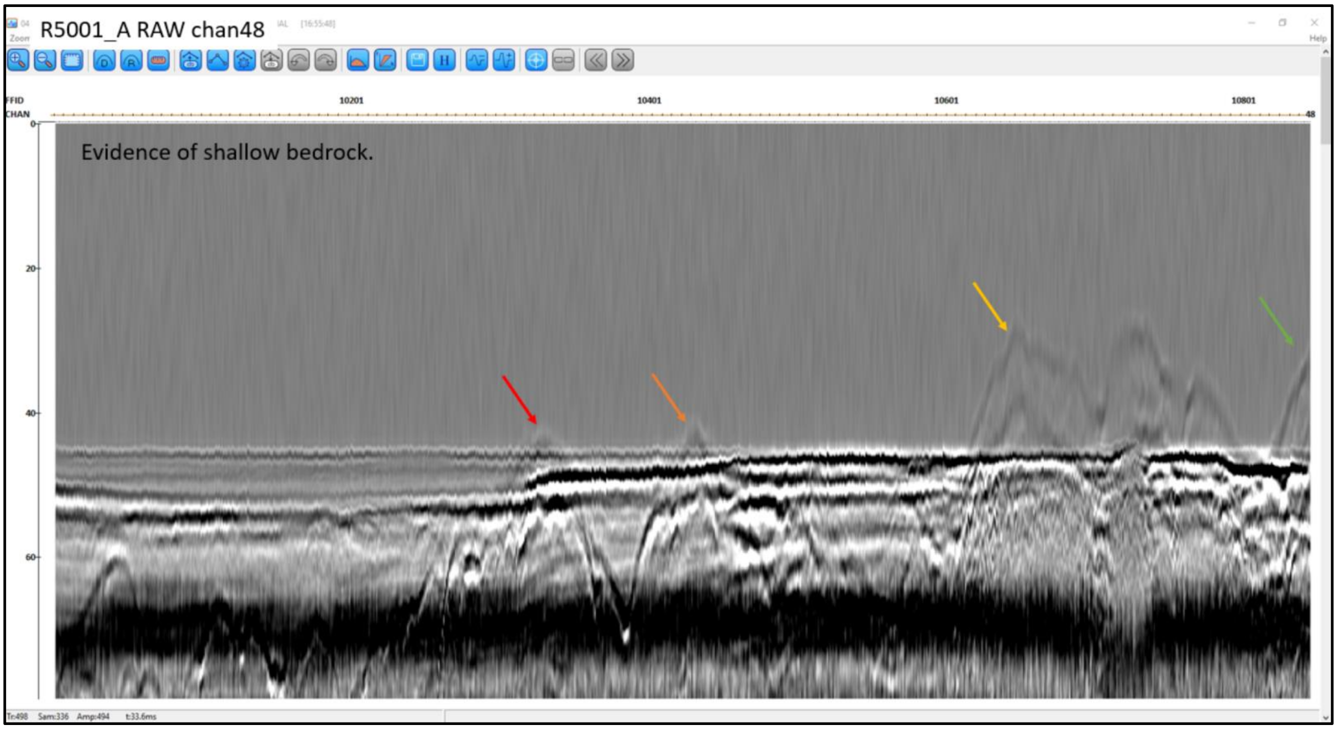

Figure 34. Geometrically corrected and minimally processed single channel profile of Channel 48 on line R5001_A. The far offset (>75m behind the source) accentuates the arrival of the refracted wave and shows substructure bedrock above the natural seabed (Colored Arrows).

Within the Inner Harbor, where there was no bedrock above -62 ft MLLW; there were large areas where no refracted energy was detected. As these areas corresponded to where geotechnical borings showed a presence of saturated organic silts and clays, the P-wave velocity was expected to be very close to the velocity of the water in the channel (nominally 4,900 ft/sec). With no refracted energy in the signal, this further supported that the p-wave velocity of these layers suggested saturated, unconsolidated sediment and no competent bedrock.

By utilizing a single Sercel Mini-G Source (20in^3) air gun, an extremely low frequency air gun source, the signal was less susceptible to the presence of shallow, biogenic gas. The lack of refracted energy in the Inner Harbor was not attributable to the presence of gas and was most likely due to the acoustic homogeneity of the subsurface in that area. An example of an area with no refracted energy received is shown below in Figure 35.

Areas with no refracted energy detected were removed from the tomographic sections accompanying this report. Where no data appeared along a refraction acquisition line, it was attributed to this lack of refracted energy. All refraction survey lines were provided as a brute stack, including those areas where refracted energy was not found.

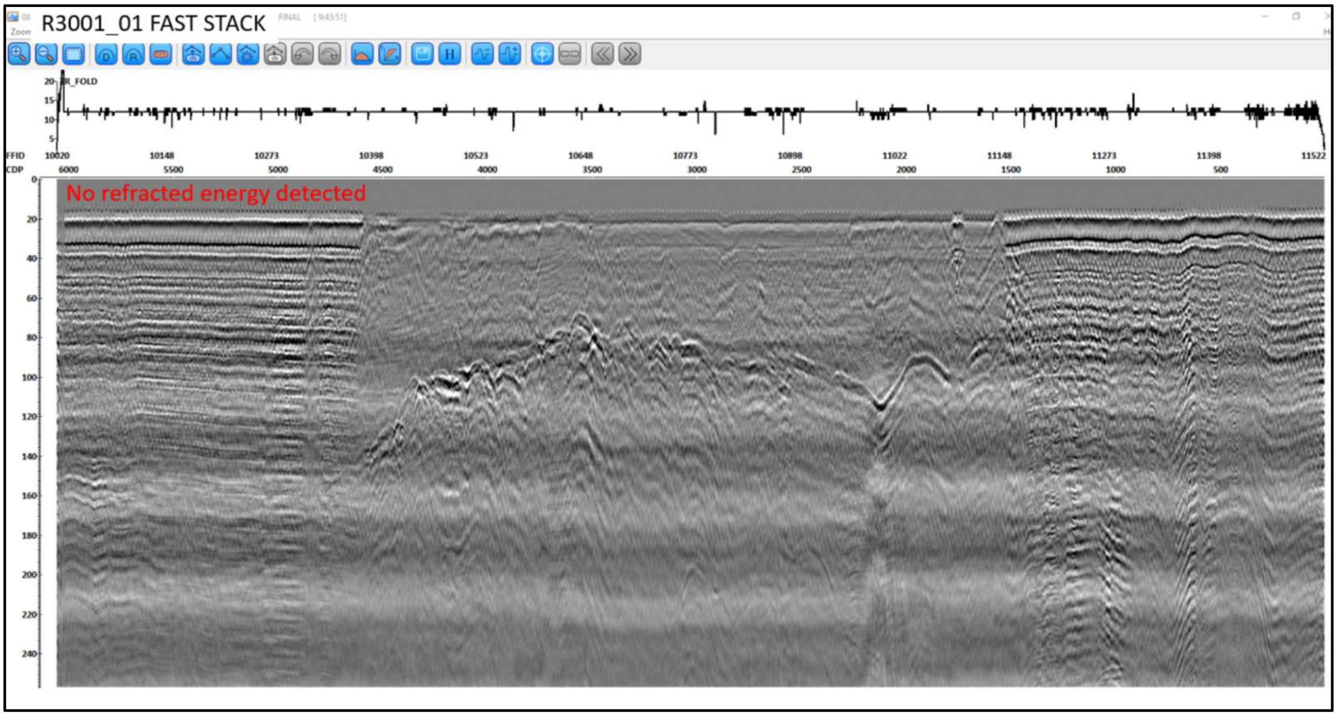

Figure 35. Example profile of R3001_01 showing no refracted energy. Lack of refraction indications a homogenous subsurface velocity within the dredge template, likely due to saturation and thickness of the organic layer

After identifying and confirming areas with refracted arrivals, the data were brought into RAYFRACT for conversion to velocity tomographic sections. Simple slope analysis was used to determine the P-wave velocity of the direct medium (seawater) and the subsequent, identifiable refracted arrivals (Figure 33). The data were exported into simple ASCII format representing the location, depth, and velocity solution for each measured, valid shot point (Figure 36). Velocity tomography was used to identify areas of expected bedrock and supplement top of rock models where reflection data was masked by shallow, biogenic gas. Due to the low frequency source used, the resolution of the refraction data was much lower than the SBP or 2D reflection data.

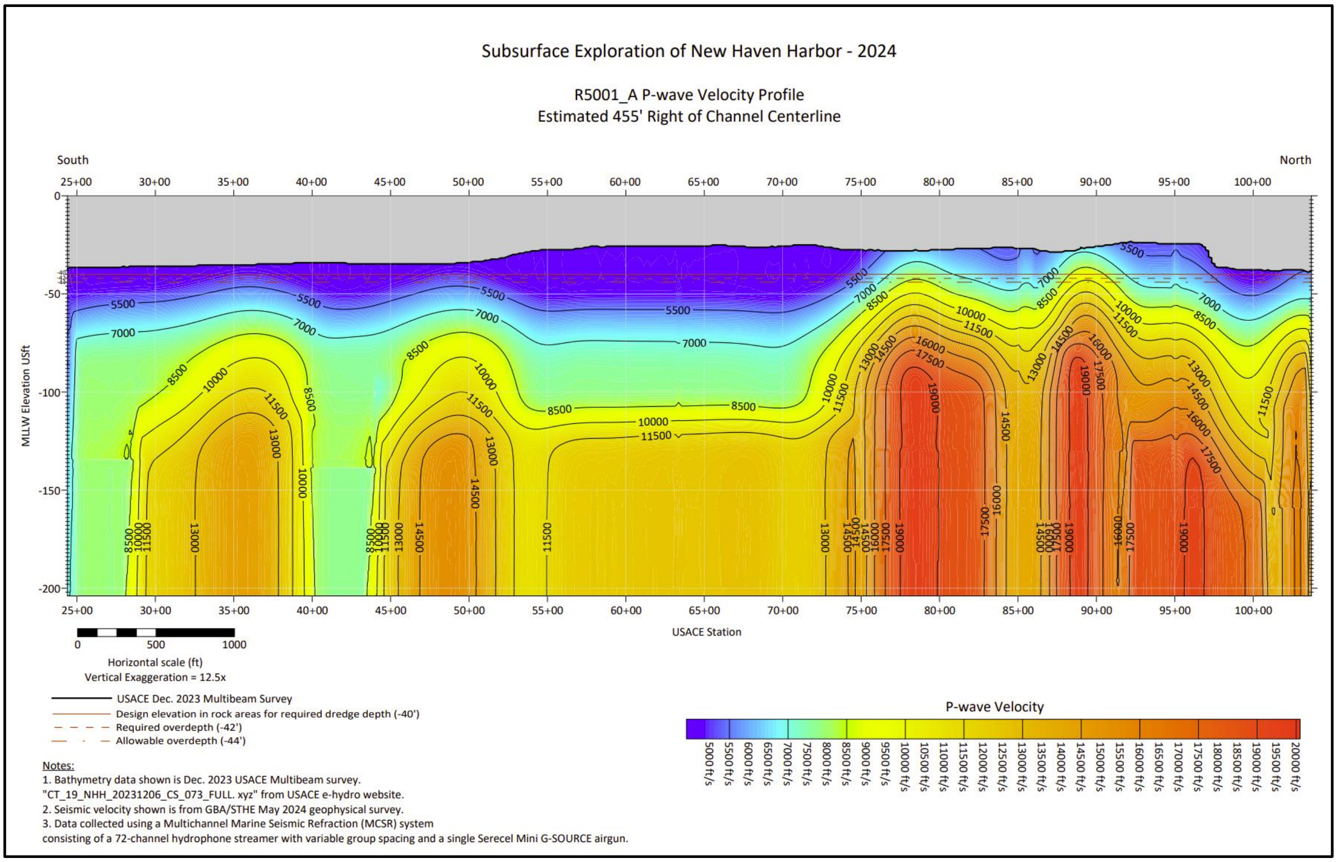

Figure 36. Example tomographic detail of Line R5004 showing the as-found horizontal and vertical variability of the P-wave velocity in the subsurface. Gray represents the seawater layer (~4,500 ft/sec).

5 Geotechnical Sample Processing and Analysis

5.1 Field Procedures

A total of thirty-six (36) borings were required for the geotechnical portion of this investigation. Twenty (20) were soil borings to assist with the classification of sediment within the harbor channel improvement project limits, six (6) borings were utilized for characterization for materials in the proposed CAD cell, and ten (10) borings were conducted as rock core borings within the rock area of interest within the vicinity of the existing breakwaters. A summary table for boring locations, northing, easting, elevation, station, offset, and termination elevation can be reviewed below.

Table 17. Boring Location Summary (MLLW, ft)

Boring ID	Northing (ft)	Easting (ft)	Top of Hole EL	Station	Offset	Boring Termination EL
FD24-B-01	640196.5	956643.2	-36.5	24+82.3	-243.9	-56.5
FD24-B-02	643342.7	955065.9	-33.3	60+01.7	-263.9	-59.3
FD24-B-03	644903.8	954968.8	-28.5	74+61.8	276.6	-60.5
FD24-B-04	646663.5	953725.5	-24.4	94+96.6	-413.7	-62.4
FD24-B-05	648476.7	954065.8	-36.1	112+30.8	-213.5	-60.1
FD24-B-06	650187.6	954731.2	-30.5	130+07.5	229.9	-49.1
FD24-B-07	651713.3	954490.3	-31.0	144+83.4	-225.6	-60.5
FD24-B-08	653153.8	955163.2	-25.2	160+04.9	235.5	-69.2
FD24-B-09	654693.6	954858.9	-28.6	174+98.6	-231.9	-60.7
FD24-B-10	657343.8	955679.3	-17.5	202+13.8	337.5	-60.0
FD24-B-11	658650.7	955766.9	-17.3	215+23.1	302.8	-59.9
FD24-B-12	659568.5	955379.1	-36.4	224+00.7	-169.0	-60.4
FD24-B-13	660674.7	955804.1	-34.1	235+07.2	258.4	-61.2
FD24-B-14	661622.6	955233.2	-33.1	244+95.2	-240.1	-61.1
FD24-B-15	662791.5	955175.7	-31.7	256+16.3	-245.60	-61.3
FD24-B-16	663859.7	955391.6	-34.2	266+19.3	-234.2	-60.0
FD24-B-17	664746.8	956025.9	-32.6	277+01.0	176.8	-60.7
FD24-B-18	666144.3	955439.9	-20.7	290+04.3	-596.4	-61.6
FD24-B-19	668042.5	956680.8	-38.7	312+59.2	367.0	-61.4
FD24-B-20	668739.3	956522.8	-30.8	317+03.3	-192.8	-62.3
FD24-CAD-01	656611.0	954152.9	-5.1	2+84.4	-238.6	-100.8
FD24-CAD-02	656869.4	954654.4	-9.0	5+90.1	235.5	-101.6
FD24-CAD-03	657210.7	954209.8	-4.5	8+86.7	-240.0	-101.0
FD24-CAD-04	657470.8	954704.6	-7.7	11+93.5	227.3	-103.0
FD24-CAD-05	657808.3	954261.7	-5.6	14+86.6	-246.2	-102.6
FD24-CAD-06	658062.2	954770.9	-8.5	17+88.6	236.0	-101.5
FD24-RC-01	643953.1	954939.9	-39.0	65+98.2	-121.9	-60.3
FD24-RC-02	648012.9	954452.4	-21.4	108+01.6	211.1	-57.6
FD24-RC-03	645964.0	954427.6	-28.7	86+92.3	165.5	-60.1
FD24-RC-04	646516.4	954612.2	-25.1	92+07.4	437.4	-60.6
FD24-RC-05	646697.0	954612.8	-25.4	93+85.5	467.3	-43.1
FD24-RC-05A	646706.8	954590.1	-25.4	93+98.9	446.5	-46.1
FD24-RC-05B	646699.7	954590.6	-25.7	93+91.7	445.8	-61.8
FD24-RC-06	645190.4	954887.4	-26.8	77+57.5	313.9	-57.8
FD24-RC-07	647931.6	954570.3	-15.4	107+30.6	335.6	-60.1
FD24-RC-08	647932.8	954162.6	-38.2	106+97.1	-70.8	-60.9
FD24-RC-09	648216.0	954554.1	-14.6	110+12.6	295.2	-73.9

Boring ID	Northing (ft)	Easting (ft)	Top of Hole EL	Station	Offset	Boring Termination EL
FD24-RC-10	646337.1	954627.1	-26.0	90+28.0	422.9	-60.9

5.1.1 SPT Overburden Sampling

All thirty-six (36) borings collected for the geotechnical investigation required SPT sampling methods for the overburden. No borings performed encountered bedrock at the surface. A CME-55 was mobilized onto the LB *Vision* platform, along with 3-in, 4-in, and 5-in casing for all water drilling activities. All spilt spoon (SPT) sampling methods were performed utilizing mud rotary drilling methods with a 4-in clay bit in soft, cohesive soils; and 4-in roller rock bit in sands and glacial till with NWJ drill rods. Continuous sampling procedures were conducted for locations in the channel where overburden was present on overlying bedrock to a target EL of -60 ft MLLW. The borings within the CAD cell, which required a termination target EL of -100 ft MLLW, were performed with 5 ft sampling intervals. Six rock core locations required 5 ft sampling intervals of the overburden to stabilize the two sets of casing, 4-inch and 3-inch, quicker than continuous sampling methods permitted. This was performed so that minimal compromise of the rock samples occurred during coring operations. For these borings, weather and/or wave conditions were bordering high-risk, and the length of time taken in order to setup and perform rock coring procedures was critical to minimize possible damage to the tooling, equipment, and the samples themselves. All SPT samples were collected in accordance with procedures outlined in ASTM D 1586, with a 140-lb automatic hammer with a 30-inch drop using a 2-inch diameter spilt spoon. The visual classification of soil samples retrieved from the split spoon were classified by field geologists in accordance with ASTM D2487 and ASTM D 2488, and specifically identified utilizing USCS. Samples were photographed prior to being placed in appropriately labeled soil jars. Identification of samples included project name, boring name, sample number, sample interval, blow counts, and total recovery.

All borings were logged by qualified field geologists and produced using an approved template as a modified version of USACE forms, ENG Form 1836 and 1836-A. Logs included start and ending dates, boring number, location, surface elevation, driller and inspector names, drilling details and methods used, listed by depth, sample number, classifications (including ASTM descriptions, moisture levels, color, density, estimated percentage of major and minor components), strata breaks, blow count data for the sample and casing drives, casing depths, sample recoveries, and other pertinent details of the drilling operations including drilling observations (rough drilling, chatter, rod drops, drill fluid, etc.) and any drilling fluid loss, location and quantity. The digitized borings logs can be viewed in Appendix B.

During project field operations, the soil boring location, FD24-B-06, was terminated earlier than its target elevation due to a last-minute request from local shipping pilots to move off the location along the edge of the existing channel toe. The LB *Vision* and crew were able to respond quickly and were off location under an hour from the request, prior to the ship's departure from the stationed sea buoy. The crew was given permission by USACE NAE to terminate the location and not reposition and re-drill since soil characterization of the material within the proposed dredge prism had met the maximum potential dredging limit of EL -44 ft MLLW.

1.1.2 Rock Coring

Ten (10) out of the thirty-six (36) borings required rock coring procedures that were performed with 4-inch casing as the outer casing vertical within the overburden on top the bedrock interface, with 3-inch casing stabilized within the 4-inch as an inner casing to provide a secondary seal for all wireline sample collection. The 3-inch casing was advanced just enough to minimize overburden material to flow between the casing and wireline barrels, but not advanced deeper than necessary to ensure collection of bedrock within the uppermost facies. An NQ-3 and NQ-2 inner core barrels were used with wireline winch line to receive the sample without lifting the advanced core barrel to minimize rock wall collapse or damage to the next sample interval for continuous and relatively seamless recovery. Each boring met the total recovery requirement of 80% during the initial attempt, with no need for an additional offset.

Bedrock was logged according to rock type, hardness, structure, degree of weathering, mineralization, discontinuities (angle of inclination measured from horizontal, planarity, roughness, aperture, infillings, coatings, mineralization, etc.). Percent recovery and Rock Quality Designation (RQD) was calculated in the field and recorded on the boring logs. Cores were securely placed in 5-foot-long wooden core boxes, with boring number, date, core run numbers, recovery, and RQD noted on the attached core box cover. All cores were immediately photographed once the core box was full and included the information on the core box cover, and a scale. Spacers, such as wooden blocks, were used to separate core runs, and bubble wrap was used for zones of core loss, and to secure the core against shifting during transport in accordance with procedures of ASTM D 5079.

During project field operations, rock core boring FD24-RC-05, required two additional offset attempts due to rig equipment failure during drilling. The location FD24-RC-05B was able to successfully meet the boring termination requirements, and boring log FD24-RC-05 COMBO, represents the overburden material encountered at FD24-RC-05 and FD24-RC-05A, integrated with the sediments and rock encountered at FD24-RC-05B. On the last day of drilling, the crew was able to complete both remaining rock core locations, FD24-RC-02 and FD24-RC-06. However, FD24-RC-06 was terminated 2.2 ft shallower than EL -60 ft MLLW due to the wave height increasing while on location and the increased need to remove tooling in order to minimize any potential of equipment damage during drilling. This location was south of the Southwest Ledge Light breakwater, so it was more exposed to the influence of waves comparatively to locations behind, or north, of the breakwater. The second location performed that day, FD24-RC-02, was terminated 2.4 ft shallower than EL -60 ft MLLW, due to the NQ double swivel inner barrel being compromised with no immediate comparable replacement onboard.

Rock Core location FD24-RC-09 was positioned in an area with the most ambiguity within the geophysical data set, due to the high organic estuary marsh silts and clays creating a gaseous layer making it difficult for the sensors to provide clear results. It was decided that there was a need for one core location to help define the reverse fault line presented on the Bedrock Geologic Map of Connecticut (USGS, 1985) and within the geophysical data collected for this investigation. At the time of the investigation, the Cross Sound Cable company provided their most recent jet probe investigative results in this area, and the location was moved to JPR-222, that had noted refusal on bedrock at EL -45.8 ft MLLW. During drilling operations, a very loose silty sand layer was encountered, with wood fragments in the spoon at this elevation, and underneath was a very dense clayey sand layer. The field crew attempted to continue drilling until the bedrock surface was met with roller bit and spoon refusal, however, the boring was terminated at EL -73.9 ft MLLW due to wave height increasing during operations.

5.2 Lab Procedures

5.2.1 Laboratory Methods

Periodically throughout the project, the site inspector would deliver available samples during inclement weather days to CDM Smith's Geotechnical Laboratory located in Chelmsford, Massachusetts. A total of one hundred four (104) soil samples were selected for the required soil analyses. Table 18 and Table 19 below provide a breakdown for how many methods were performed. For the rock cores, a total of twenty-two (22) samples were selected for the required rock analyses outlined in the rock testing plan.

Table 18. Soil Laboratory Tests

Soil Laboratory Test Method	Total Samples Submitted
Standard Test Method for Particle-Size Distribution (Gradation) of Soils Using Sieve Analysis; [ASTM D6913-04 (2017) and ASTM D422-63 (2014)]	54
Standard Test Method for Particle-Size Distribution (Gradation) of Fine-Grained Soils Using the Sedimentation (Hydrometer) Analysis; [ASTM D7928-17 (2021) and ASTM D1140-17 (2017)]	50
Standard Test Methods for Liquid Limit, Plastic Limit, and Plasticity Index of Soils (Atterberg Limits); [ASTM D 4318-00 (2018)]	35
Standard Test Method for Laboratory Determination of Water (Moisture) Content of Soil and Rock by Mass; [ASTM D2216-98 (2019)]	104

Table 19. Rock Laboratory Tests

Rock Laboratory Test & Method	Total Samples Submitted
Unconfined Compressive Strength w/ Young's Modulus (ASTM D7012, Method D, and ASTM D 3148; core preparation by ASTM D 4543)	21
Point Load Index (ASTM D 5731)	18
Splitting Tensile Strength (Brazilian) (ASTM D 3967)	27
Cerchar Abrasivity Index (CAI) (ASTM D7625-10)	18
Total Hardness	18
Unit Weight & Classification	21
Petrographic Analysis (ISRM procedures)	18
Acoustic Velocity	21

1.1.2 Sediment Laboratory Results

One hundred-four (104) samples collected from 36 boring locations were submitted for moisture content (104), grain size (54), hydrometer (50), and Atterberg limits (35). A summary table for laboratory results for the soil overburden material can be reviewed in Table 20 below, Figure 37 below presents the soil lab results as gradation distribution vs. sample elevation; for an in-depth review, the gradation curves and Atterberg graphs can be found in Appendix C. A summary of the results are as follows:

- The samples of the surficial estuary marsh were classified as high plasticity, organic silts and clays and determined by calculating the liquid limit from the Atterberg tests per ASTM D 2487, and not by loss of ignition.
- The samples encountered beneath the organic sediments were predominantly sands, grading into silty sands with interbedded layers of silts.
- None of the samples submitted were classified as gravel, however, 33 samples had a gravel percentage ranging from 0.1 to 31.4.
- The silts and clays had a liquid limit range from 33 to 151, a plastic limit range from 23 to 65, and a plasticity index range of 9 to 86.
- Out of 104 samples, 53 were classified as poorly graded sands, with varying degrees of silt content and the remaining 51 were classified as silts and clays with varying degrees of plasticity and organics.

Table 20. Soil Laboratory Results

Boring ID	Sample Depth(ft)	Grain Size Analysis			Moisture Content %	Liquid Limit %	Plastic Limit %	Plasticity Index %	USCS Lab Classification
		Gravel %	Sand %	Fines %					
FD24-B-01	2.0-4.0	0.1	91.7	8.2	18.1	-	-	-	SP-SM
FD24-B-01	10.0-12.0	3.3	78.3	18.4	30.8	-	-	-	SM
FD24-B-01	12.5-14.0	0.2	97.0	2.8	24.4	-	-	-	SP
FD24-B-01	16.0-18.0	0.0	3.9	96.1	96.9	117	59	58	OH
FD24-B-02	2.0-4.0	0.0	94.5	5.5	26.0	-	-	-	SP-SM
FD24-B-02	10.0-12.0	0.0	85.7	14.3	27.8	-	-	-	SM
FD24-B-02	18.0-20.0	0.0	88.5	11.5	23.8	-	-	-	SP-SM
FD24-B-03	2.0-4.0	1.0	84.0	15.0	33.7	-	-	-	SM
FD24-B-03	14.0-16.0	11.1	75.1	13.8	30.4	-	-	-	SM
FD24-B-04	2.0-4.0	0.5	92.3	7.2	19.0	-	-	-	SP-SM
FD24-B-04	8.0-10.0	0.0	58.6	41.4	25.2	-	-	-	SM
FD24-B-04	16.0-18.0	0.0	23.5	76.5	28.0	-	-	-	ML
FD24-B-04	28.0-30.0	0.0	3.3	96.7	37.4	-	-	-	ML/OH
FD24-B-05	2.0-4.0	2.0	91.2	6.8	21.4	-	-	-	SP-SM
FD24-B-05	6.0-8.0	1.4	97.2	1.4	19.0	-	-	-	SP
FD24-B-06	4.6-6.6	0.0	0.6	99.4	102.2	106	47	59	OH
FD24-B-06	12.6-14.6	0.0	1.6	98.4	114.5	132	49	83	OH
FD24-B-07	2.0-4.0	0.0	10.3	89.7	114.4	106	48	58	OH
FD24-B-07	15.5-17.5	0.0	56.3	43.7	38.9	33	24	9	SM
FD24-B-07	21.5-23.5	0.6	95.9	3.5	24	-	-	-	SP
FD24-B-08	2.0-4.0	0.0	10.6	89.4	90.7	88	39	49	OH
FD24-B-08	10.0-12.0	0.3	92.5	7.2	17.4	-	-	-	SP-SM
FD24-B-08	16.0-18.0	26.6	69.9	3.5	13.1	-	-	-	SP
FD24-B-08	20.0-22.0	0.2	78.5	21.3	24.5	-	-	-	SM
FD24-B-08	32.0-34.0	0.0	51.6	48.4	25.4	-	-	-	SM
FD24-B-09	3.8-5.8	0.0	8.5	91.5	106.8	102	42	60	OH
FD24-B-09	9.8-11.8	0.0	12.9	87.1	71.7	77	34	43	OH
FD24-B-09	24.1-26.1	0.8	92.3	6.9	17.3	-	-	-	SP-SM
FD24-B-10	2.0-4.0	0.0	7.9	92.1	92.2	92	42	50	OH
FD24-B-10	8.2-10.2	0.0	2.6	97.4	127.1	108	44	64	OH
FD24-B-10	24.2-26.2	0.0	89.5	10.5	20.5	NP	NP	NP	SP-SM
FD24-B-10	30.5-32.5	10.6	85.5	3.9	15.1	-	-	-	SP
FD24-B-11	7.4-9.4	0.0	4.9	95.1	113.7	108	44	64	OH
FD24-B-11	21.4-23.4	0.0	45.2	54.8	45.3	41	24	17	CL
FD24-B-11	26.6-28.6	7.0	87.4	5.6	17.5	-	-	-	SP-SM
FD24-B-11	37.0-38.6	0.0	46.9	53.1	23.7	-	-	-	ML
FD24-B-12	2.0-4.0	0.0	28.8	71.2	38.5	NP	NP	NP	ML
FD24-B-12	6.0-8.0	0.7	94.2	5.1	22.6	-	-	-	SP-SM
FD24-B-12	12.0-14.0	21.4	69.9	8.7	16.2	-	-	-	SW-SM
FD24-B-12	16.0-18.0	0.0	3.9	96.1	28.4	NP	NP	NP	ML
FD24-B-13	0.0-2.0	0.0	1.8	98.2	117.0	95	44	51	OH
FD24-B-13	4.9-6.9	0.0	91.2	8.8	24.2	-	-	-	SP-SM
FD24-B-13	8.6-10.6	0.0	65.6	34.4	25.9	-	-	-	SM

Boring ID	Sample Depth(ft)	Grain Size Analysis			Moisture Content %	Liquid Limit %	Plastic Limit %	Plasticity Index %	USCS Lab Classification
		Gravel %	Sand %	Fines %					
FD24-B-13	17.0-19.0	0.0	10.4	89.6	27.9	-	-	-	ML
FD24-B-14	2.0-4.0	0.0	1.2	98.8	146.2	113	46	67	OH
FD24-B-15	12.0-14.0	0.0	62.2	37.8	27.4	-	-	-	SM
FD24-B-15	16.0-18.0	12.4	77.1	10.5	16.3	-	-	-	SP-SM
FD24-B-15	22.0-24.0	0.0	27.6	72.4	23.7	-	-	-	ML
FD24-B-15	3.7-5.7	0.0	3.0	97.0	134.0	119	51	68	OH
FD24-B-15	11.6-13.6	17.3	80.0	2.7	18.0	-	-	-	SP
FD24-B-15	17.6-19.6	0.0	44.7	55.3	28.5	-	-	-	ML
FD24-B-16	2.0-4.0	0.0	6.4	93.6	115.2	120	54	66	OH
FD24-B-16	8.0-10.0	0.0	28.9	71.1	25.0	-	-	-	ML
FD24-B-16	19.8-21.8	0.0	30.4	69.6	27.3	-	-	-	ML
FD24-B-17	0.0-2.0	0.0	1.3	98.7	179.6	119	51	68	OH
FD24-B-17	10.1-12.1	0.0	20.3	79.7	124.9	-	-	-	OL
FD24-B-17	18.1-20.1	0.0	86.8	13.2	29.6	-	-	-	SM
FD24-B-18	3.9-5.9	0.0	1.0	99.0	134.9	117	55	62	OH
FD24-B-18	18.9-20.9	0.0	2.0	98.0	110.2	151	65	86	OH
FD24-B-18	33.9-35.9	0.0	70.9	29.1	26.3	-	-	-	SM
FD24-B-19	4.7-6.7	0.0	91.3	8.7	31.1	NP	NP	NP	SP-SM
FD24-B-19	6.7-8.7	0.0	57.2	42.8	23.5	-	-	-	SM
FD24-B-20	4.5-6.5	0.0	4.8	95.2	167.3	121	63	58	OH
FD24-B-20	14.5-16.5	0.0	13.5	86.5	128.0	96	43	53	OH
FD24-B-20	19.5-21.5	31.4	50.0	18.6	15.8	-	-	-	SM
FD24-B-20	24.5-26.5	0.0	92.8	7.2	20.4	-	-	-	SP-SM
FD24-B-20	29.5-31.5	0.0	72.0	28.0	20.6	-	-	-	SM
FD24-CAD-01	9.2-10.7	0.0	90.9	9.1	19.3	-	-	-	SP-SM
FD24-CAD-01	14.2-16.2	0.0	27.6	72.4	66.0	-	-	-	OH
FD24-CAD-01	29.2-31.2	0.0	28.0	72.0	66.2	-	-	-	OH
FD24-CAD-01	44.2-46.2	0.7	93.7	5.6	19.7	-	-	-	SP-SM
FD24-CAD-02	20.3-22.3	0.0	8.3	91.7	104.0	-	-	-	OH
FD24-CAD-02	40.6-42.6	0.2	94.5	5.3	21.1	NP	NP	NP	SP-SM
FD24-CAD-02	50.6-52.6	0.0	10.5	89.5	29.7	NP	NP	NP	ML
FD24-CAD-02	70.6-72.6	0.0	0.8	99.2	35.6	-	-	-	ML
FD24-CAD-03	4.5-6.5	1.0	94.2	4.8	22.4	NP	NP	NP	SP
FD24-CAD-03	14.5-16.5	0.0	8.5	91.5	67.5	-	-	-	OH
FD24-CAD-03	29.5-31.5	0.0	13.3	86.7	77.4	-	-	-	OH
FD24-CAD-03	44.5-46.5	12.1	81.1	6.8	16.6	NP	NP	NP	SP-SM
FD24-CAD-04	15.8-17.8	0.0	6.4	93.6	91.2	112	42	70	OH
FD24-CAD-04	41.7-42.8	7.9	87.0	5.1	15.9	-	-	-	SP-SM
FD24-CAD-04	63.3-65.3	0.0	0.8	99.2	36.7	44	23	21	CL
FD24-CAD-04	73.3-75.3	0.0	7.8	92.2	28.4	-	-	-	ML
FD24-CAD-05	6.0-8.0	0.0	35.1	64.9	51.3	73	31	42	OH
FD24-CAD-05	35.0-37.0	0.0	19.9	80.1	99.3	82	39	43	OH
FD24-CAD-05	40.0-42.0	0.5	93.6	5.9	23.6	-	-	-	SP-SM
FD24-CAD-05	55.0-57.0	0.0	29.1	70.9	24.6	-	-	-	ML

Boring ID	Sample Depth(ft)	Grain Size Analysis			Moisture Content %	Liquid Limit %	Plastic Limit %	Plasticity Index %	USCS Lab Classification
		Gravel %	Sand %	Fines %					
FD24-CAD-06	5.7-7.7	0.0	8.6	91.4	101.8	89	43	46	OH
FD24-CAD-06	25.7-27.7	0.0	9.1	90.9	89.5	104	39	65	OH
FD24-CAD-06	40.7-42.7	4.3	88.8	6.9	19.3	-	-	-	SP-SM
FD24-CAD-06	56.0-58.0	0.0	3.3	96.7	29.5	-	-	-	ML
FD24-RC-01	1.7-3.7	0.2	97.0	2.8	23.8	-	-	-	SP
FD24-RC-02	5.7-7.1	0.4	31.3	68.3	89.2	-	-	-	ML
FD24-RC-03	2.0-3.9	0.0	81.1	18.9	26.8	-	-	-	SM
FD24-RC-03	7.9-9.9	12.6	82.4	5.0	17.4	-	-	-	SP-SM
FD24-RC-04	2.0-4.0	0.7	91.8	7.5	21.9	-	-	-	SP-SM
FD24-RC-05	5.7-7.7	1.6	75.5	22.9	28.9	-	-	-	SM
FD24-RC-05	13.7-15.7	0.0	26.8	73.2	19.6	-	-	-	ML
FD24-RC-06	2.3-4.3	0.7	70.4	28.9	33.5	-	-	-	SM
FD24-RC-07	5.5-7.5	0.0	11.2	88.8	123.5	114	44	70	OH
FD24-RC-07	15.5-17.5	0.0	83.9	16.1	17.8	-	-	-	SM
FD24-RC-09	8.3-10.3	0.0	8.9	91.1	155.8	95	44	51	OH
FD24-RC-09	22.3-24.3	0.0	85.8	14.2	20.4	-	-	-	SM
FD24-RC-10	3.7-5.7	0.0	90.8	9.2	24.9	-	-	-	SP-SM

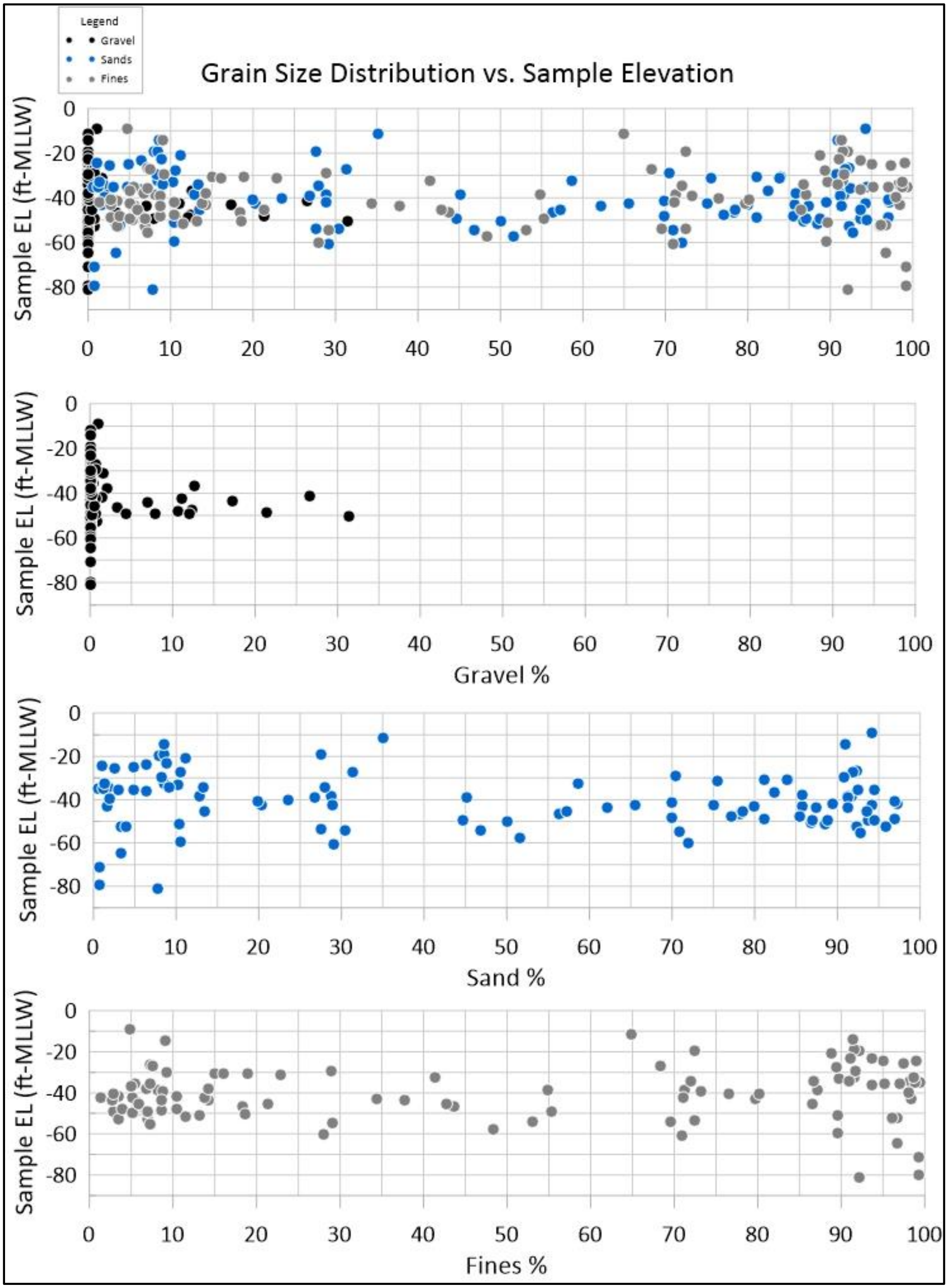

Figure 37. Sample Grain Size Distribution vs Sample Elevation

5.2.1 Rock Coring Data and Laboratory Results

Rock Quality Designation (RQD) was measured and determined in the field at the nine (9) rock core locations where bedrock was encountered. Location FD24-RC-09 has no rock analysis performed since bedrock was not encountered. RQD was calculated by dividing the sum of the recovered, intact pieces of 4-inches or greater in length by the total length of the run and expressed as a percentage for each run. Sections of the recovered core with vertical fractures were considered in the calculation if the section was 4-inches or greater in length.

Table 21. Rock Quality Designation

RQD	Rating
0-25%	Very Poor
25-50%	Poor
50-75%	Fair
75-90%	Good
90-100%	Excellent

Please note, that the RQD ratings presented in Table 21 are an estimated range and only reflect RQD where boring data was collected. Any interpretation between boring locations was variable to onsite conditions. The summary Table 22 provides recovery and RQD results for all runs performed at 9 boring locations. Figure 38 and Figure 39 present the RQD results sequentially, and verses top of core run elevation, respectively. The following observations were made:

- The predominant rock type was metamorphosed granite schist that was observed to be generally vertically fractured with some horizontal jointing.
- Core recoveries varied from 60% to 100% for individual runs, with an average total recovery of 93% for the 9 rock core borings.
- RQDs relatively varied between locations, with an average RQD of 86%.
- The core recovery and RQD results were of generally high standards expected for the coring locations where igneous metamorphic bedrock was encountered.

Table 22. Rock Coring Data

Boring ID	Coring Run Number	Sample Depth (ft)	Elevation (ft, MLLW)	Predominant Rock Type	Recovery (%)	RQD (%)
FD24-RC-01	Run 1	15.3-21.3	-54.3 to -60.3	Altered Granite Schist	85	82/Good
FD24-RC-02	Run 1	26.4-30.0	-47.8 to -51.4	Altered Granite Schist	80	37/Poor
	Run 2	30.0-36.2	-51.4 to -57.6	Altered Granite Schist	100	61/Fair
FD24-RC-03	Run 1	13.4-15.4	-42.1 to -44.1	Altered Granite Schist	95	50/Fair
	Run 2	15.4-18.4	-44.1 to -47.1	Altered Granite Schist	90	30/Poor
	Run 3	18.4-23.4	-47.1 to -52.1	Altered Granite Schist	94	68/Fair
	Run 4	23.4-28.4	-52.1 to -57.1	Altered Granite Schist	98	96/Excellent
	Run 5	28.4-31.4	-57.1 to -60.1	Altered Granite Schist	60	23/Very poor
FD24-RC-04	Run 1	8.0-13.0	-33.1 to -38.1	Altered Granite Schist	100	66/Fair
	Run 2	13.0-18.0	-38.1 to -43.1	Altered Granite Schist	94	70/Fair
	Run 3	18.0-23.0	-43.1 to -48.1	Altered Granite Schist	96	74/Fair
	Run 4	23.0-28.0	-48.1 to -53.1	Altered Granite Schist	96	88/Good
	Run 5	28.0-33.0	-53.1 to -58.1	Altered Granite Schist	100	98/Excellent
	Run 6	33.0-35.5	-58.1 to -60.6	Altered Granite Schist	80	80/Good
FD24-RC-05B	Run 1	21.1-26.1	-46.8 to -51.8	Altered Granite Schist	84	40/Poor

Boring ID	Coring Run Number	Sample Depth (ft)	Elevation (ft, MLLW)	Predominant Rock Type	Recovery (%)	RQD (%)
FD24-RC-05B	Run 2	26.1-31.1	-51.8 to -56.8	Altered Granite Schist	84	54/Fair
	Run 3	31.1-36.1	-56.8 to 61.8	Altered Granite Schist	92	68/Fair
FD24-RC-06	Run 1	6.0-11.0	-32.8 to -37.8	Altered Granite Schist	100	80/Good
	Run 2	11.0-16.0	-37.8 to -42.8	Altered Granite Schist	94	88/Good
	Run 3	16.0-21.0	-42.8 to -47.8	Altered Granite Schist	100	72/Fair
	Run 4	21.0-26.0	-47.8 to -52.8	Altered Granite Schist	100	88/Good
	Run 5	26.0-31.0	-52.8 to -57.8	Altered Granite Schist	88	84/Good
FD24-RC-07	Run 1	19.7-24.7	-35.1 to -40.1	Altered Granite Schist	94	84/Good
	Run 2	24.7-28.7	-40.1 to -44.1	Altered Granite Schist	100	93/Excellent
	Run 3	28.7-34.7	-44.1 to -50.1	Altered Granite Schist	97	80/Good
	Run 4	34.7-39.7	-50.1 to -55.1	Altered Granite Schist	98	96/Excellent
	Run 5	39.7-44.7	-55.1 to -60.1	Altered Granite Schist	100	84/Good
FD24-RC-08	Run 1	4.9-9.7	-43.1 to -47.9	Altered Granite Schist	85	60/Fair
	Run 2	9.7-14.7	-47.9 to -52.9	Altered Granite Schist	90	74/Fair
	Run 3	14.7-18.7	-52.9 to -56.9	Altered Granite Schist	85	40/Poor
	Run 4	18.7-22.7	-56.9 to -60.9	Altered Granite Schist	95	73/Fair
FD24-RC-10	Run 1	7.7-12.7	-33.7 to -38.7	Altered Granite Schist	96	12/Very Poor
	Run 2	12.7-17.7	-38.7 to -43.7	Altered Granite Schist	100	66/Fair
	Run 3	17.7-22.7	-43.7 to -48.7	Altered Granite Schist	100	76/Good
	Run 4	22.7-27.7	-48.7 to -53.7	Altered Granite Schist	98	92/Excellent
	Run 5	27.7-32.7	-53.7 to -58.7	Altered Granite Schist/Quartz-Biotite-Plagioclase Schist	98	84/Good
	Run 6	32.7-34.9	-58.7 to -60.9	Altered Granite Schist/Quartz-Biotite-Plagioclase Schist	100	64/Fair

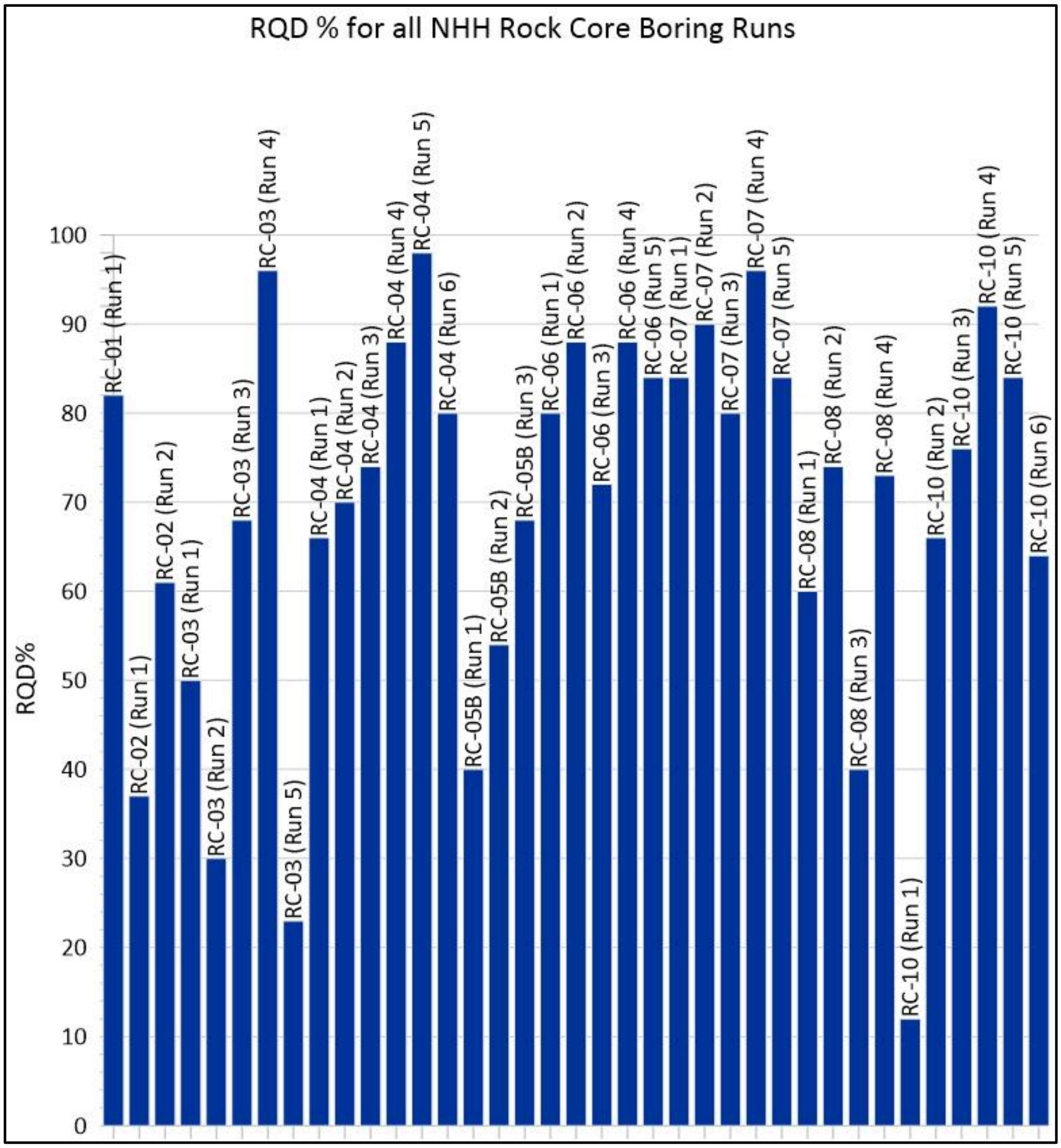

Figure 38. RQD Percentages for Individual Rock Core Runs

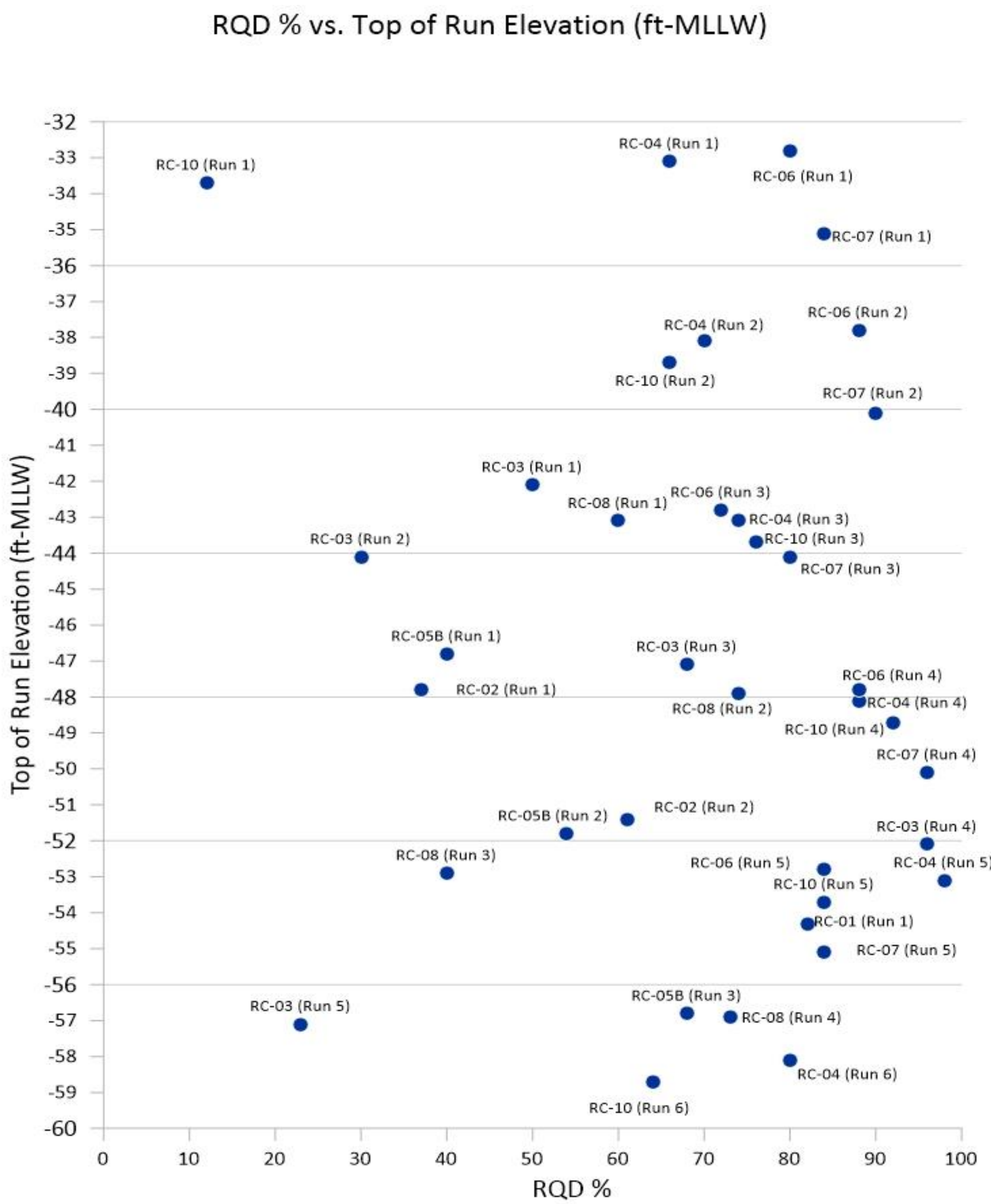

Figure 39. RQD % vs Top of Core Run Elevation (ft-MLLW)

A total of eighteen (18) samples were submitted for petrographic analysis to Spectrum Petrographics, Inc. located in Vancouver, WA. A summary of their results can be viewed in Table 23. Petrographic Analysis. The following observations were noted:

- The predominant rock type recovered was granite as the parent material bedrock and defined as a schist for its metamorphic grade, therefore being defined as Altered Granite Schist.
- One sample was determined to be a fully metamorphosed schist with biotite (20%), quartz (20%), and plagioclase (60%) being the primary mineralogical composition.

- A varying amount of minor mineral constituents were noted during analysis which were biotite (<1% to 8%), muscovite/sericite (<1% to 2%), smectite (<1% to 2%), chlorite (<1% to 2%), apatite (<1%), opaques (<1%), zircon (<1%), carbonate (<1%), leucoxene (<1%), and sphene (<1%).

Table 23. Petrographic Analysis

Boring ID	Sample Depth (ft)	Elevation (FT MLLW)	Quartz %	Alkali-feldspar %	Plagioclase %	Predominant Rock Type
FD24-RC-01	16.9-17.0	-55.9 to -60.0	31	32	30	Altered Granite Schist
FD24-RC-01	19.9-20.1	-58.9 to -59.1’	29	35	31	Altered Granite Schist
FD24-RC-02	27.3-27.4	-48.7’ to -48.8’	31	32	30	Altered Granite Schist
FD24-RC-02	35.0-35.1	-56.4 to -56.5	32	39	25	Altered Granite Schist
FD24-RC-03	16.0-16.1	-44.7 to -44.8	35	41	20	Altered Granite Schist
FD24-RC-03	19.9-20.2	-48.6 to -48.9	32	32	32	Altered Granite Schist
FD24-RC-04	16.9-17.0	-41.7 to -41.8	41	41	17	Altered Granite Schist
FD24-RC-04	21.4-21.5	-46.5 to -46.6	31	37	24	Altered Granite Schist
FD24-RC-05B	29.8-30.0	-55.5 to -55.7	29	43	22	Altered Granite Schist
FD24-RC-05B	32.5-32.6	-58.2 to -58.3	32	32	27	Altered Granite Schist
FD24-RC-06	9.2-9.3	-36.0 to -36.1	33	33	33	Altered Granite Schist
FD24-RC-06	24.6-24.7	-51.4 to -51.5	44	44	9	Altered Granite Schist
FD24-RC-07	21.1-21.2	-36.5 to -36.6	30	31	30	Altered Granite Schist
FD24-RC-07	29.1-29.3	-44.5 to -44.7	28	56	9	Altered Granite Schist
FD24-RC-08	8.9-9.0	-47.1 to -47.2	26	53	18	Altered Granite Schist
FD24-RC-08	21.1-21.2	-59.3 to -59.4	34	55	7	Altered Granite Schist
FD24-RC-10	17.4-17.6	-43.4 to -43.6	44	44	7	Altered Granite Schist
FD24-RC-10	26.0-26.1	-52.0 to -52.1	20%	N/A	60%	Biotite-Quartz-Plagioclase Schist

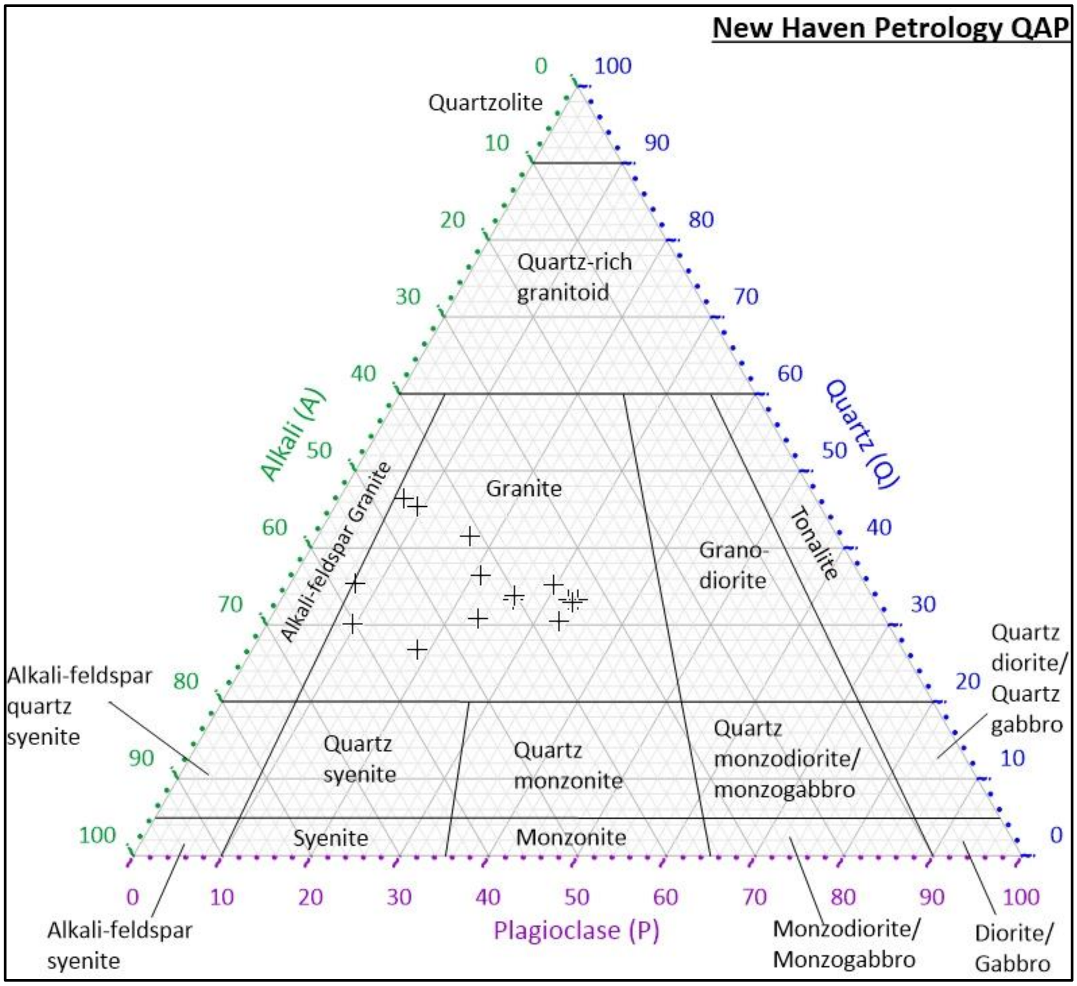

Figure 40. Petrographic Analysis Plotted on QAP Igneous Diagram. All Samples are depicted with a "+." All samples were located within the "Granite" classification area.

Twenty-one (21) rock core samples were submitted for Unconfined Compressive Strength (UCS) with Young's Modulus, including bulk density. The results are summarized below in Table 24, and the full laboratory report can be reviewed in Appendix C.

- Bulk density values showed very little variation, ranging from 162.6 to 173.3 pounds per cubic foot (lb/ft³).
- UCS results had a variable range of strengths from 8,860 to 27,190 pounds per square inch (psi).
- Double shear failure was observed in 13 of 21 samples, single plane shear failure was observed in 4 of 21 samples, Y-shaped shear or failure was observed in 2 of 21 samples, one sample was observed to have axial splitting, and one sample failed along a foliation plane.

Table 24. UCS Results, Bulk Density, and Failure Type

Boring ID	Depth of Sample (ft)	Elevation (ft MLLW)	Bulk Density (lb/ft^3)	Failure Stress (psi)	Failure Type
FD24-RC-01	15.9-16.2	-54.9 to -55.2	163.7	18,690	Double Shear
	18.2-18.5	-57.2 to -57.5	165.0	21,470	Double Shear
FD24-RC-02	35.4-35.7	-56.8 to -57.1	164.0	15,560	Single Plane Shear
FD24-RC-03	17.1-17.4	-45.8 to -46.1	163.4	8,860	Axial Splitting
	20.8-21.0	-49.5 to -49.7	163.9	21,040	Single Plane Shear
FD24-RC-04	16.0-16.3	-41.1 to -41.4	163.9	27,190	Double Shear
	20.7-21.1	-45.8 to -46.2	164.0	12,060	Single Plane Shear
FD24-RC-05B	28.7-29.0	-54.4 to -54.7	164.9	21,270	Double Shear
	31.6-31.9	-57.3 to -57.6	165.1	24,580	Double Shear
FD24-RC-06	10.0-10.3	-36.8 to -37.1	163.2	17,120	Double Shear
	14.7-15.0	-41.5 to -41.8	163.2	22,510	Double Shear
	23.7-23.9	-50.5 to -50.7	164.2	21,240	Double Shear
	24.9-25.2	-51.7 to -52.0	163.2	19,760	Single Plane Shear
FD24-RC-07	20.2-20.5	-35.6 to -35.9	164.6	23,800	Double Shear
	29.8-30.2	-45.2 to -45.6	165.0	21,430	Double Shear
FD24-RC-08	7.9-8.2	-46.1 to -46.4	162.6	24,220	Double Shear
	13.3-13.6	-51.5 to -51.8	163.3	23,140	Double Shear
	20.0-20.4	-58.2 to –58.6	163.4	15,480	Y-Shaped Shear
FD24-RC-10	16.7-17.0	-42.7 to -43.0	163.8	20,670	Double Shear
	26.7-27.0	-52.7 to -53.0	173.3	12,450	Failed Along Foliation
	29.6-29.9	-55.6 to -55.9	162.9	16,550	Y-Shaped Failure

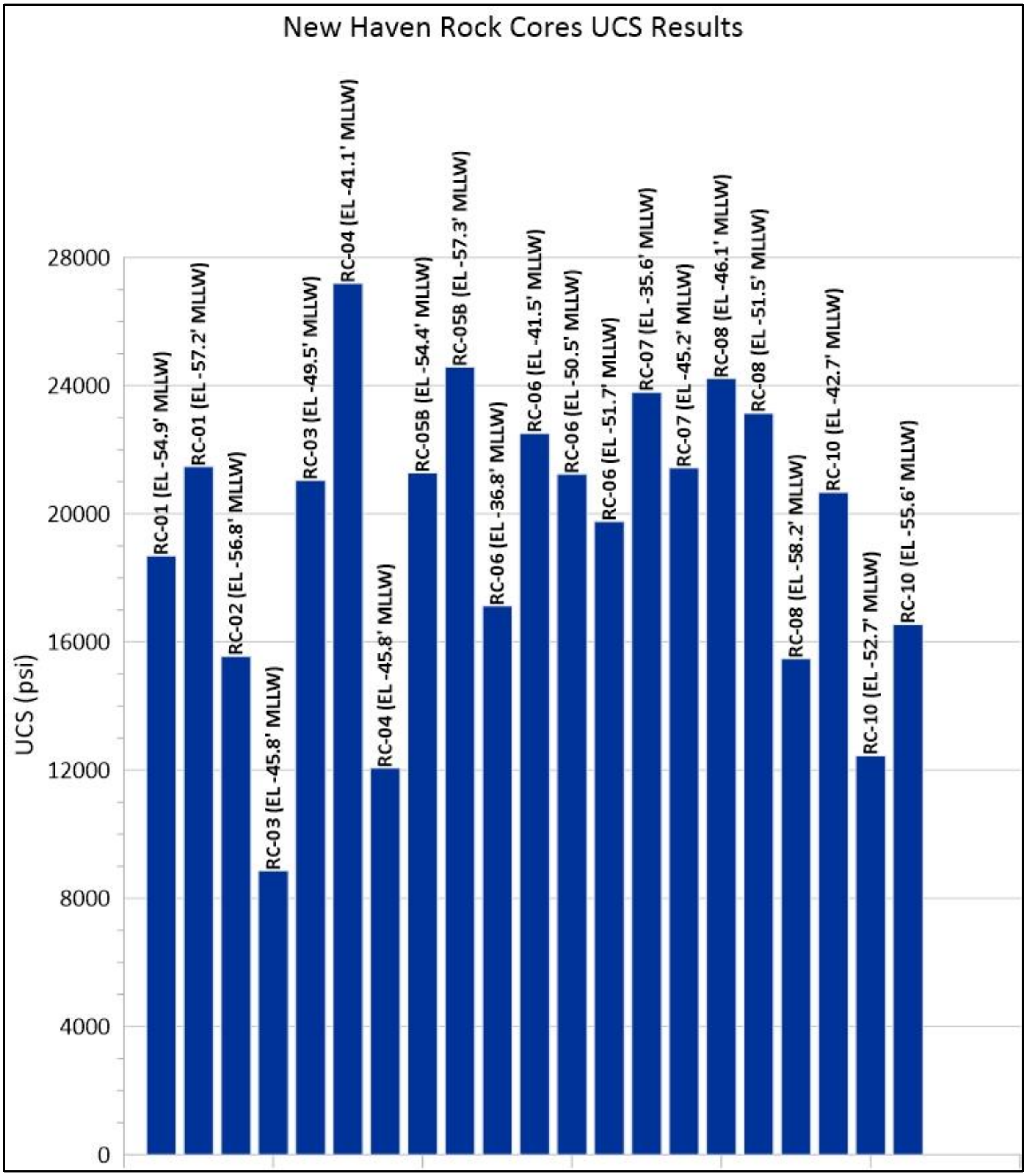

Figure 41. Unconfined Compressive Strength Results

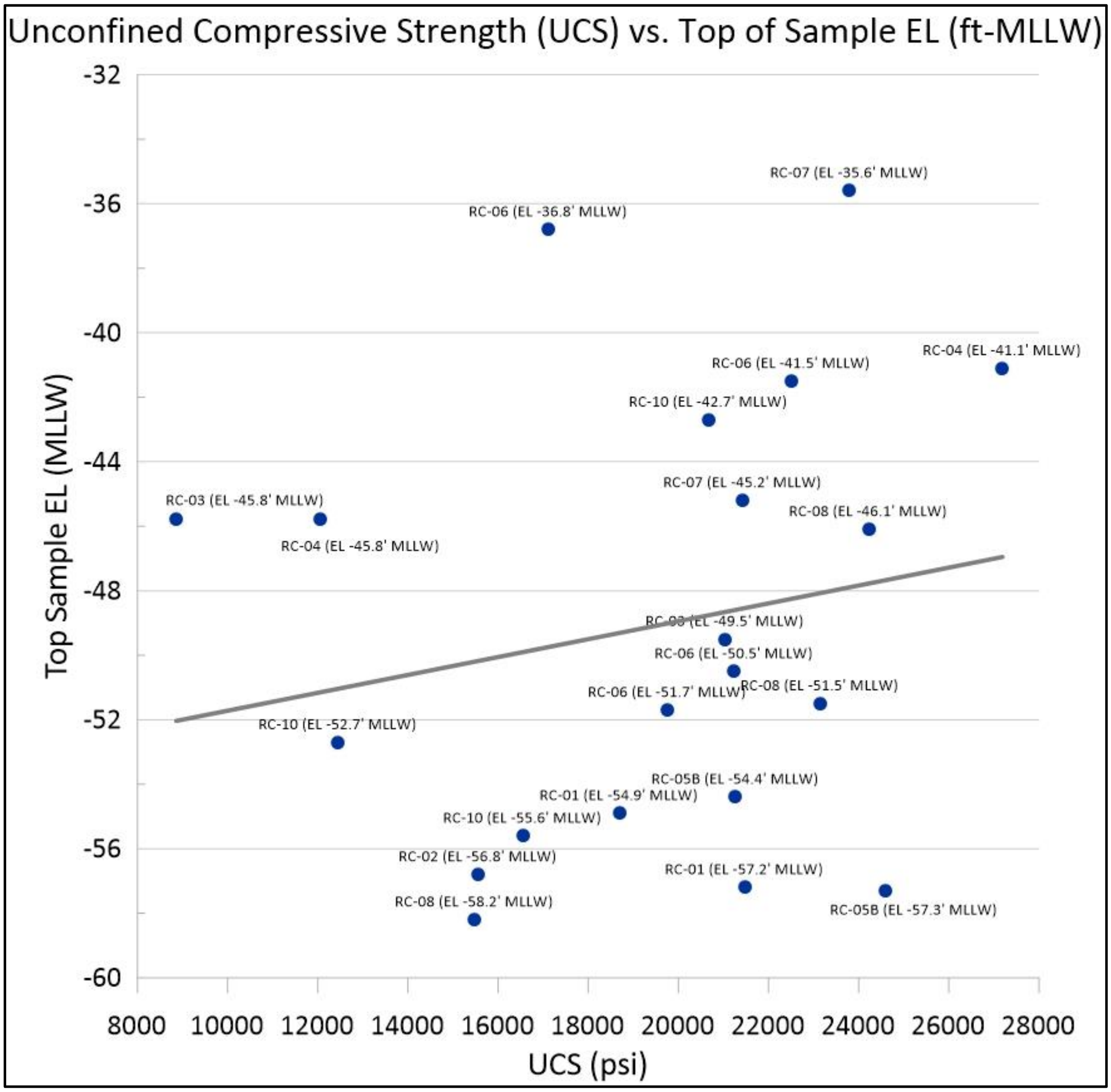

Figure 42. Unconfined Compressive Strength Results (psi) vs Top of Sample Elevation (ft-MLLW)

For the Young's Modulus performed by the CDM Smith Laboratory, summarized results are present in Table 25, where the following observations were noted:

- Young's Modulus values at failure ranged from 4,067,100 psi to 30,472,400 psi, and Poisson's Ratio values at failure ranged from 0.22 to 3.90.

Table 25. UCS Results, Young's Modulus, and Poisson's Ratio

Boring ID	Depth of Sample (ft)	Elevation (ft MLLW)	Failure Stress (psi)	Young's Modulus (psi)	Poisson's Ratio
FD24-RC-01	15.9-16.2	-54.9 to -55.2	18,690	5,915,900	0.78
	18.2-18.5	-57.2 to -57.5	21,470	7,144,100	0.60
FD24-RC-02	35.4-35.7	-56.8 to -57.1	15,560	5,282,700	0.73
FD24-RC-03	17.1-17.4	-45.8 to -46.1	8,860	5,375,700	2.95

Boring ID	Depth of Sample (ft)	Elevation (ft MLLW)	Failure Stress (psi)	Young's Modulus (psi)	Poisson's Ratio
FD24-RC-03	20.8-21.0	-49.5 to -49.7	21,040	7,815,400	1.69
FD24-RC-04	16.0-16.3	-41.1 to -41.4	27,190	30,472,400	2.56
	20.7-21.1	-45.8 to -46.2	12,060	8,900,200	3.62
FD24-RC-05B	28.7-29.0	-54.4 to -54.7	21,270	9,149,200	0.29
	31.6-31.9	-57.3 to -57.6	24,580	6,227,900	0.33
FD24-RC-06	10.0-10.3	-36.8 to -37.1	17,120	4,679,000	0.71
	14.7-15.0	-41.5 to -41.8	22,510	7,605,600	0.60
	23.7-23.9	-50.5 to -50.7	21,240	7,734,900	0.68
	24.9-25.2	-51.7 to -52.0	19,760	10,323,500	2.53
FD24-RC-07	20.2-20.5	-35.6 to -35.9	23,800	9,036,300	1.30
	29.8-30.2	-45.2 to -45.6	21,430	8,137,300	0.70
FD24-RC-08	7.9-8.2	-46.1 to -46.4	24,220	8,045,800	0.22
	13.3-13.6	-51.5 to -51.8	23,140	27,344,000	1.05
	20.0-20.4	-58.2 to –58.6	15,480	11,339,200	3.90
FD24-RC-10	16.7-17.0	-42.7 to -43.0	20,670	9,775,200	1.44
	26.7-27.0	-52.7 to -53.0	12,450	4,067,100	0.32
	29.6-29.9	-55.6 to -55.9	16,550	11,057,300	1.37

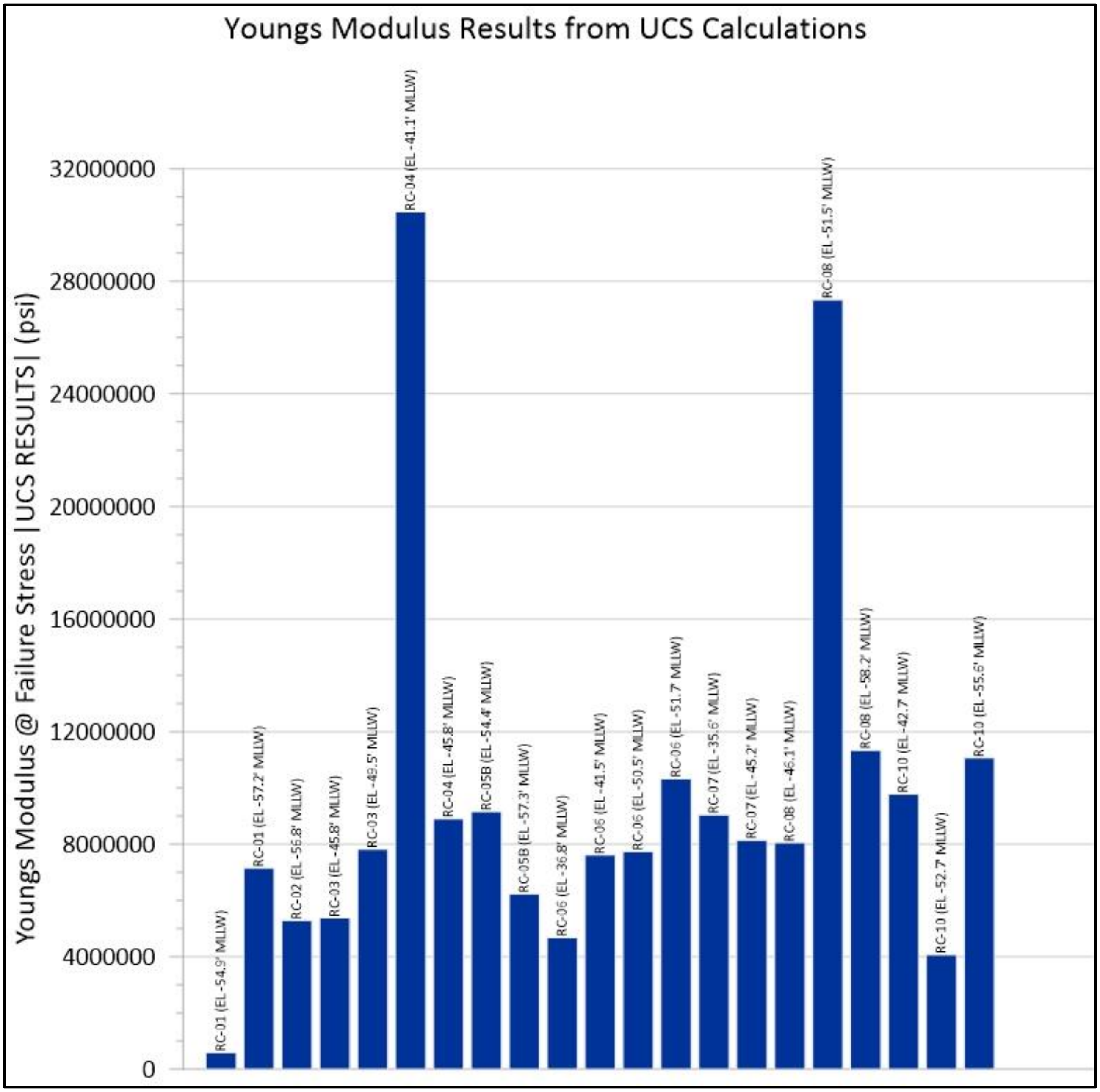

Figure 43. Youngs Modulus at Failure (psi) results from UCS Testing

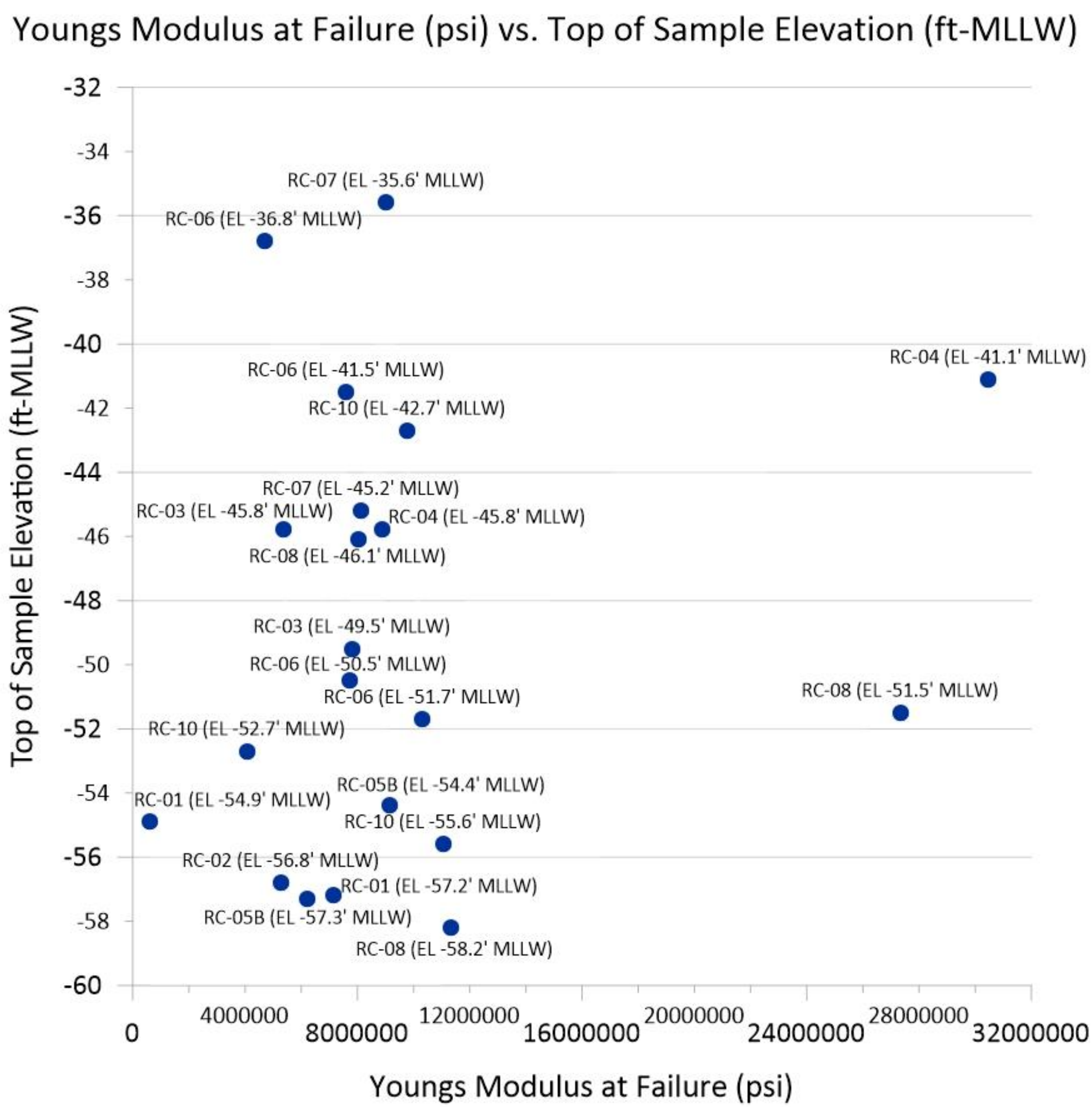

Figure 44. Youngs Modulus at Failure (psi) results from UCS Testing vs. Top of Sample Elevation (ft-MLLW)

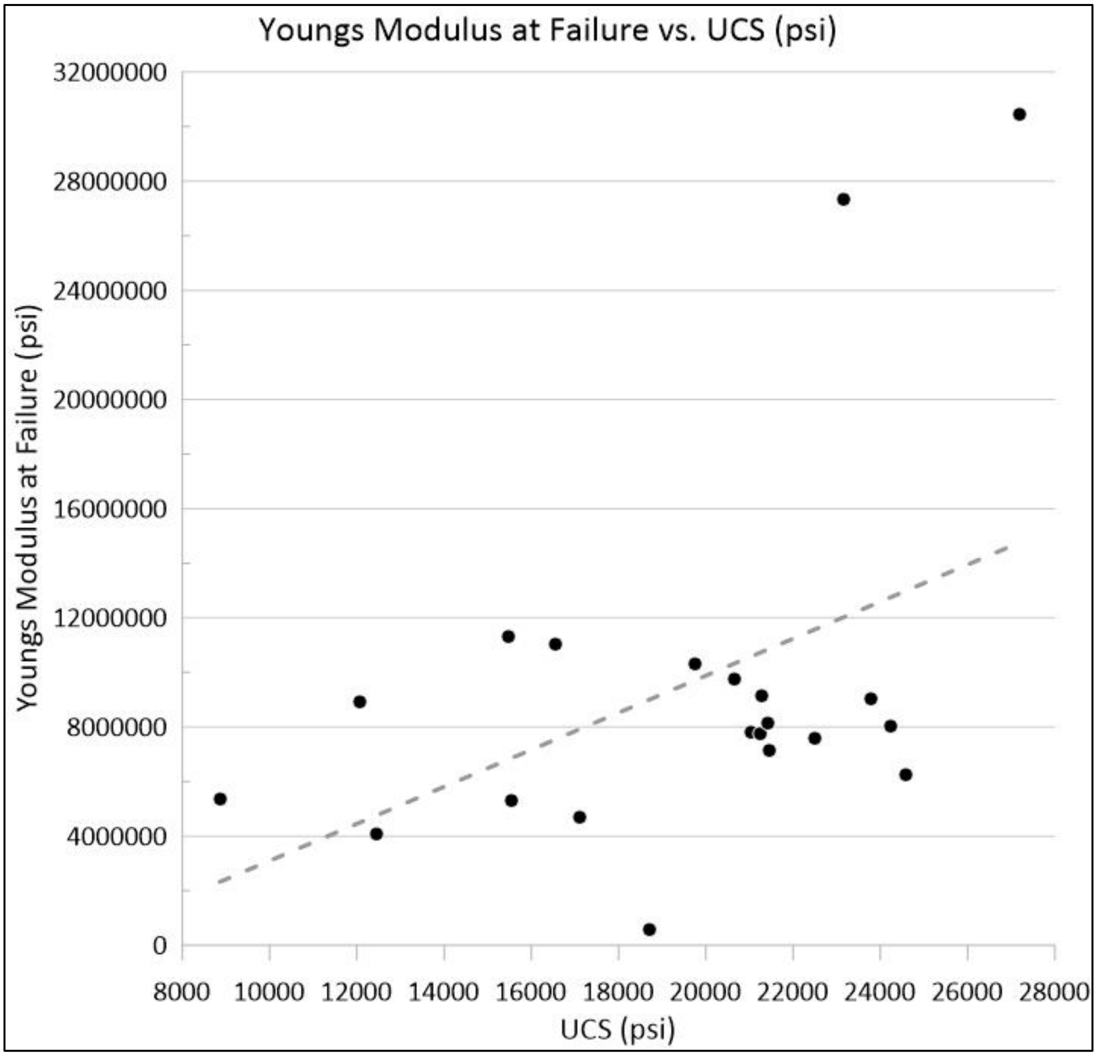

Figure 45. Unconfined Compressive Strength Results vs Youngs Modulus at Failure

Twenty-seven (27) samples were submitted for splitting tensile strength, summarized results are presented in Table 26, where the following observations were noted:

- Failure loads ranged from 1,442 pound-force (lbf) to 7,396 lbf.
- Splitting tensile strengths ranged from 542.7 psi to 2,405.6 psi.
- Only one sample failed on contact.

Table 26. Splitting Tensile Results

Boring ID	Depth of Sample (ft)	Elevation (ft MLLW)	Thickness (in)	Diameter (in)	Failure Load (lbf)	Splitting Tensile Strength (psi)
FD24-RC-01	16.2	-55.2	0.95	1.979	6,150	2,082.40
FD24-RC-01	19.1	-58.1	0.827	1.976	2,466	960.75
FD24-RC-02	26.9	-48.3	0.848	1.981	1,442	546.51
FD24-RC-02	30.0	-51.4	0.875	1.980	4,020	1,477.00

Boring ID	Depth of Sample (ft)	Elevation (ft MLLW)	Thickness (in)	Diameter (in)	Failure Load (lbf)	Splitting Tensile Strength (psi)
FD24-RC-02	35.3	-56.7	0.859	1.981	4,576	1,711.81
FD24-RC-03	13.5	-42.2	0.894	1.758	4,626	1,873.63
FD24-RC-03	13.6	-42.3	0.756	1.758	2,946	1,410.96
FD24-RC-03	21.6	-50.3	0.760	1.766	2,777	1,317.13
FD24-RC-04	15.2	-40.3	0.902	1.982	6,175	2,199.01
FD24-RC-04	20.1	-45.2	0.938	1.977	3,824	1,312.74
FD24-RC-05B	23.1	-48.8	0.824	1.979	Sample failed on contact	
FD24-RC-05B	26.6	-52.3	1.076	1.982	5,239	1,563.97
FD24-RC-05B	29.1	-54.8	1.023	1.977	6,328	1,991.85
FD24-RC-05B	32.0	-57.7	0.976	1.981	5,744	1,808.03
FD24-RC-06	9.4	-36.2	0.819	1.981	2,347	921.04
FD24-RC-06	14.1	-40.9	0.882	1.981	3,038	1,106.79
FD24-RC-06	24.5	-51.3	0.904	1.987	4,073	1,443.62
FD24-RC-06	24.8	-51.6	0.850	1.984	2,992	1,255.96
FD24-RC-07	20.9	-36.3	0.938	1.757	3,878	1,497.86
FD24-RC-07	30.2	-45.6	0.940	1.981	5,093	1,741.32
FD24-RC-08	8.3	-46.5	0.917	1.767	5,162	2,028.30
FD24-RC-08	13.6	-51.8	0.759	1.767	3,068	1,456.48
FD24-RC-08	20.4	-58.6	0.907	1.999	1,546	542.72
FD24-RC-10	15.9	-41.9	0.977	1.983	5,465	1,795.94
FD24-RC-10	17.1	-43.1	0.931	1.984	5,055	1,742.28
FD24-RC-10	25.4	-51.4	0.988	1.981	7,396	2,405.63
FD24-RC-10	27.4	-53.4	0.879	1.983	6,427	2,347.30

A total of twenty-one (21) samples were submitted for Acoustic Velocity to GeoTesting Express located in Acton, Massachusetts. The following observations were noted:

- P-wave velocity ranged from 8,018 to 13,591 feet per second (ft/sec).
- S-wave velocity ranged from 3,385 to 8,063 ft/sec.

Two p-wave velocity values in Table 27 were discarded from the analysis of this report's findings due to their results being extremely low, with values similar to the velocity of water. The lab informed that these were due to a vertical fracture through one sample and a mineralized band of mica in the other. According to the lab manager, the best sections of core at FD24-RC-06 were selected to utilize in the analysis and a comparable section could not be found. These results from FD24-RC-06 are presented in the table below for review purposes only. Two samples from nearby cores, FD24-RC-03 (23.5'-23.9') and FD24-RC-10 (23.0'-23.4'), were submitted to replace these values.

The Young's Modulus values from this method largely differ than the results calculated from the Unconfined Compressive Strength method provided in this report. It is suggested that the more conservative results between the two methods (the UCS values) be incorporated into the design of this project, aiming to reduce the risk of underestimating the volume of bedrock that would need to be blasted during construction.

Table 27. Acoustic Velocity Results

Boring ID	Depth of Sample (ft)	Elevation (ft MLLW)	P-Wave Velocity (ft/sec)(Axial)	S-Wave Velocity (ft/sec)(Axial)	Young's Modulus (psi)	Poisson's Ratio
FD24-RC-01	16.4-16.8	-55.4 to -55.8	9,971	5,805	2,950,000	0.24
FD24-RC-01	18.6-18.9	-57.6 to -57.9	10,316	5,915	3,090,000	0.26
FD24-RC-02	35.4-35.7	-56.8 to -57.1	8,957	5,166	2,330,000	0.25
FD24-RC-03	13.8-14.1	-42.5 to -42.8	9,261	7,238	2,560,000	0.28
FD24-RC-03	20.4-20.8	-49.1 to -49.5	10,187	8,063	2,990,000	0.34
FD24-RC-03	23.5-23.9	-52.2 to -52.6	10,382	5,415	2,690,000	0.31
FD24-RC-04	16.5-16.9	-41.6 to -42.0	9,958	5,771	2,900,000	0.25
FD24-RC-04	20.3-20.7	-45.4 to -45.8	12,275	6,521	3,830,000	0.30
FD24-RC-05B	27.9-28.2	-53.6 to -53.9	12,596	6,337	3,710,000	0.33
FD24-RC-05B	31.1-31.5	-56.8 to -57.2	12,806	5,854	3,300,000	0.37
FD24-RC-06	11.6-12.0	-38.4 to -38.8	4,191	3,385	450,000	0.44
FD24-RC-06	23.2-23.6	-50.0 to -50.4	4,974	3,889	750,000	0.29
FD24-RC-06	24.9-25.2	-51.7 to -52.0	9,636	5,407	2,580,000	0.27
FD24-RC-07	19.8-20.2	-35.5 to -35.9	8,018	6,399	1,790,000	0.38
FD24-RC-07	29.4-29.8	-45.1 to -45.5	13,591	6,862	4,420,000	0.33
FD24-RC-08	7.5-7.9	-45.7 to -46.1	13,479	7,659	5,170,000	0.26
FD24-RC-08	19.4-19.8	-57.6 to -58.0	13,487	7,578	5,090,000	0.27
FD24-RC-10	14.9-15.3	-40.9 to -41.3	11,145	6,023	3,240,000	0.29
FD24-RC-10	23.0-23.4	-49.0 to -49.4	10,385	5,482	2,730,000	0.31
FD24-RC-10	26.2-26.6	-52.2 to -52.6	9,498	5,081	2,490,000	0.30
FD24-RC-10	29.1-29.6	-55.1 to -55.6	13,476	6,738	4,200,000	0.33

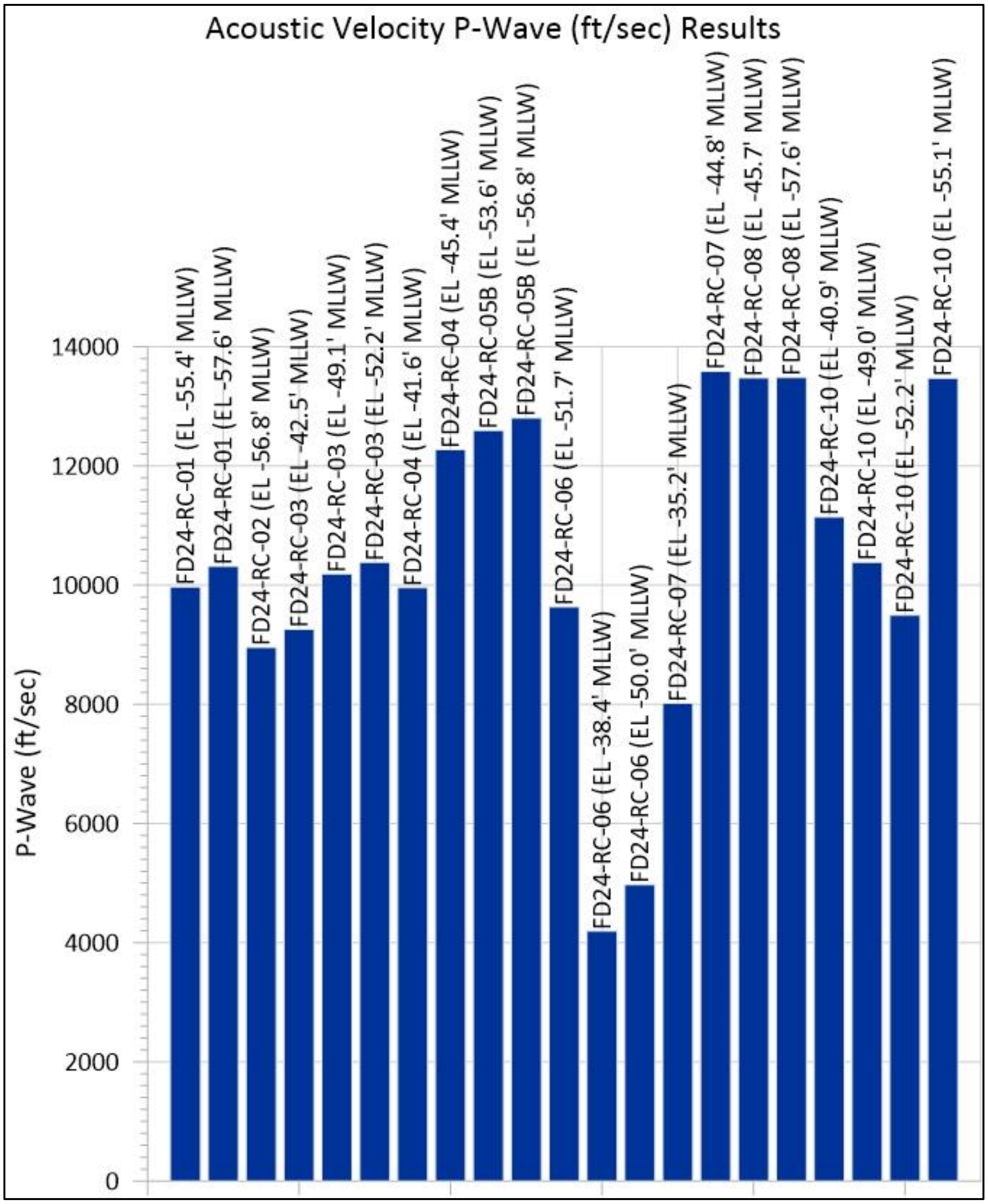

Figure 46. Acoustic Velocity P-Wave (ft/sec) Results

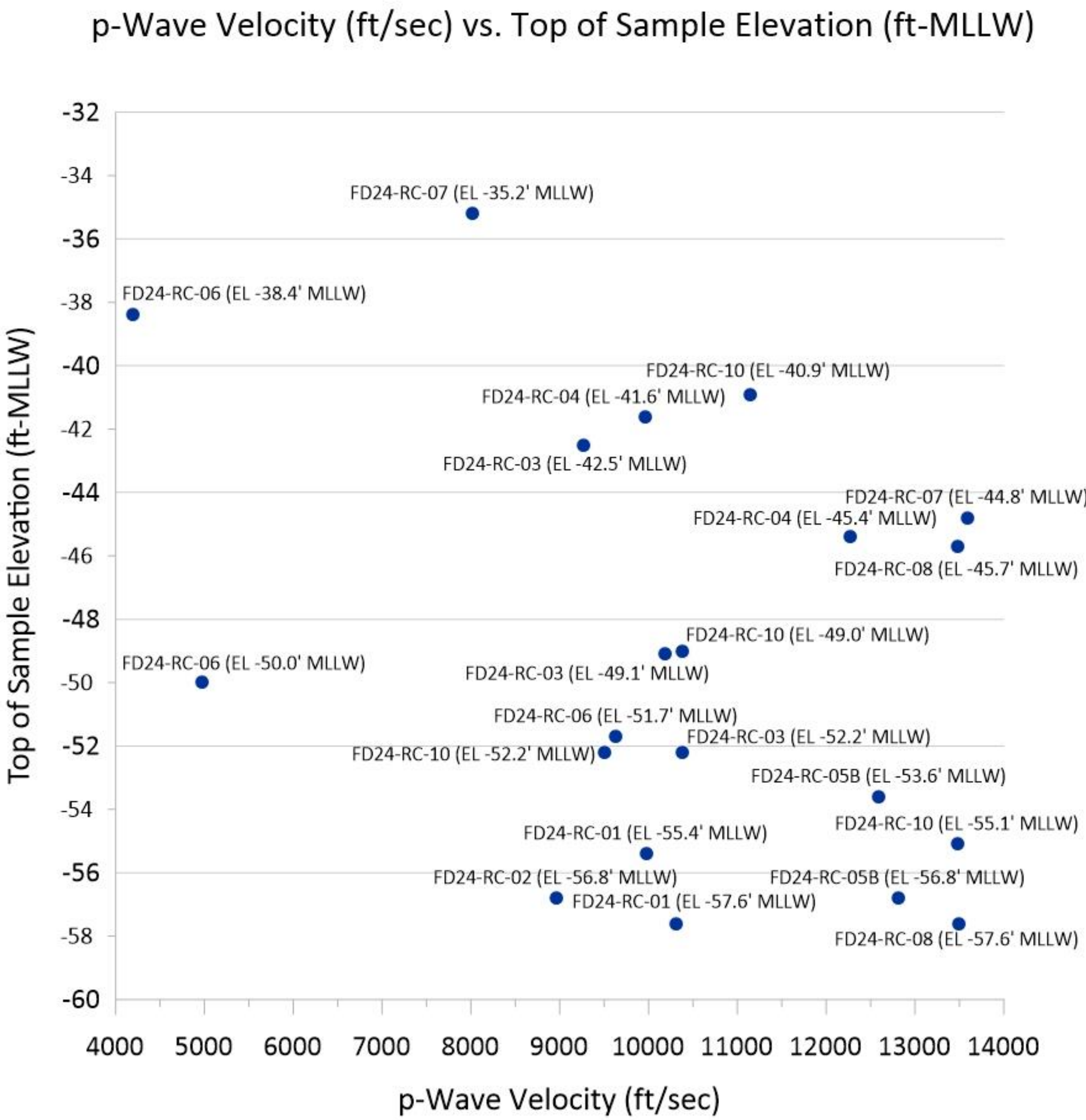

Figure 47. p-Wave Velocity (ft/sec) Results vs. Top of Sample Elevation (ft-MLLW)

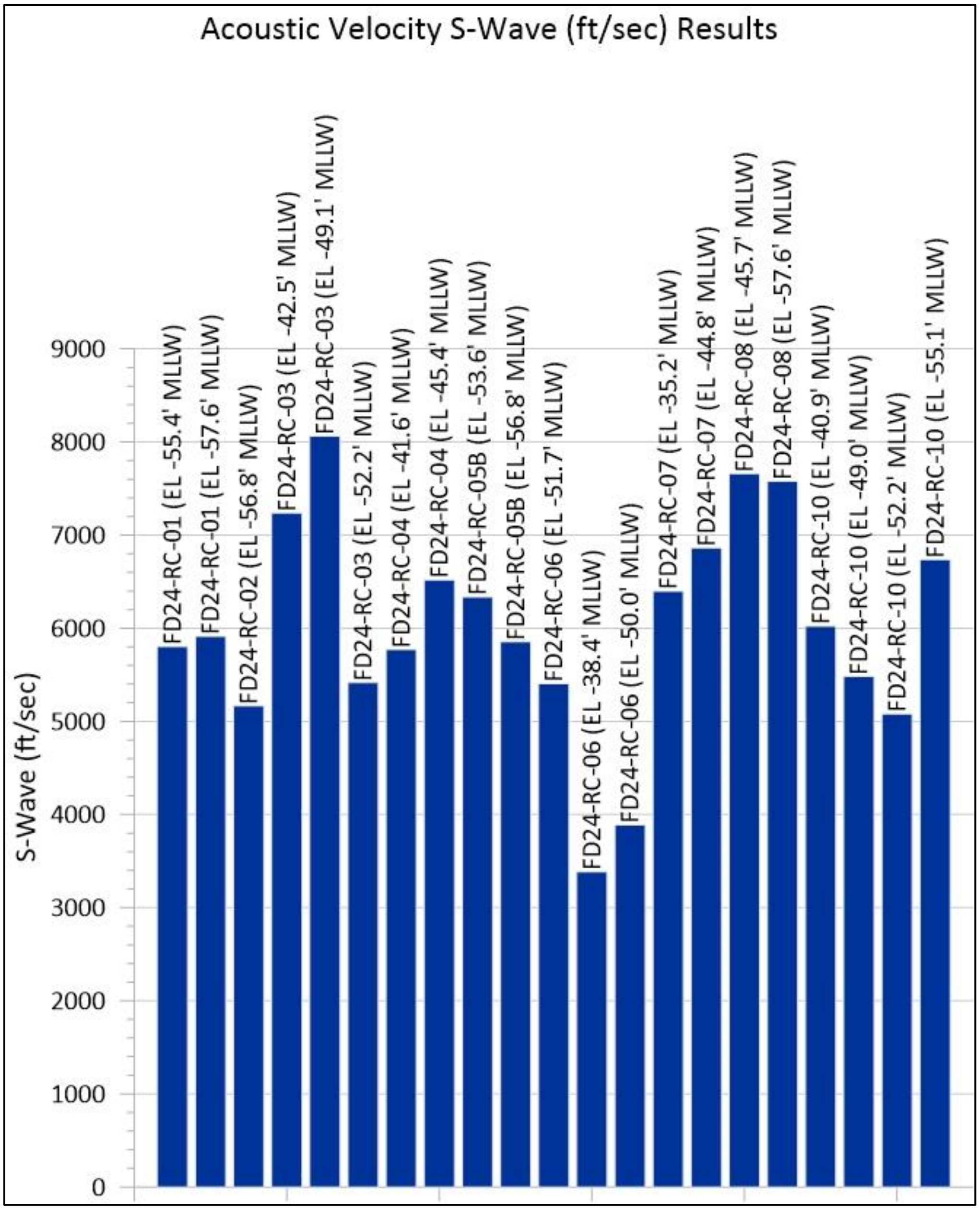

Figure 48. Acoustic Velocity S-Wave (ft/sec) Results

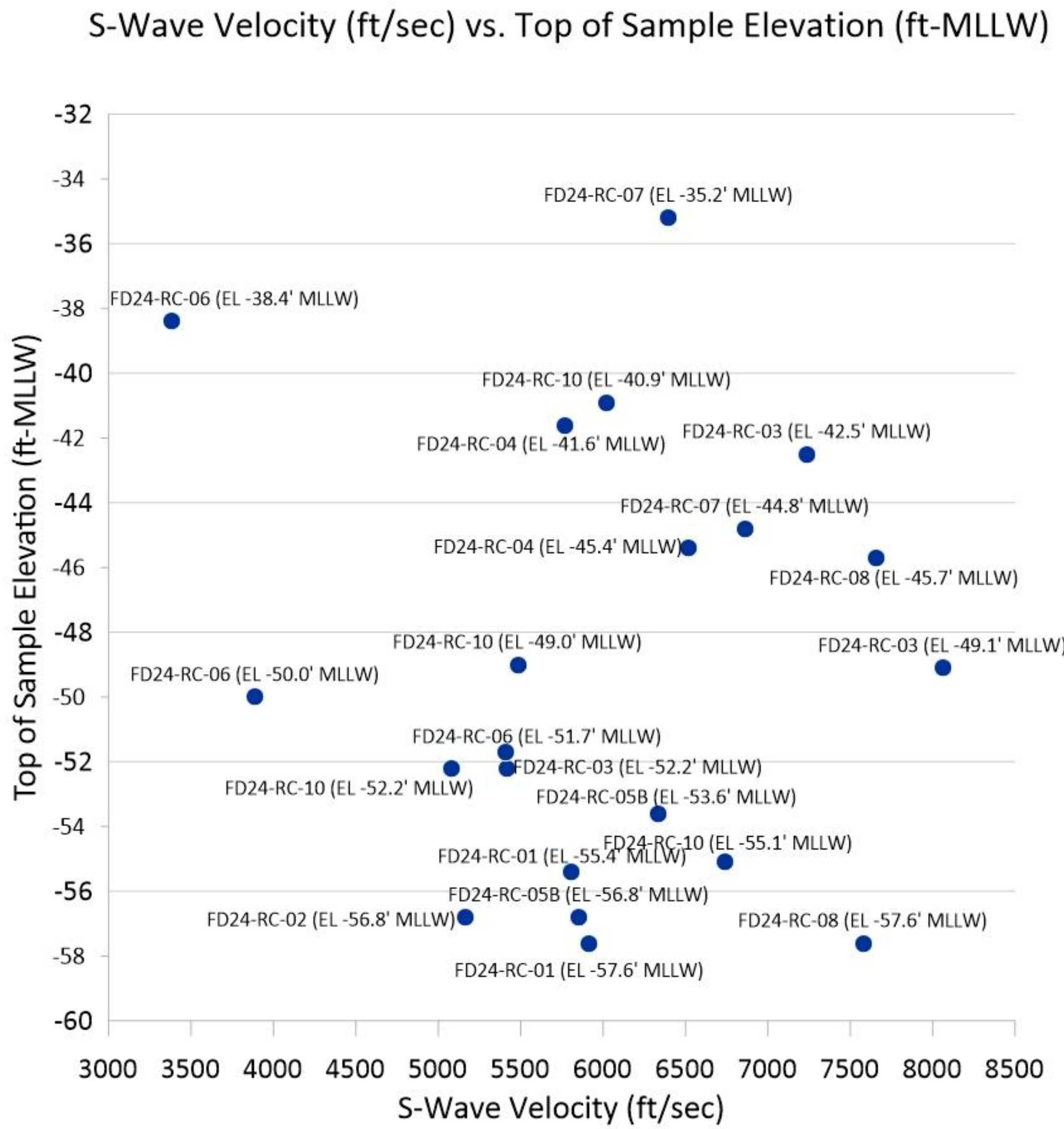

Figure 49. S-Wave Velocity (ft/sec) Results vs. Top of Sample Elevation (ft-MLLW)

6 Investigation Results

Prior to analysis of the data results, a desktop study was provided illuminating the geologic history and morphological setting of the current project area, New Haven Harbor. This history and setting provide the context for understanding these specific results and provide confidence for the interpretation of the data. After gathering and processing all data acquired during the geophysical and geological survey phases, a very robust model and body of results were compiled that fit in quite well with the expected physiographic setting

In the following sections, this physiographic history and current setting introduces the background on which the specific interpretations are based. The sources of the background information include previous public and private research as well as available peer reviewed data. A comprehensive list and detail of these citations is provided in Section 8.

6.1 Geologic Background and Physiographic Setting

The area of interest (AOI), defined here as New Haven Harbor and the relevant adjacent terrestrial landscapes and waters of Long Island Sound, is located at ~41°N along the western margin of the Atlantic Ocean (Figure 50). The inception of the Atlantic Ocean and its continental margins [regional physiographic context of the AOI] are tied to Triassic rifting and the breakup of the super continent Pangea (Miall, Balkwill and McCracken, 2008). Triassic rifting fostered continental thermal uplift and produced conditions favorable for crustal separation (Favre and Stampfli, 1992). Further and substantial development of the proto-Atlantic Ocean occurred as the result of seafloor spreading through the Jurassic (Bird et al. 2007). The combined phenomena of thermal cooling, subsidence, and sediment deposition through the late Mesozoic and Tertiary produced the mature passive margin that encompasses the AOI today (Favre and Stampfli, 1992). Devonian/Silurian aged Gneiss is found in the area and is a product of the Acadian Orogeny, the collision and incorporation of Avalonia with the Euramerica continental mass during the late Silurian/early Devonian (Golonka, 2002). These Avalonia metamorphic units are found across New England and Scandinavia. In the New Haven Harbor Area, portions of this metamorphic unit are known as the Lighthouse Gneiss.

Figure 50. Satellite imagery depicting the geographic position of the Area of Interest (AOI) along the western margin of the North Atlantic Ocean. The AOI is located on the east coast of the U.S.A. in the state of Connecticut.

The three figures presented below depict the evolution of the New Haven Harbor area in a global, tectonic context. Figure 51 and Figure 52 below depict the source of the Paleozoic metamorphic rocks that outcrop in southern Connecticut the Acadian Orogeny (Glonka, 2002). Figure 53 depicts the beginning and evolution of the passive continental margin setting that is seen today (McKraken, et al. 2008)

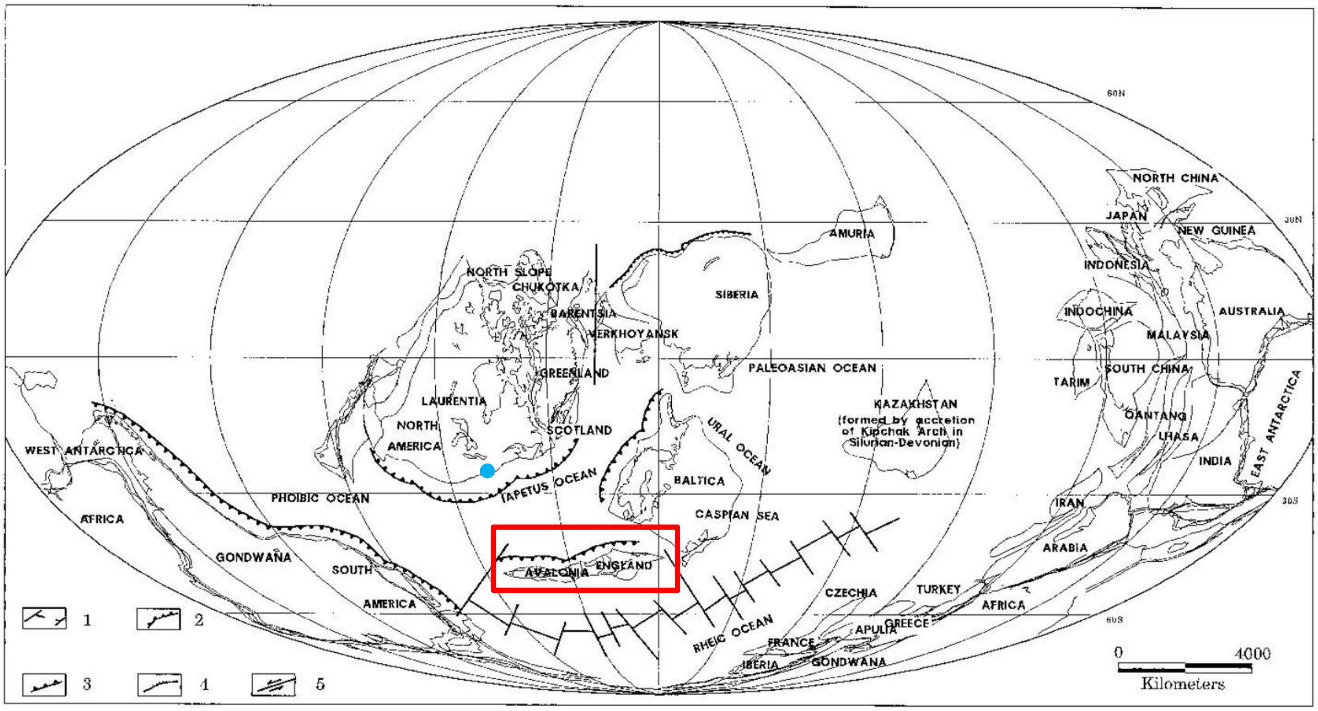

Figure 51. Plate tectonic reconstruction from Golonka, 2002 Depicting the approximate Middle Ordovician (~470Ma) positions of the project site (blue dot) and Avalonia (red box)

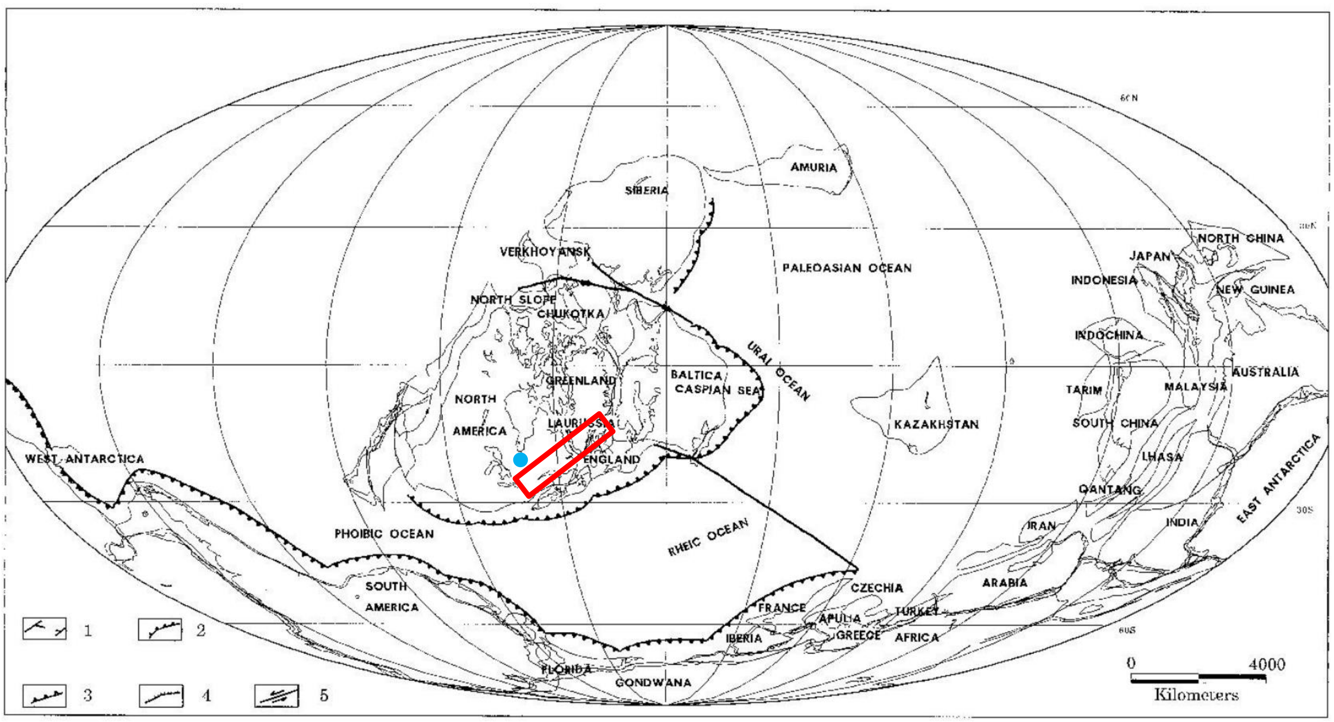

Figure 52. Plate tectonic reconstruction from Golonka, 2002 Depicting the approximate late Silurian (~420Ma) positions of the project site (blue dot) and Avalonia (red box)

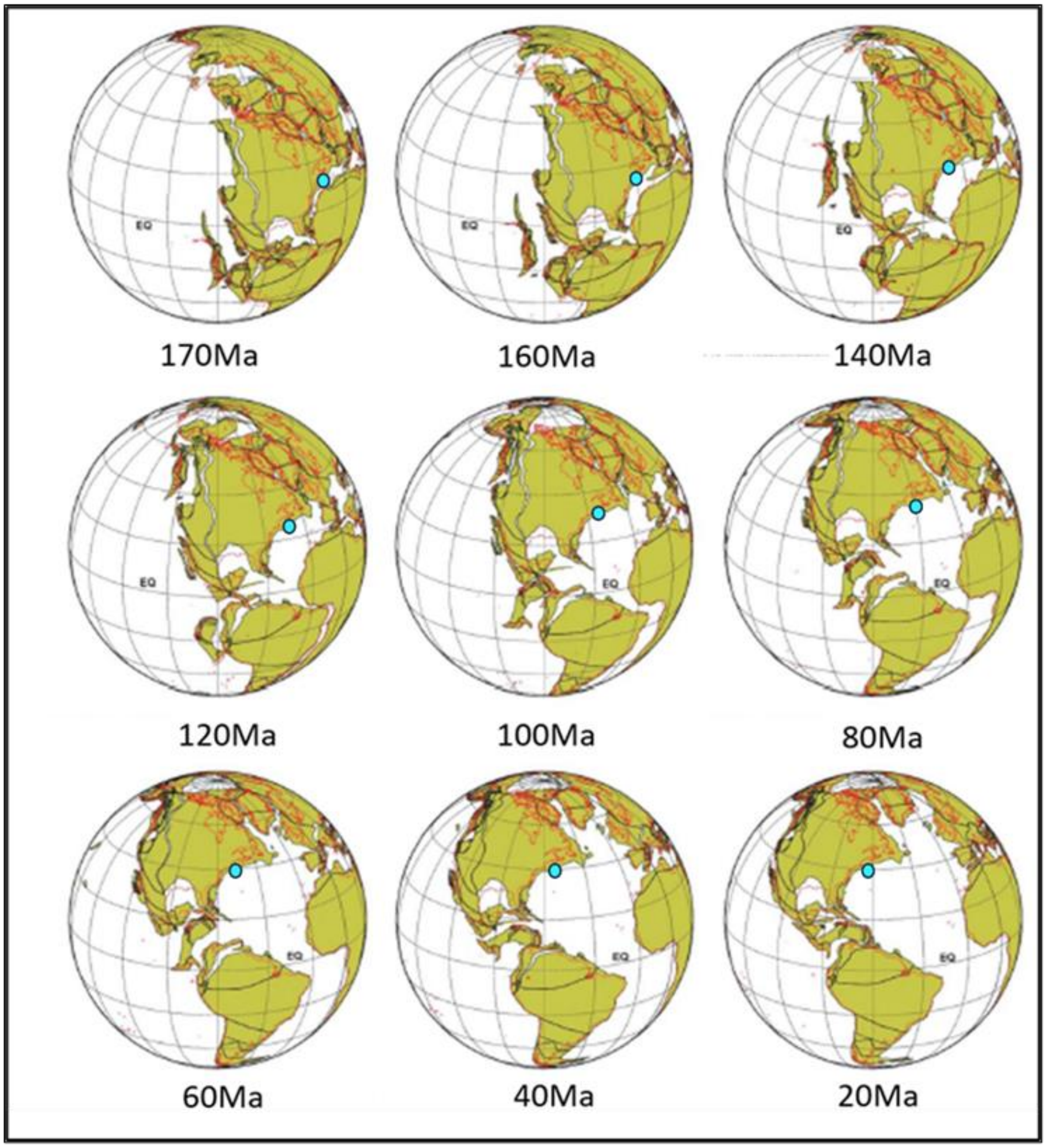

Figure 53. Plate tectonic reconstruction of the opening and evolution of the Atlantic Ocean and adjacent margins. The blue dot represents the approximate location of New Haven Harbor. Adapted from Fig. 3 in Miall, Balkwill and McCracken, 2008.

In modern geographic terms, the AOI is situated within the state of Connecticut along the northern shore of Long Island Sound (LIS). New Haven Harbor, specifically, is positioned in the seaward extension of Connecticut's Central Lowlands province (Figure 54) (Poppe et al. 2001). The harbor sits at the southern tip of the Hartford Basin, which is mostly Early Jurassic in age (Cornet and Traverse, 1975; Lewis and DiGiacomo-Cohen, 2000). Bedrock in the AOI is Mesozoic, namely, late Triassic sedimentary rocks [arkose sandstones] with Jurassic igneous intrusions (Bjerklie, 2012), and Silurian/Devonian metamorphic rocks [Gneiss/Schist]. Being less susceptible to erosion, the igneous and metamorphic rocks often comprise the topographic highs in the AOI. The Mesozoic units unconformably overlay deeper Paleozoic rocks (Deasy, Wathen, and Wintsch, 2017). The Paleozoic units are comprised of polymetamorphic argillites and mafic rocks that have a singular outcrop in southern Connecticut, the Lighthouse Gneiss.

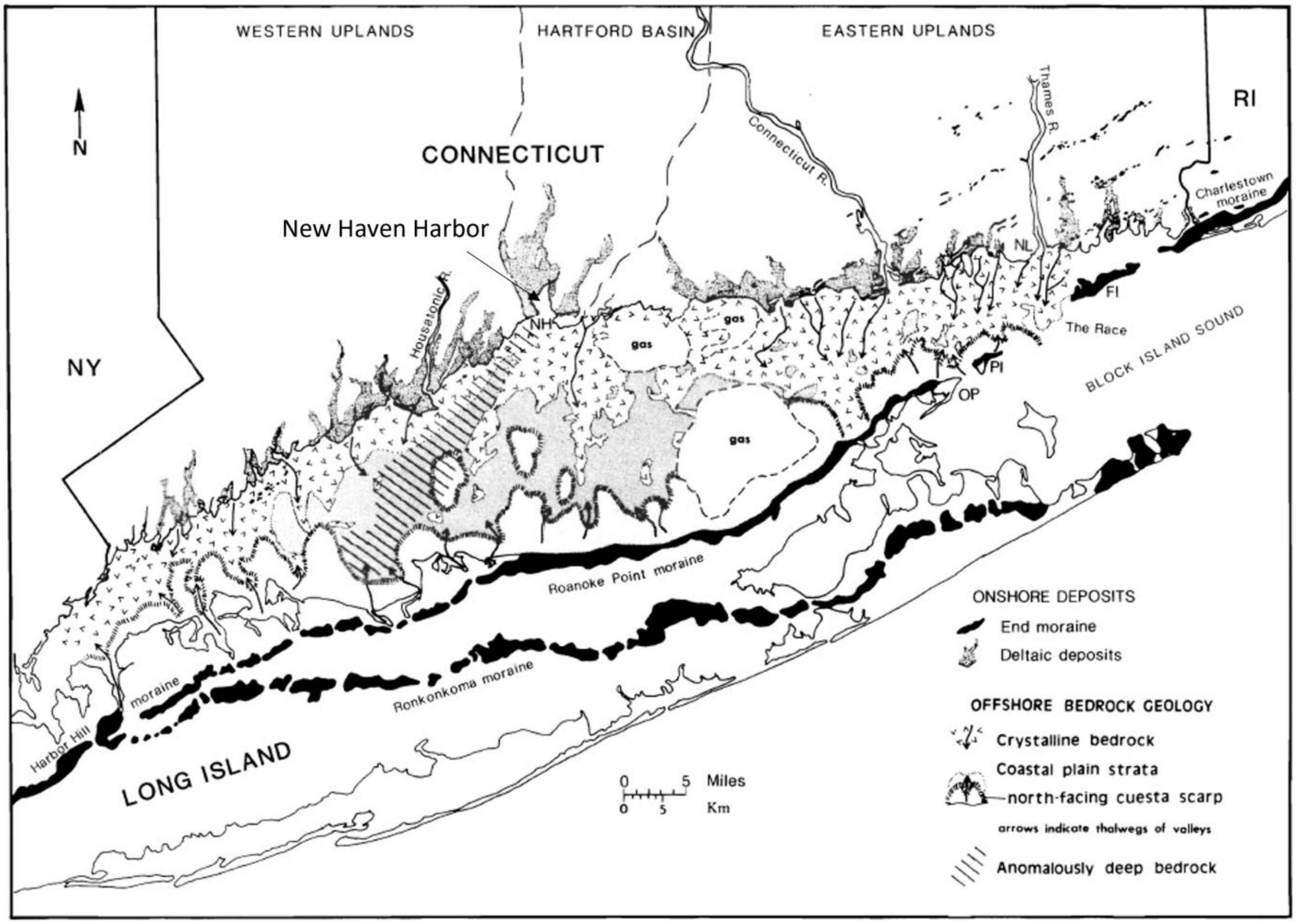

Figure 54. Physiographic and geologic map of the region surrounding the Area of Interest. Figure 2 from Lewis and Stone (1991).

The upper bedrock surface undulates in the New Haven region and may exhibit ~300m of relief (Bjerklie et al. 2012). A prominent trough in the bedrock exists within New Haven Harbor that has been interpreted as the union of the ancestral, Farm, West, and Quinnipiac River channels (Figure 55) (Sanders, 2010). Mesozoic rock outcrops do occur within the AOI. However, much of the present-day terrestrial geomorphology and surficial deposits (Figure 57) [land and marine] of the AOI and Connecticut more broadly, were produced during the Quaternary Period (Stone, 2005). As such, from the standpoint of most engineering concerns, the most relevant epochs of geologic history for the AOI are the Silurian/Devonian (443.8Ma – 358.9Ma), Pleistocene (2.6Ma-10Ka), and the Holocene (10Ka-present day).

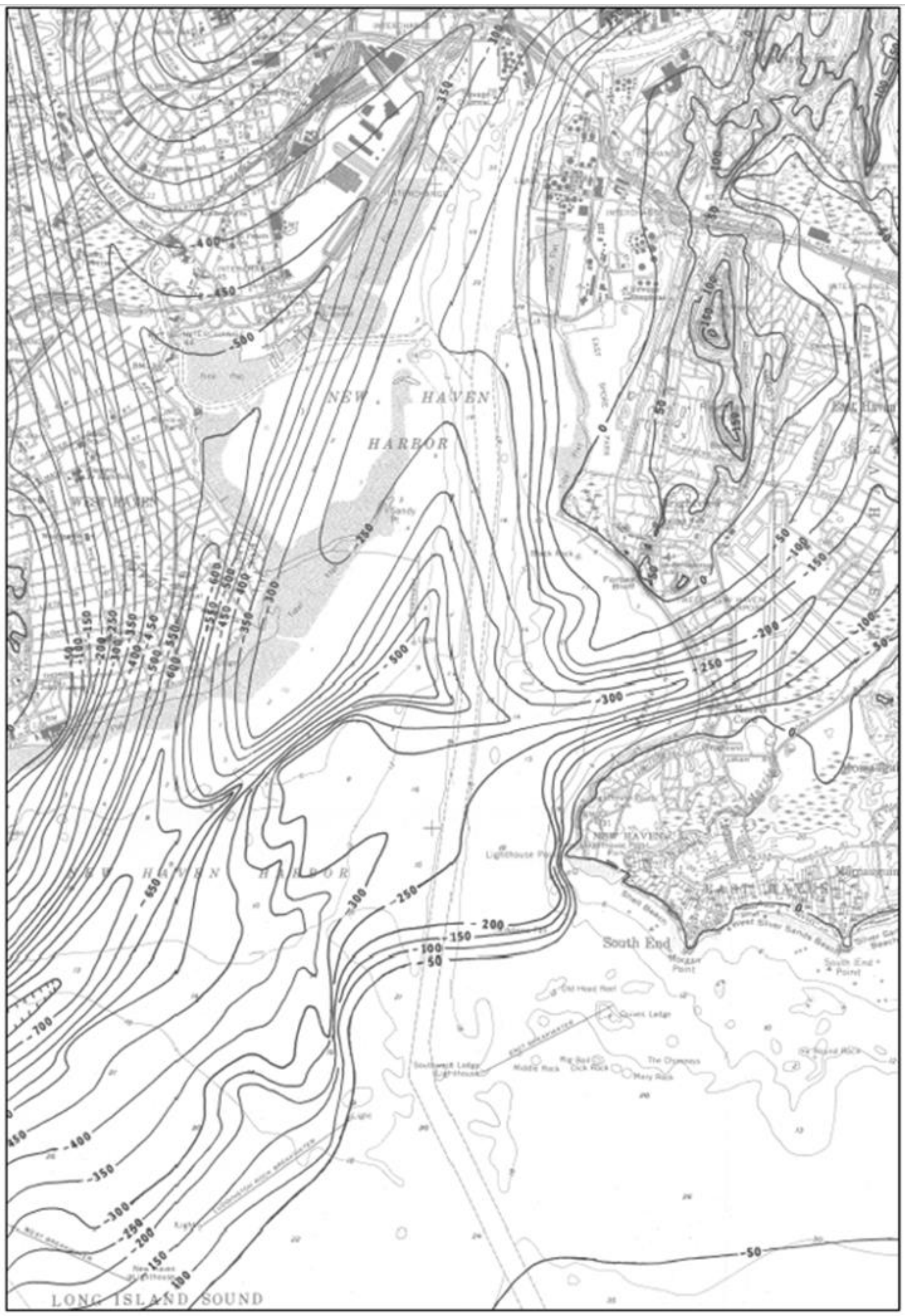

Figure 55. Vintage bedrock surface elevation map from Haeni and Sanders, 1974. The deep trough feature that exists within New Haven harbor has been interpreted as the coalesced channels of paleo rivers entering the embayment from the north.

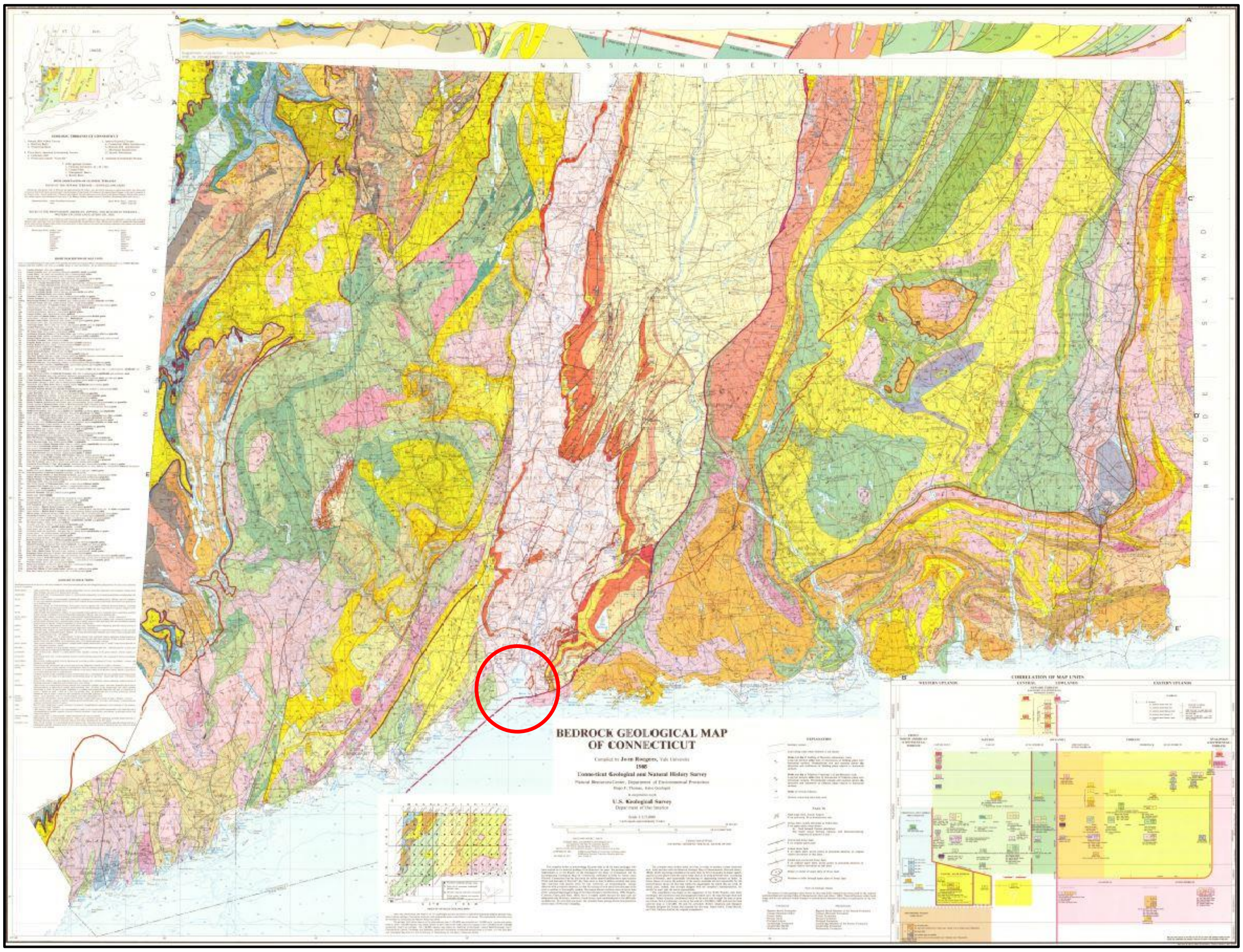

Figure 56. Generalized Bedrock Geological Map of Connecticut with the project area circled in RED.

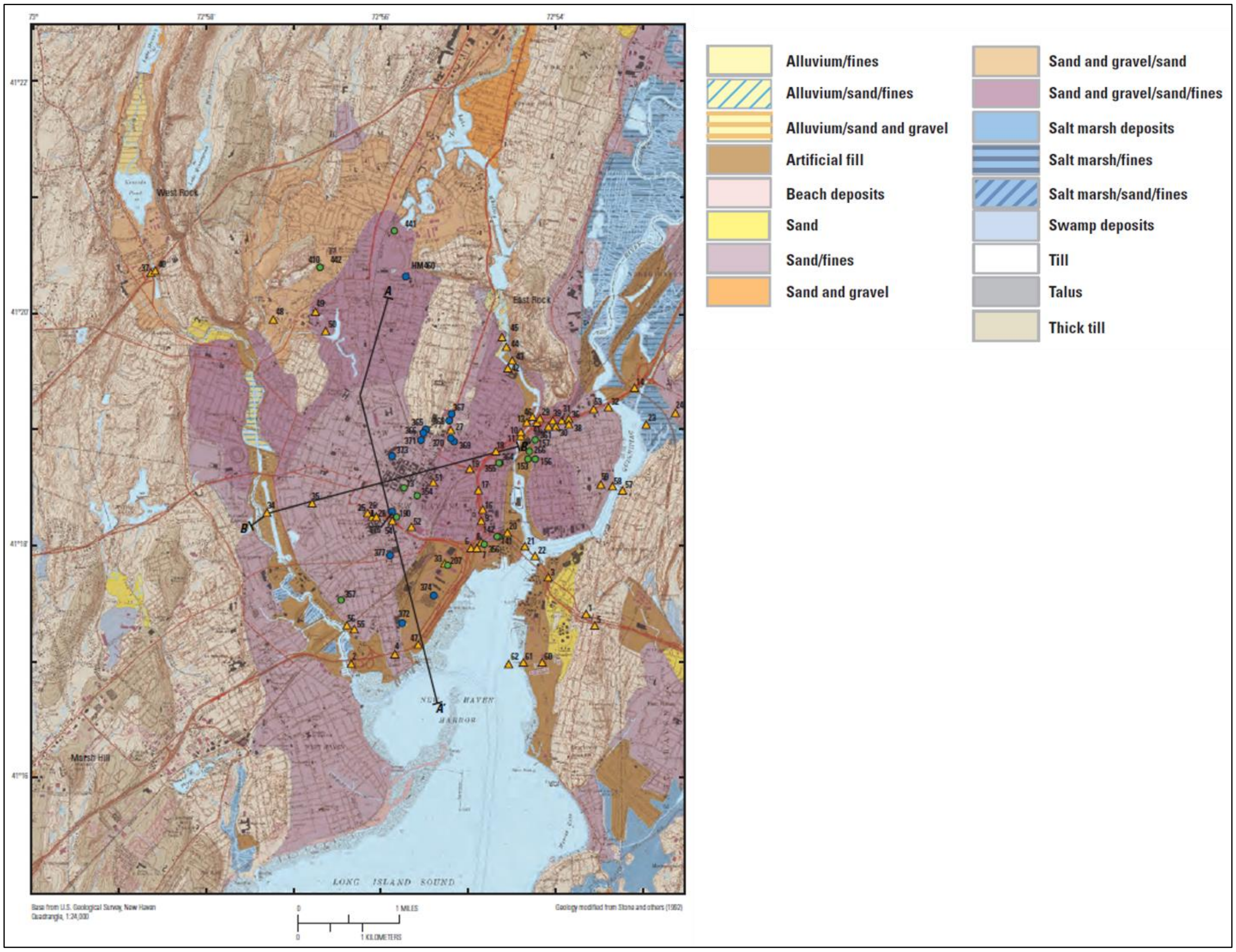

Figure 57. Map of the surficial geologic material for the greater New Haven area, adapted from Figure 1-1 from Bjerklie et al. (2012).

The Quaternary was, and continues to be, a period of high-amplitude, high-frequency, eustatic sea-level fluctuations, driven by oscillations in global climate and related ice volume (Figure 58) (Pisias and Moore, 1981). The external forcing mechanism invoked as the major control on Quaternary climate is astrophysical in nature, having to do with the celestial mechanics of the earth-sun orbital relationship, commonly referred to as Milankovitch cycles (Figure 59) (Pillans et al. 1998). The near-surface geology and stratigraphic architecture of formerly glaciated terranes, e.g., higher latitude shelves of the northern hemisphere, to include the AOI, are in large part, the result of the interplay of glaciation, sediment supply and sea-level change (McHugh & Olson, 2002; McHugh et al. 2010; Zecchin, Catuneanu & Rebesco 2015).

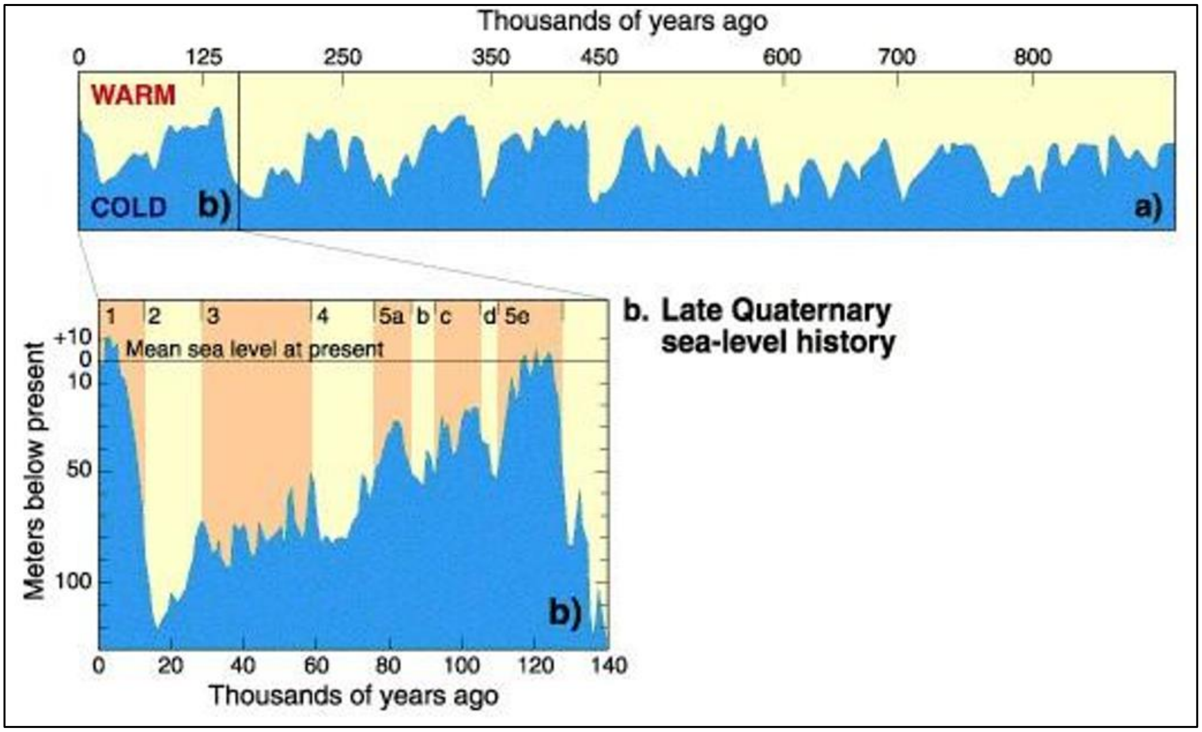

Figure 58. Sea level curve for the Late Quaternary period with an emphasis on the last 140ka. The high frequency, high amplitude nature of sea level is clearly on display in the time series. Source NOAA.

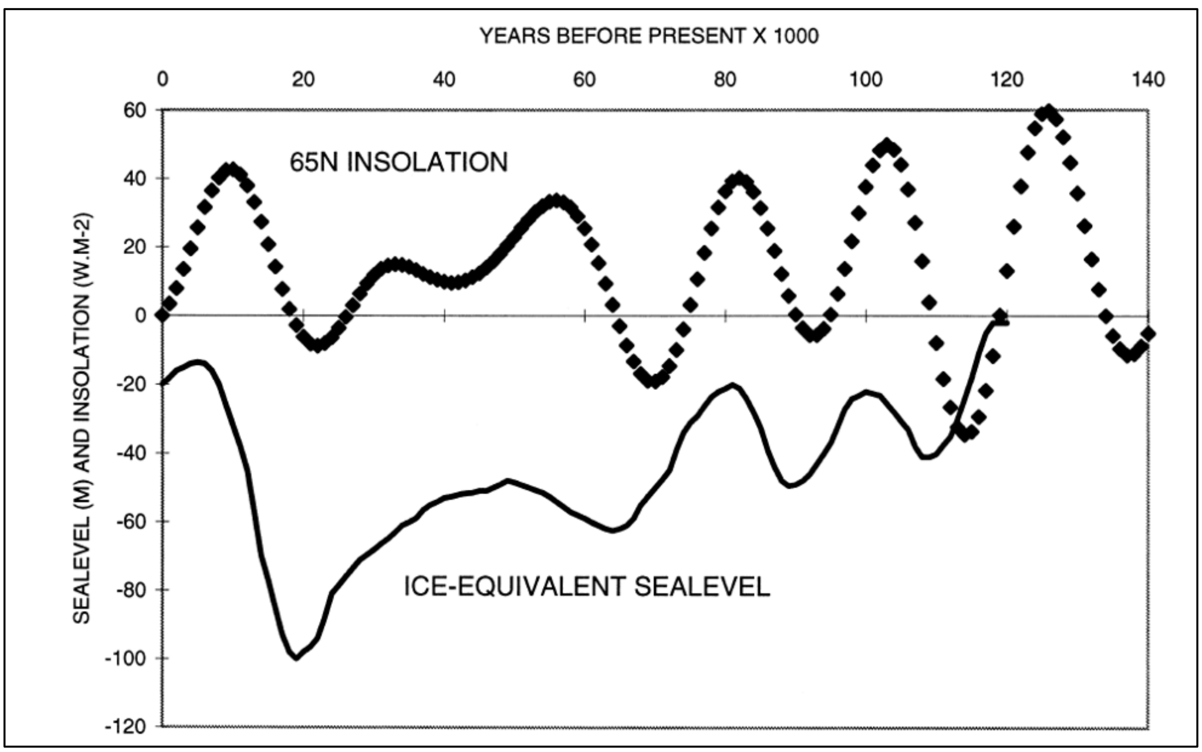

Figure 59. Time series of insolation at 65 degrees N. latitude and eustatic sea-level – The upper curve, insolation, is closely correlated with Milankovitch cycles that influence the glacial and interglacial periodicity of the planet. The lower curve represents the behavior of sea-level that is also coupled to Milankovitch cycles through global ice volume. Adapted from Fig. 1 in Pillans, Chappell and Naish, 1998.

New Haven Harbor, the primary feature of concern within the AOI, is an embayment within the greater LIS basin, (Figure 60) (Rozan and Benoit, 2001). LIS is a linearly shaped estuary that runs parallel to the mainland U.S. coast (Lewis and DiGiacomo-Cohen, 2000). The LIS estuary has connections to the Atlantic Ocean at its opposing ends, east and west, via a series of straits adjacent to Block Island Sound and the East River, respectively (Parker and O'Reilly, 1991). The latter being a conduit to the Hudson River Estuary that has broad communication with the coastal Atlantic. The genesis and sedimentological structure of Long Island Sound is directly connected to Milankovitch cyclicity and related glacier dynamics. The southern shore of LIS, i.e., Long Island, is a terminal moraine (Williams, 1976). The Long Island moraine was formed during the Wisconsinan Glaciation [≈75,000 to 11,000 YBP] near the time of the Last Glacial Maxima [LGM] around 26Ka to 19Ka, (Clark et al. 2009; Uchupi et al. 2001). During this time period, sea level is estimated to have been ~127m below present-day (Clark and Mix, 2002).

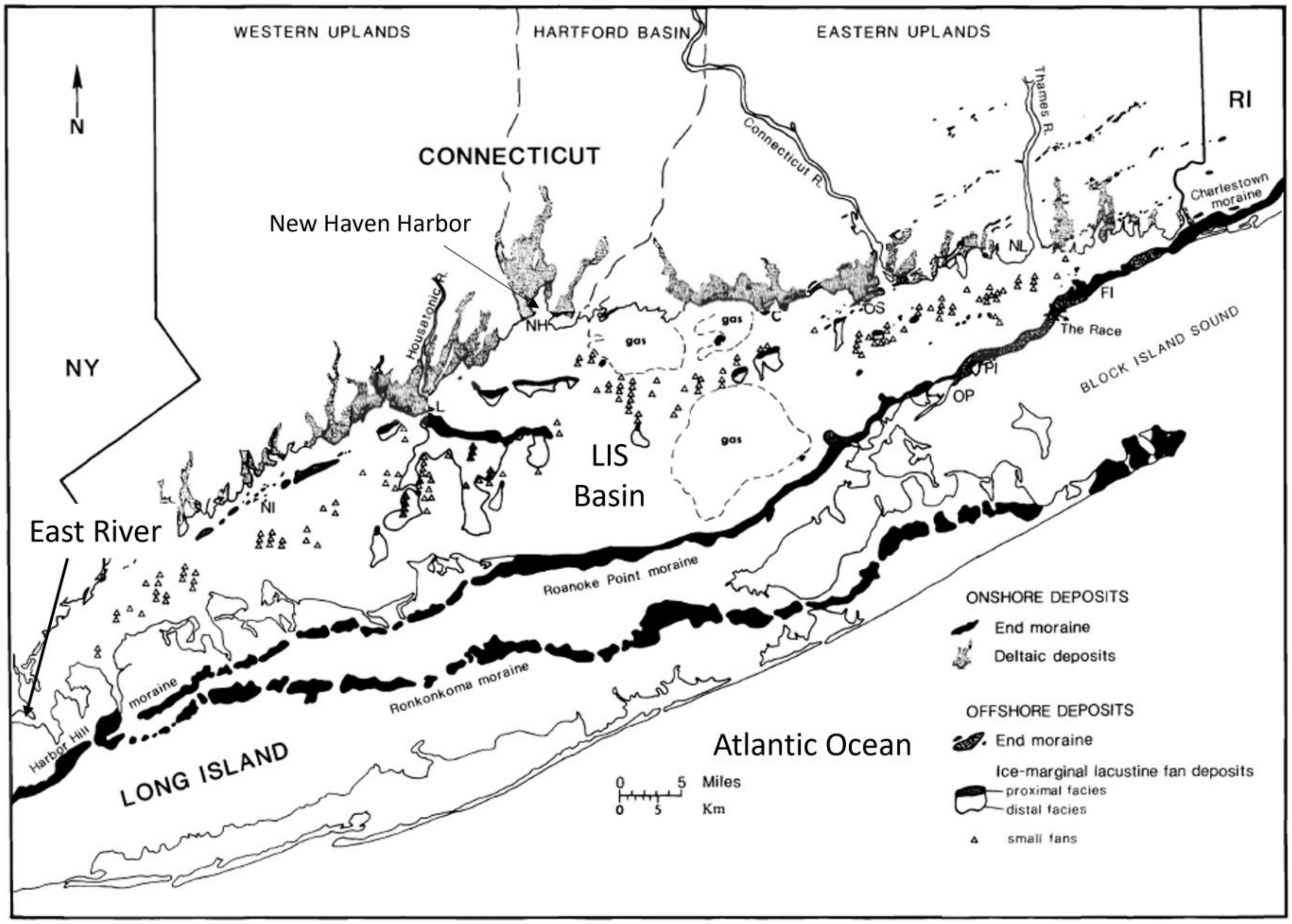

Figure 60. Map of the Long Island Sound basin and the glacial deposits that occur throughout the area. Figure 3 from Lewis and Stone (1991).

The maximum southeastern extension of the Laurentide Icesheet is represented by an assemblage of terminal moraine deposits offshore the northeastern U.S. coast, to include Long Island (Mickelson and Colgan, 2003). Long Island Sound was the site of a large glacial lake (Uchupi et al 2001) and all of Connecticut was covered by the Laurentide ice sheet near the end of the Wisconsinan glaciation (Figure 61) (Bjerklie et al. 2012). Glacial Lake Connecticut covered the New Haven Habor area and provided the accommodation space for the glaciofluvial deltaic deposits found here, as well as the glaciolacustrine sediments (Figure 62) (Poppe et al. 1998). Given the proximity of the AOI to the icesheet margin, glacial deposits predominate the landscape and subsurface, and may include boulders, tills, clays, gravel, sand, and varieties of glaciotectonites (Bennett & Glasser, 2011).

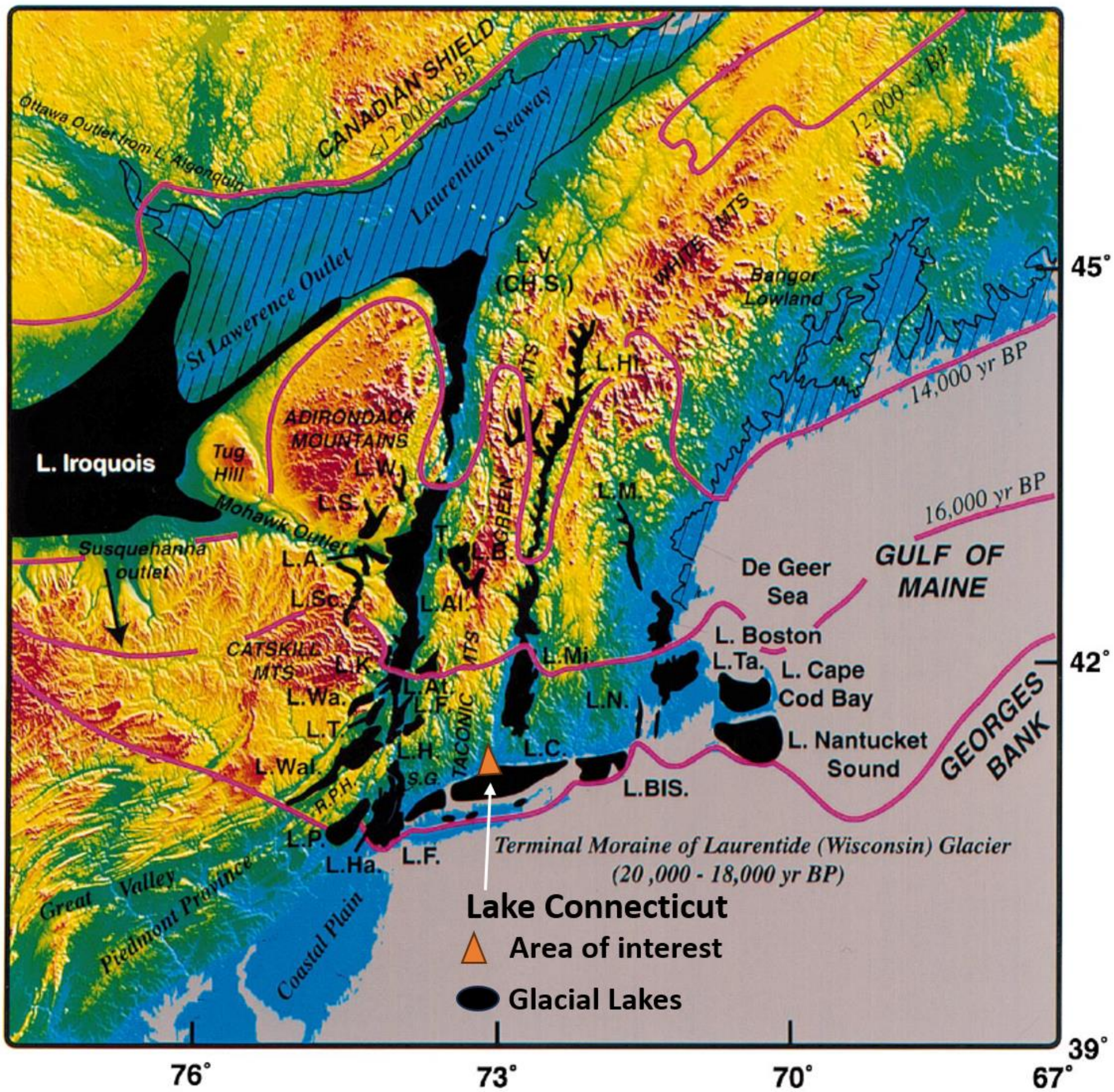

Figure 61. Map depicting the distribution of glacial lakes around the time of the Last Glacial Maxima. Lake Connecticut, on the backside of the Long Island terminal moraine covered what is now New Haven Harbor. Adapted from Figure 4 from Uchupi et al. (2001).

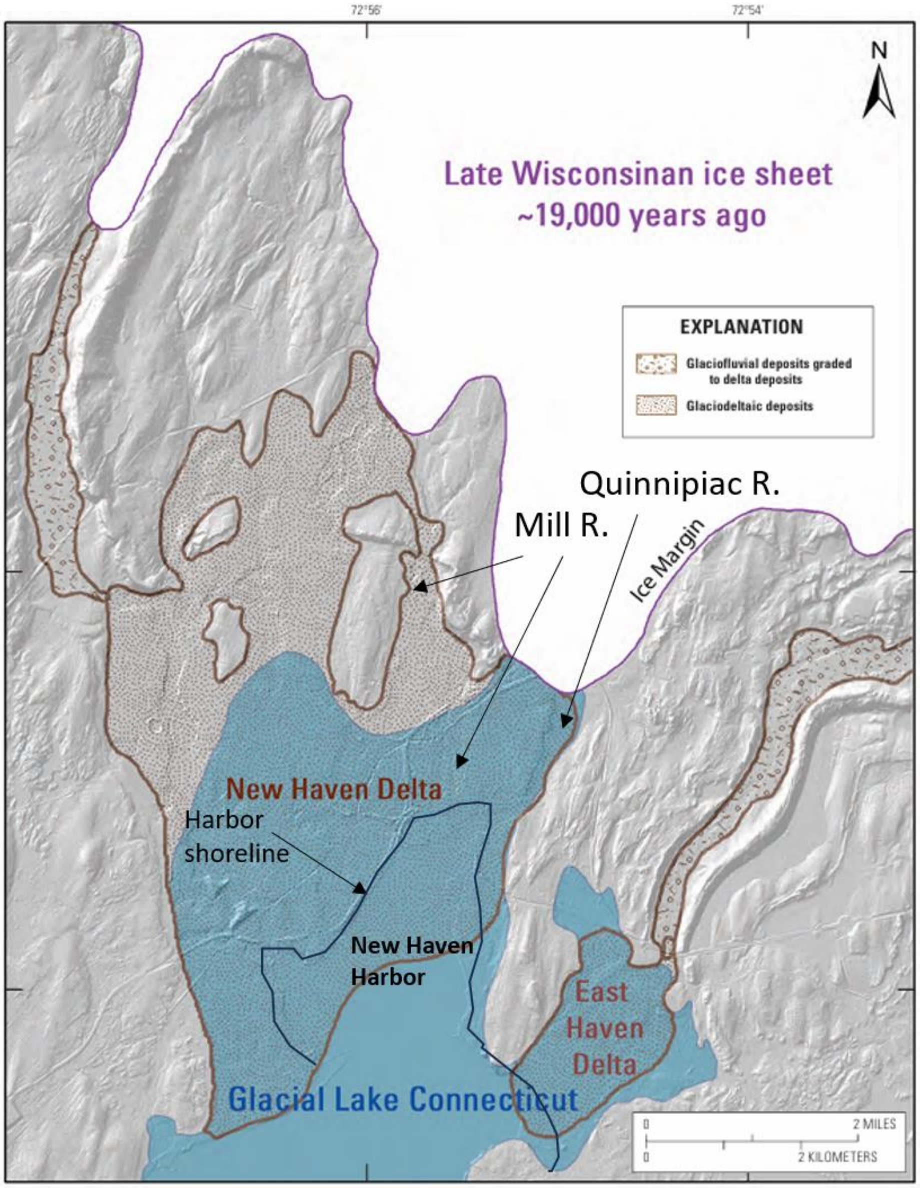

Figure 62. Map depicting the interpreted boundaries of glacial Lake Connecticut during the Late Pleistocene. Also shown are the major depocenters associated with meltwater inputs. Lake Connecticut covered New Haven Harbor 19,000 years ago. Adapted from Figure 1-2 from Bjerklie et al. (2012).

Broadly speaking, two forms of glacial deposits occur within the AOI, i.e., glacial till and glacial meltwater deposits (Bjerklie et al. 2012). Two, age distinct, till deposits unconformably overlie bedrock in the AOI. However, only the younger, Wisconsinan-aged till, has been mapped around New Haven Harbor (Poppe et al. 2001). The older till, likely deposited during the Illinoian ice age, tends to be thicker and comprises the hill features west of the harbor in West Haven (Bjerklie et al. 2012). The till is generally sandy containing larger lithoclasts, up to the size of "large" boulders and may be compacted or loose (Poppe et al. 1998). The Wisconsinan tills overlie the bedrock at variable thicknesses across the New Haven area and extend offshore into the harbor (Figure 63). Outcrops of this till are present at Oyster River, Lighthouse, and Morgan Points, as well as around Morris Cove, see Figure 64, for locations, (Stone et al. 1992). Figure 65 shows the complete spatial distribution of surficial geologic material across the AOI, to include the relevant till outcrops.

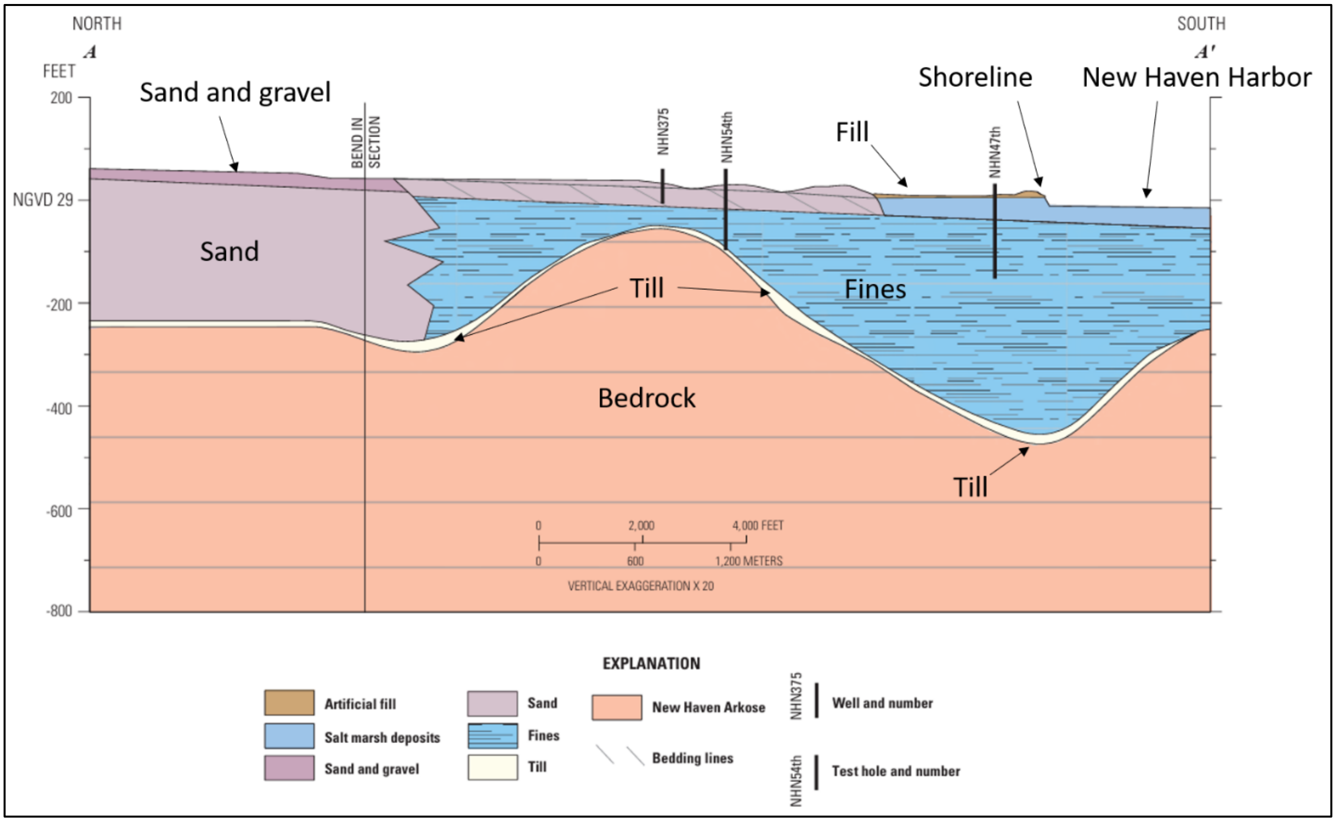

Figure 63. Schematic profile of the subsurface for New Haven and the northern extent of its harbor. The location of the profile, A – A' is shown in Figure 57. Original work is from Bjerklie et al. (2012).

Figure 64. Satellite imagery depicting landmarks to which geological conditions are referenced.

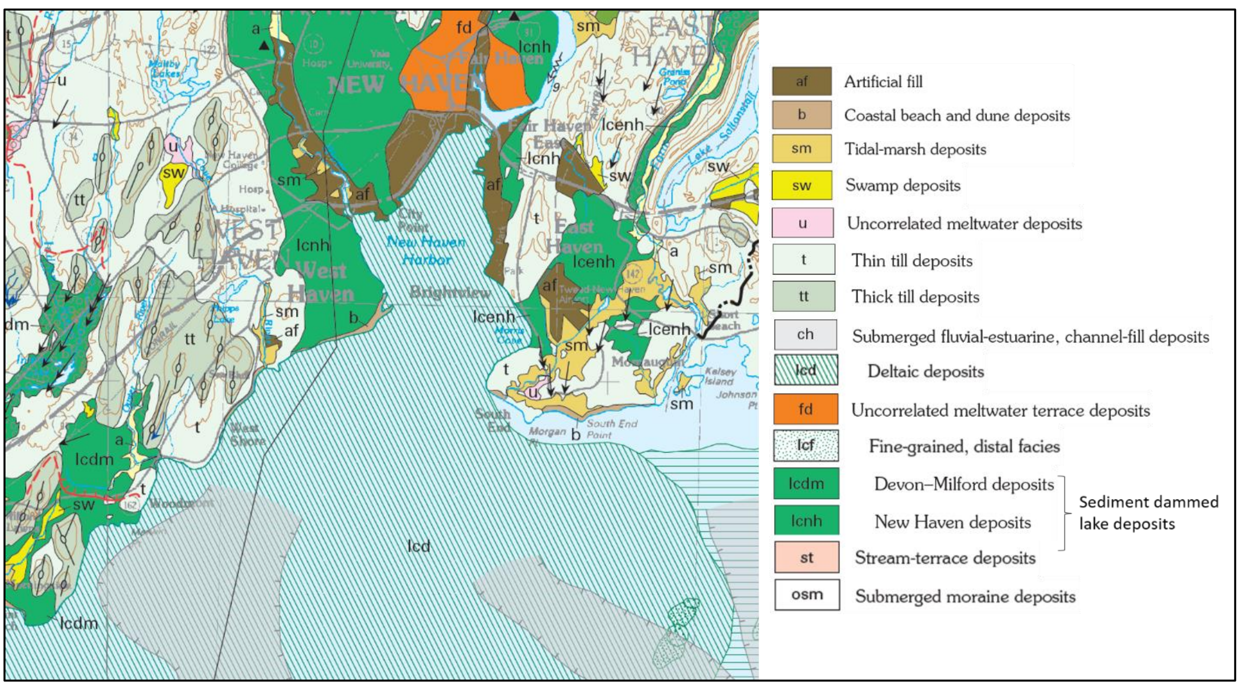

Figure 65. Geologic map of the AOI showing the spatial distribution of till outcrops (t and tt) and other surficial deposits. USGS.gov.

Stratified, glacial drift deposits predominate the New Haven Harbor and surrounding areas (Bjerklie et al. 2012). These sediments were deposited by glaciofluvial processes in outwash plains and now overlie the till and bedrock in much of the AOI (Poppe et al. 2001). Glacial meltwater deposits may exhibit deltaic sequences, where topset beds are coarse-grained and overlie foreset and bottomset beds that are finer-grained. Bottomset beds may be glaciolacustrine deposits (Bjerklie et al. 2012). Deltaic sediment units deposited in Lake Connecticut, the large glacial lake that covered much of LIS basin in the Pleistocene, now overlie drift deposits and bedrock in New Haven Harbor (Poppe et al. 2001 and references therein).

Presently and during the Holocene, New Haven Harbor represents the terminus of three rivers, the Quinnipiac, West and Mill (Rozan and Benoit, 2001). The rivers flow through salt marshes prior to entering the harbor (Rozan and Benoit, 2001), that are comprised of a mixture of peat and mud (Poppe et al. 2001). Sediments within the modern river channels approaching the harbor are mostly sand (Rozan and Benoit, 2001). During periods of lower sea-level, while in a subaerial state, the harbor contained the outwash plains of the aforementioned rivers (Sanders, 1994). Today, the paleovalleys of these rivers exist in the subsurface of the harbor as sediment filled channels with bedrock walls. The ancestral rivers preferentially incised the relatively soft, sedimentary units of the bedrock. The subsurface, valley-fill sediments may be 35 m thick in the outer reaches of the harbor, and based on cores from Sanders (1994), are mostly sandy, Pleistocene, outwash deposits. Further north, in the interior of the harbor, organic silts are present, with thicknesses up to 13m (Sanders, 1994). According to Bjerklie et al. (2012), some of the earliest post glacial sediments are stream deposits incised into the deltas formed within Lake Connecticut. Also, talus deposits accumulated adjacent to bedrock cliffs as the glacier retreated. Alluvium deposits, typically mixtures of clay, silt, sand, and gravel, were also deposited as deglaciation continued (Bjerklie et al. 2012).

A regional unconformity truncates both the Lake Connecticut glaciolacustrine and drift deposits. The unconformity was generated from the combination of subaerial exposure, following the drainage of Lake Connecticut, and subsequent marine transgression (Lewis and Stone, 1991). Marine deposits, the product of Holocene transgression and highstand conditions, when present, unconformably overlie the glacial sediments (Poppe et al. 2001). Presently, along the harbor's coast, thin beach deposits occur above the glaciogenic sediments (Bjerklie et al. 2012).

Surficial sediments in New Haven Harbor are described in Poppe et al. (1998) and Poppe et al. (2001) and are summarized as follows. Gravel and boulder deposits occur off of Oyster River Point, Lighthouse Point, and Morgan Point. Exposures of glaciogenic deltaic deposits are also located near the aforementioned points. Fine-grained Holocene sediments, e.g., poorly sorted silts, flank the main shipping channel near Lighthouse Point and occur in protected areas adjacent to the breakwaters. Sandy silts are present in the shallow parts of Morris Cove. Sand deposits occur off of Oyster River Point and Sandy Point, as well as through the central part of the outer harbor. Sands are also present outside of the breakwaters in the open water of LIS.

The distribution of sediments in and around New Haven Harbor largely conforms to expectations related to energy levels and the antecedent geologic conditions. The shallower and unprotected areas of the harbor, where currents and waves impinge on the seabed, contain coarser materials. This is owing to the process of winnowing, as the finer grained materials are transported away, exposing the glaciogenic deposits that include gravel and boulders. Quieter depositional environments, e.g., deeper water, restricted embayments, and the lee of breakwaters, host finer-grained sediments (Poppe et al. 1998; Poppe et al. 2001).

Today, New Haven Harbor is considered an urban estuary (Mattei et al. 2015), and its port is the most active within the state of Connecticut (Rozan and Benoit, 2001). Unsurprisingly, given its urban estuary status, the majority of the harbor's shoreline has been engineered (Poppe et al. 2001). It is also one of the most contaminated regions of LIS (Rozan and Benoit, 2001). Pollution input sources to the harbor are its rivers, treated sewage, atmospheric fall-out, sewer overflow, and legal industrial discharge. Pollution sinks inside the harbor are its sediments and salt marshes, and it exports contaminants via outflow to LIS and through dredging (Rozan and Benoit, 2001). The southern extent of New Haven Harbor is bounded by three breakwaters that limit its connection to Long Island Sound. The breakwaters form a partial barrier to hydrologic mass and energy transfer between the open LIS waters and the harbor. As a result of the aforementioned and according to Rozan and Benoit (2001), New Haven Harbor inhibits a "substantial" amount of metal contaminants from reaching LIS. Additionally, the Central Long Island Sound Disposal Site (CLISDS), the EPA designated placement site for formerly dredged material, is located 7 miles south of the New Haven Harbor breakwaters.

Urban development has led to large land reclamation projects that have advanced the coastline around the perimeter of New Haven Harbor (Figure 66) (Wu and Barrett, 2022). Currently, much of the coastal land surrounding New Haven Harbor is less than 3 m above sea level. Also, from Wu and Barret (2022), most of the land advancement into the harbor was to accommodate transportation and industry expansion. However, under projected estimates of sea-level rise and flooding intensification some are predicting a future retreat from the reclaimed land areas.

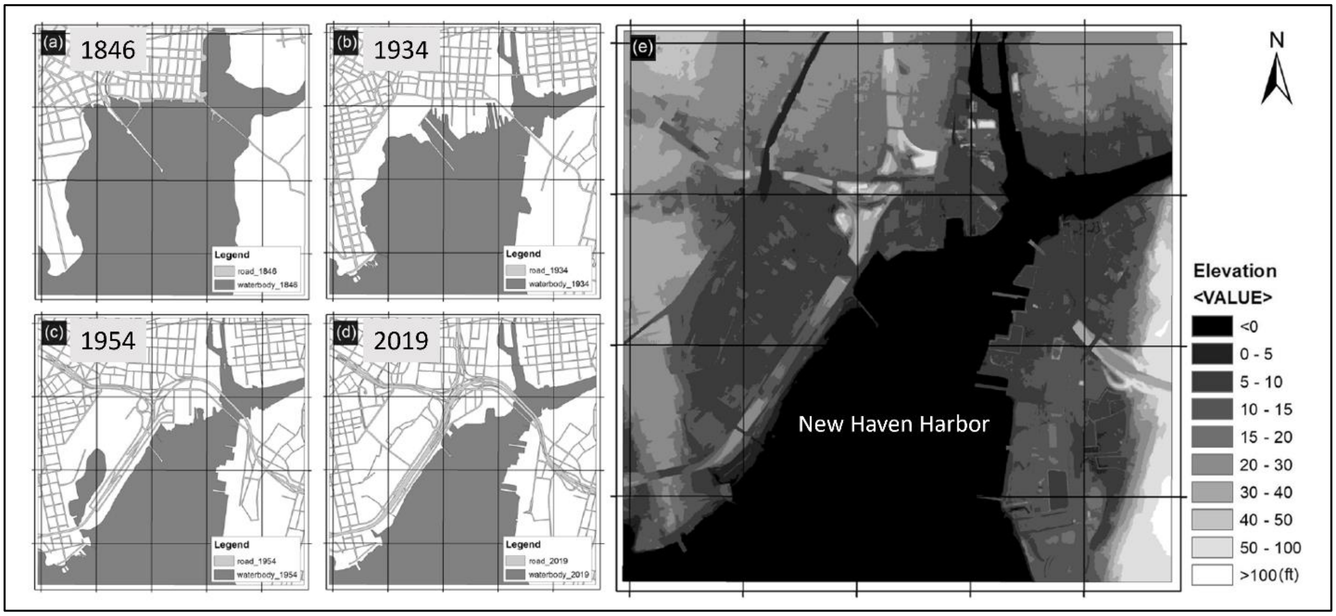

Figure 66. Left, sequence of maps depicting the progress of land reclamation in New Haven Harbor. Right, DTM of New Haven Harbor. Adapted from Figure 3 in Wu and Barrett (2021).

Exacerbating the flood potential in the AOI, despite its relatively northern latitude, is the threat of tropical storm impacts (Poulos, 2010). The AOI is subject to hurricane passages and landfalls by "mature" and "late season" storms that track northward from warmer tropical and subtropical waters (Boose et al. 2001). Tropical storm risk analysis for New England, published in Poulos (2010), incorporated data from 248 storms that crossed the region from 1851 to 2006, demonstrating a "high probability" of occurrence for these events (Figure 67).

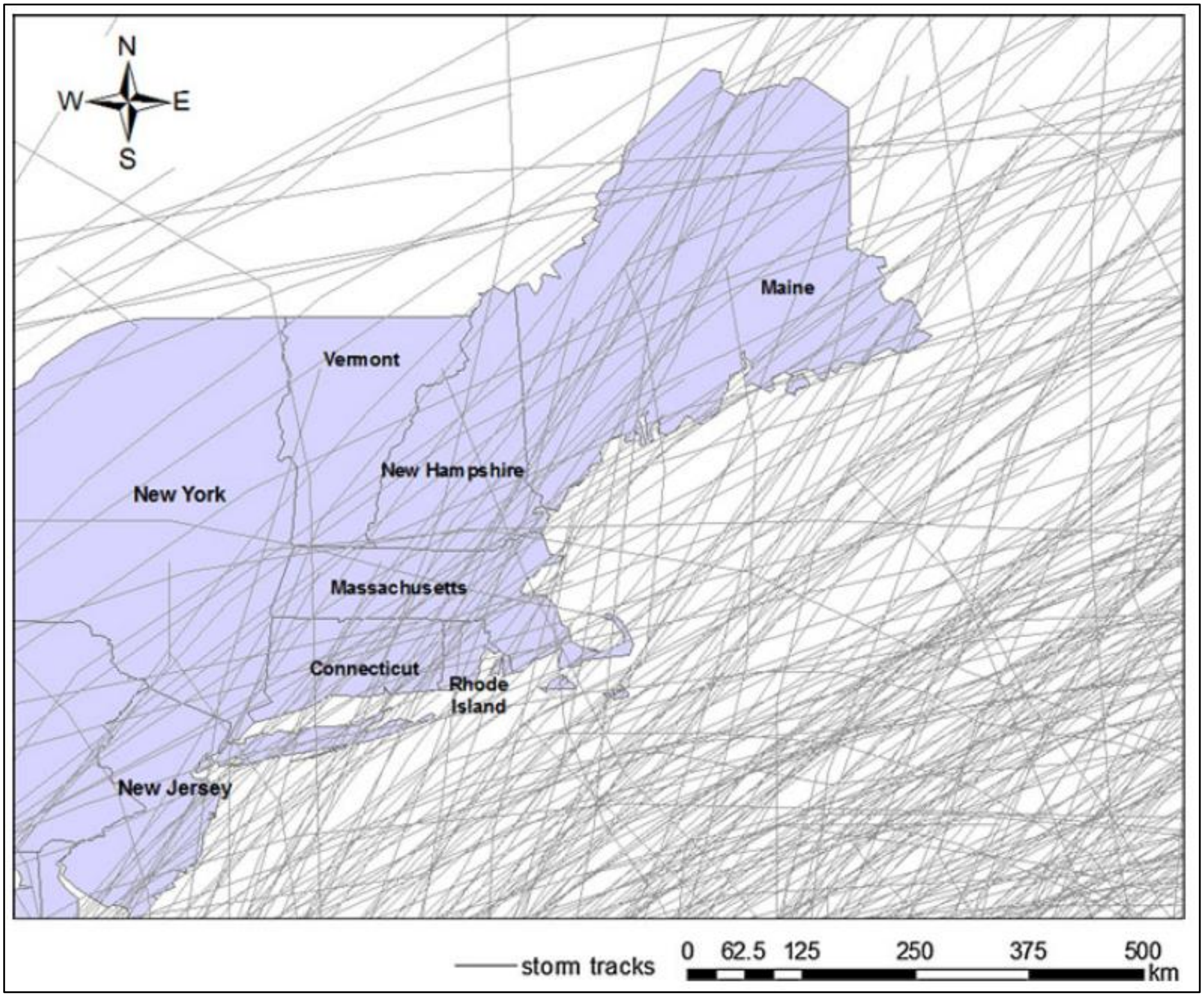

Figure 67. Tropical storm tracks across the N.E. from 1851 to 2006. Figure 1 from Poulos (2010).

The strongest storms that reach New England are those that track northward in the footprint of the Gulf Stream, benefiting from its warm surface water thereby maintaining their intensity (Boose et al. 2001). Further intensification of storm surge and flooding from tropical storms is related to the east-west orientation of Long Island and Connecticut that allows for direct landfalls for northerly tracking storms (Poulos, 2010). Two major hurricanes made landfall near the AOI in the 20th century, i.e., the Great New England Hurricane of 1938 and Hurricane Carol in 1954, that led to the construction of storm mitigation structures in the region (Ullman et al. 2019). However, earlier this century, FEMA declared Southern New England the “Achilles heel of the Northeast” in light of the region’s vulnerability to future tropical storms.

6.2 Investigation Summary

Bathymetric and geophysical data acquired in May 2024 aboard the R/V *Pricus* were processed in Hudson’s Cherry Hill, NJ office using the methods described in Section 4 Geophysical Data Processing. Geophysical results from both Reflection and Refraction data were able to discern clear and consistent horizons representing the various sediments and rock within the survey area. Interpretation priorities were set by the purpose of the survey, and it was determined that specific interfaces between the defined As-Found Geologic units (described further in section 6.2.1) would be defined where relevant to future channel planning. Not all visible interfaces were interpreted.

Horizons created by seismic reflection and refraction are found below in Table 28.

Table 28. Identified and Delineated Seismic Reflectors

Name	Digitized Color	Correlating Geotech	Description	Distribution	Comments
H1_MS_OS	Dark Green	FD24-B-01	Interface Between Marine Sediment and Organic Sediment	0+00 – 75+00 And CAD Cell	Created using 2D reflection and refraction only.
TOR	Red	All Rock Cores	Top of Rock	60+00 – 110+00 AND 180+00 – 220+00	Composite of 3D, 2D, refraction and rock cores

Geotechnical exploration data were collected onboard the LB *Vision* during July and August 2024, where materials were classified on site and samples were temporarily stored at CDM Smiths Geotechnical Laboratory in Acton, MA. The details of the full investigation can be reviewed in Sections 2 and 5. During this portion of the investigation, five main geologic units were encountered; specific characteristics for each unit are reviewed in detail below.

6.2.1 Definition of As-found Geologic Units

Physical sampling of soil units throughout the survey area showed a variety of sediment and bedrock. The geotechnical coring campaign was undertaken to provide physical examples of the subsurface for analysis and categorization. After reviewing the range of physical properties (grain size, color, cohesion, mineral content, plasticity, etc.), broad categories were developed to aid in discussion of the subsurface variability across the site.

Five unique, broad units were identified in the project area: Bedrock, Organic Sediment, Marine Sand, Glacio-marine Silt, and Glacio-marine Sand. Most (>95%) samples taken in the project area fell within one of these five broad categories. Initially, gravel and Glacial Till units were expected in greater abundance and volume, so a gravel and till unit was anticipated. However, data suggested that gravel and till were rarer in this area than expected and in quantities that did not merit separate, identified units.

In the following sections, each unit was defined within the context of this project. The specific values of any physical property (grain size, plasticity, organic content, etc.) should be reviewed in the core logs and laboratory results appendices.

6.2.1.1 ORGANIC SEDIMENT (OS)

Organic Sediments are Modern (Holocene) sediments classified as organic silts and clays as determined by the Atterberg liquid limit method classified in ASTM D 2487. This unit is a depositional setting typical of an estuary marsh, very soft, with higher water content. Most of this sediment unit is found within the CAD Cell and Inner Harbor. With very few exceptions, this unit begins at the seabed to an estimated subsurface elevation between -27' MLLW to -52' MLLW, based on the boring data . These sediments are gray to black in color with medium to high plasticity and low sand percentages (lower than 35%) (Figure 68).

Figure 68. Sample of ORGANIC SEDIMENT (OS) as recovered during field acquisition of soil boring CAD-03

6.2.1.2 MARINE SAND (MS)

Marine Sands are unconsolidated sands deposited and maintained within a marine setting. These sands are black to dark gray with variable silt content in the outer harbor, and in a small area of the CAD Cell. This unit is typically encountered as reddish-brown outwash deposit within the Inner Harbor underlying the organic sediments, with a variable subsurface estimated elevation between -32’ MLLW to -62’ MLLW, based on the boring data. In the outer harbor, this is the most modern unit, including the seabed to the top of rock in most instances. In the CAD Cell, it is found as a small seabed unit near the breakwaters, then reappears underlying the estuary marsh silts as the outwash deposit encountered within the Inner Harbor, with an estimated elevation range of -42’ MLLW to -78’ MLLW based on the six boring locations. These sands are typically subangular to subrounded and homogenous (Figure 69).

Figure 69. Sample of MARINE SAND (MS) as recovered during field acquisition, boring FD24-B-01 and FD24-B-08.

6.2.1.3 GLACIO-MARINE SILT (GM)

Glacio-marine silts are silts deposited from both marine and glaciofluvial/glaciolacustrine sources, pre-Holocene. This unit is primarily found in the outer harbor and within the CAD Cell at elevations below -50.5 to -78.1 ft MLLW. This unit is both red and gray in color due to differing parent material, mica content, and depositional dynamics. Relative density differs between the two areas it was encountered in. The gray material sampled from FD24-B-01 in the outer harbor is a very soft, high plasticity silt, and likely deposited as a glacio-estuary environment. This red unit encountered within the anticipated dredge design template for the CAD call is soft to hard silts and clays, with varying thicknesses of lensing and lamination exhibited within the glaciolacustrine, subset of material. Lensing is not seen in the gray/black marine/estuary subset seen in the outer harbor (Figure 70).

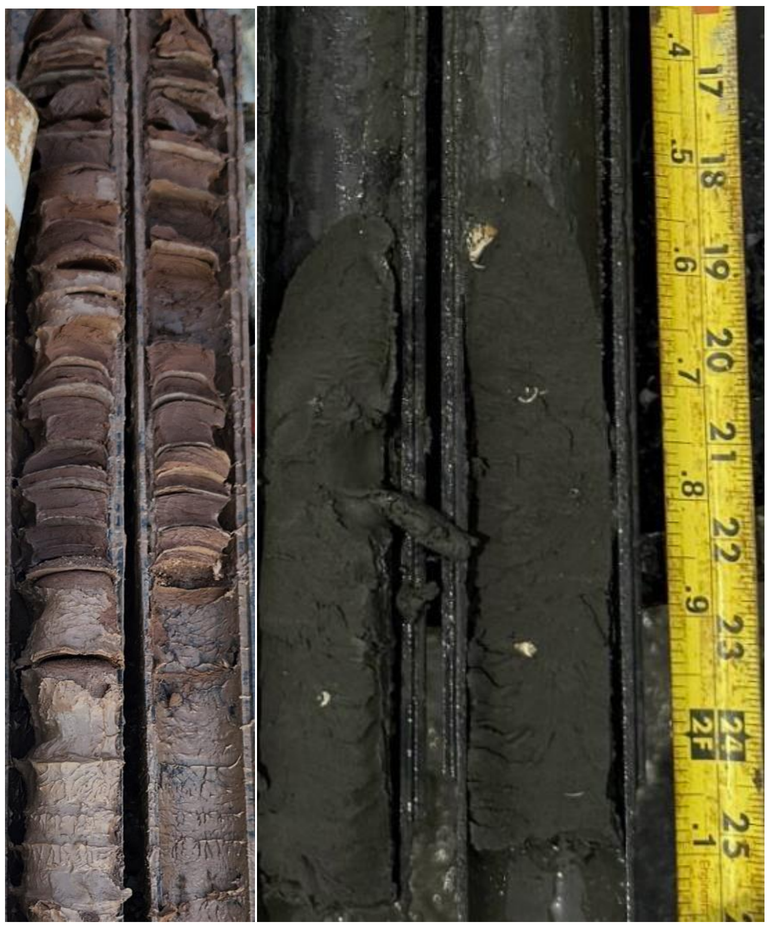

Figure 70. Samples of GLACIO-MARINE SILT (GM) as recovered during field acquisition of soil borings FD24-CAD-01 (left) and FD24-B-01 (right)

6.2.1.4 GLACIO-MARINE SAND (GS)

Glacio-marine sand is primarily found within the CAD Cell. These sands are red/brown in color and are interpreted to be weathered Arkose and deposited during the most recent glacial retreat approximately 11-20kya. This unit is differentiated from the outwash Marine Sands unit due to its higher degree of consolidation, denser N-values ranging from 13 to 89, and is found at lower elevations between -42.1 and -100 ft MLLW underlying the Glacio-Marine Silt in the CAD Cell (Figure 71).

Figure 71. Sample of GLACIO-MARINE SAND (GS) as recovered during field acquisition of soil boring CAD-03.

6.2.1.5 TOP OF ROCK (TOR)

Top of Rock is the interpreted and modeled top of the competent bedrock unit. The surface created from the top of rock interpretation was created from geotechnical cores, seismic reflection, and seismic refraction results. The bedrock encountered during the investigation, between stations 65+00 and 113+25, is a complicated area filled with sharp undulations of extremely hard, altered granite schists that outcrop at the surface, and then dive to over -100 ft or more in some areas. Core petrology results report 100% of samples are Altered Granite Schist with a median UCS of 19,480 psi and a range of 8,860 psi to 27,190 psi. Rock cores were typically fair RQD, with a median percentage of 74% and an average of 70% over thirty-seven rock core runs, and Solid Core Recovery (SCR). P wave velocity analysis from both laboratory testing and in-situ refraction range from 8,018 to 13,591 ft/sec. This unit is interpreted to be the Continental Terrane Lighthouse Gneiss, Paleozoic in age and found on the downthrown (south) side of the Eastern Border Fault as it crosses New Haven Harbor (Figure 72).

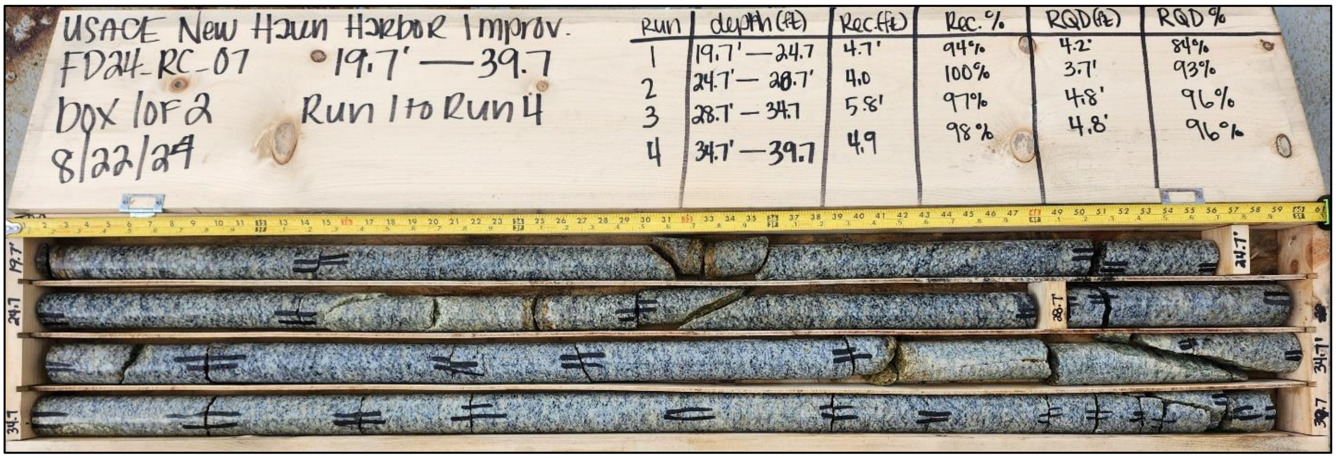

Figure 72. Sample of Rock at FD24-RC-07

6.3 Integrated Results

6.3.1 Outer Harbor (Station 0+00 to 65+00)

6.3.1.1 Surface Results

The seabed of the outer harbor is a homogenous surface consisting of Marine Sands (MS) that have been moved into various, small scale bedforms (ripples, small sand waves, etc.). Here, outside the breakwaters, the seabed is unprotected from the dynamics of Long Island Sound. The surface units found in the borings taken in this area are Poorly Graded Sand with Silt with the silt content being less than 9% and the sand being primarily fine to medium sized. Minor constituents of fine shell fragments, likely bivalves, are present within these surficial marine sands. This is consistent with the high energy environment outside the breakwaters.

Backscatter data results in this area depict a relatively high backscatter intensity when compared to the entire channel. Most variation in this area are attributable to limitations in the frequencies used to image the backscatter and survey direction. Taken as an entire area (0+00 to 65+00) the data presents a homogenous and consistent seabed. Backscatter results between these stations are found below in figures Figure 73 and Figure 74.

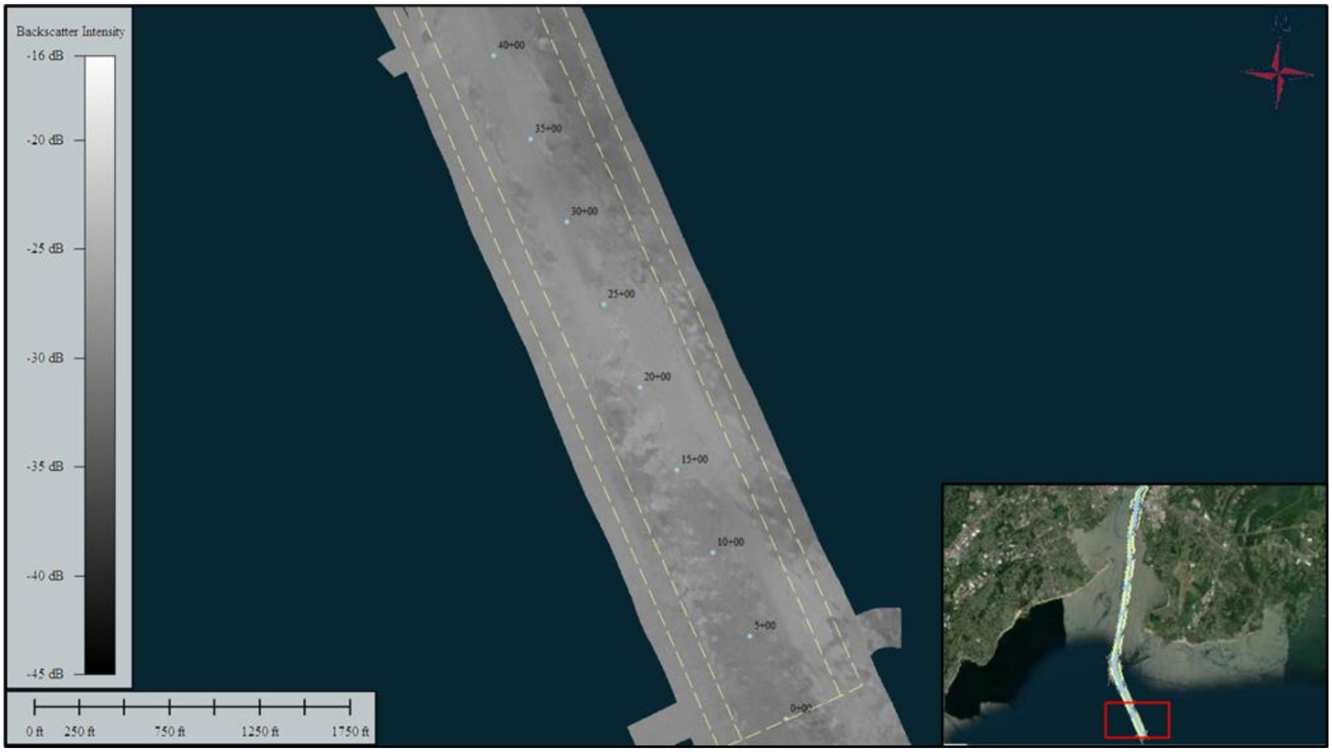

Figure 73. Acoustic backscatter mosaic depicting relative reflectivity of the seabed between stations 0+00 and 45+00

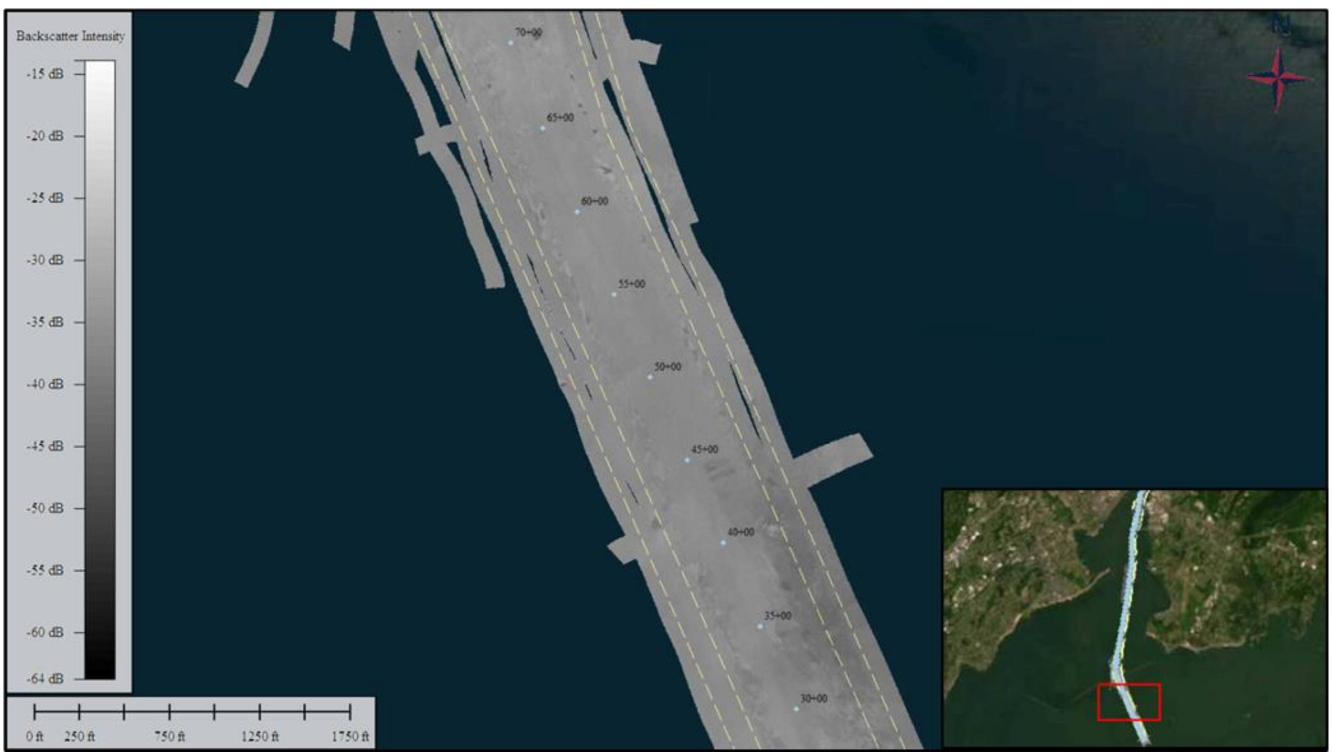

Figure 74. Acoustic backscatter mosaic depicting relative reflectivity of the seabed between stations 30+00 and 70+00

6.3.1.2 Subsurface Results

The Outer Harbor subsurface was found to be primarily Marine Sands within the anticipated dredging design template. Seismic results indicate a highly dynamic history of deposition through the last 20,000 years of sea-level rise. Boring FD24-B-01 (Figure 75) shows a clear interface between the Marine Sand unit (MS) which dominates the surface and sediments within the template, and Organic Sediment (OS) interpreted to be deposited in a paleo-estuary environment before the most recent sea-level rise cycle.

The most relevant borings that capture this Marine Sand (MS) unit from station 0+00 to 65+00 are FD24-B-01 and FD24-B-02.

ELEV	DEPTH	LEGEND	FIELD CLASSIFICATION OF MATERIALS (Description)	% REC	Samp No.
			POORLY GRADED SAND WITH SILT (SP-SM) (2.5Y 3/1), very dark gray, wet, very loose to loose, homogeneous, rapid dilatancy, medium to coarse sand, few shell fragments, Marine Sediments	75	SS-01
				100	SS-02
-40.5	4.0		Some shell fragments	35	SS-03
				100	SS-04
				40	SS-05
-46.5	10.0		SILTY SAND (SM) (2.5Y 3/1), very dark gray, wet, very loose, homogeneous, rapid dilatancy, fine to medium sand, few shell fragments	95	SS-06
-48.5	12.0		POORLY GRADED SAND (SP) (2.5Y 3/1), very dark gray, wet, very loose, homogeneous, rapid dilatancy, medium to coarse sand, some shell fragments	70	SS-07
-50.5	14.0		ORGANIC SILT (OH) (2.5Y 3/1), very dark gray, wet, very soft, homogeneous, rapid dilatancy, trace fine sand, Organic Sediments	20	SS-08
				75	SS-09
				50	SS-10
-56.5	20.0		BOTTOM OF BOREHOLE AT 20.0 ft		

Figure 75. Boring FD24-B-01 Geologic Classifications to 56.5ft MLLW showing Marine Sands (MS) to -50.5ft MLLW and Organic Silt beyond the bottom of the borehole at 56.5ft.

Seismic Horizon, H1 is interpreted to be the interface between Marine Sands and the Organic Sediment. H1 is found in almost all locations below the dredge template and is unlikely to be encountered during excavations. For example, in Boring FD24-B-01 the interface is found at -50.5 ft (Figure 76). The borings were used to correlate the seismic horizons in this area to help define this interface through the area. A small area near station 65+00 the interface pinches out where it encounters the bedrock. This small amount of Silt is potentially within the template.

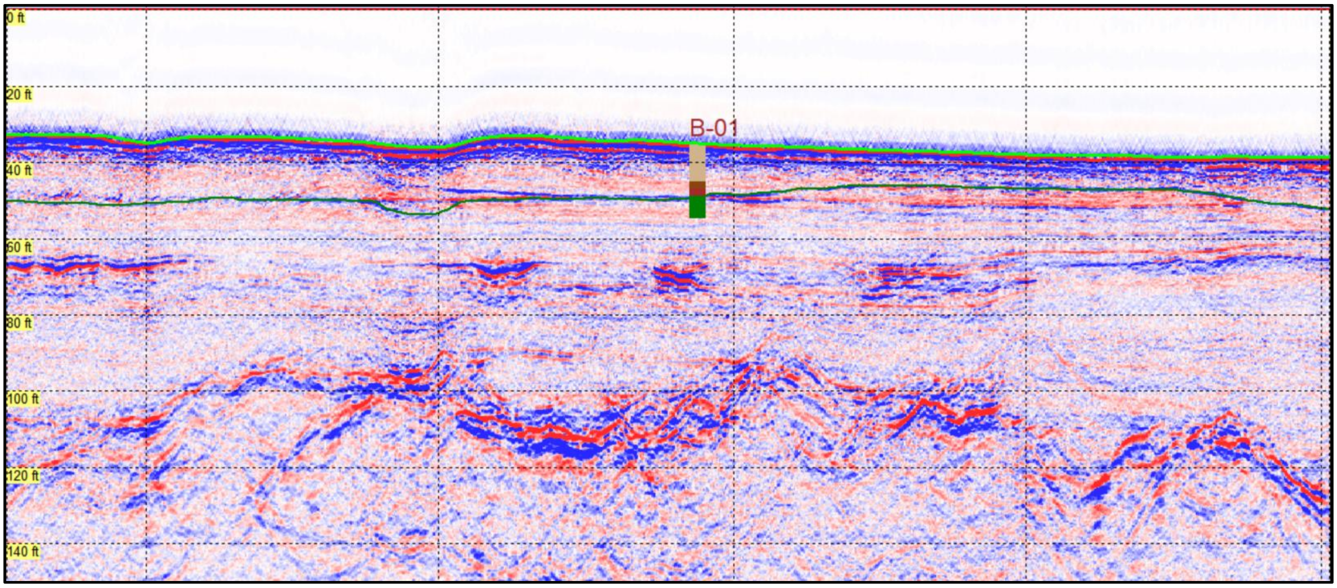

Figure 76. 2D seismic reflection profile with color coded core results from FD24-B-01 shown referenced to the bottom elevation. The interface between MS (Tan, brown and Red) and OS (Dark Green) is seen at approximately -50MLLW. A prominent reflector is seen at this depth.

Bedrock in the outer harbor is found at -175 ft MLLW at station 0+00 and gently rises toward the surface with increasing station. An acute expression of the bedrock is encountered between station 60+00 and 65+00 the bedrock rises from 60 ft below the surface to 7 ft below the surface. This is in the immediate vicinity of rock core FD24-RC-01. At this point, the rock remains significantly present until station 113+25.

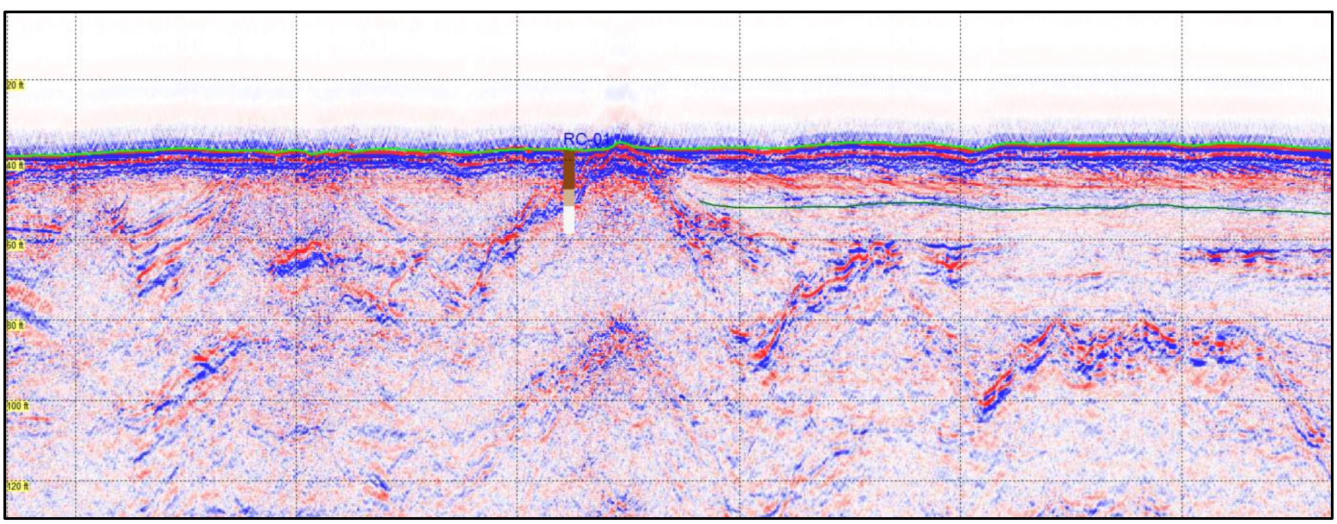

Figure 77. Seismic profile along RC-01 depicting the abrupt rise and near-outcropping of bedrock near station 65+00.

Refraction Tomography sections accompany this report in Appendix E. These profiles depict the results of the refraction survey and within the specific Outer Harbor stations the results match the expectations of the seismic reflection data.

For the Outer Harbor, please refer to refraction profiles R5001, R5003, R5004, and R5007 to view the P-wave velocity profiles within these station ranges 0+00 to 65+00. The refraction profiles begin approximately at station 15+00 because from station 0+00 to station 15+00 the bedrock is too deep to image and therefore the tomography results are null in this area. Once the bedrock rises to approximately Elevation -130 ft the refraction array can reliably detect it. An example profile acquired relatively along the centerline is shown below in Figure 78.

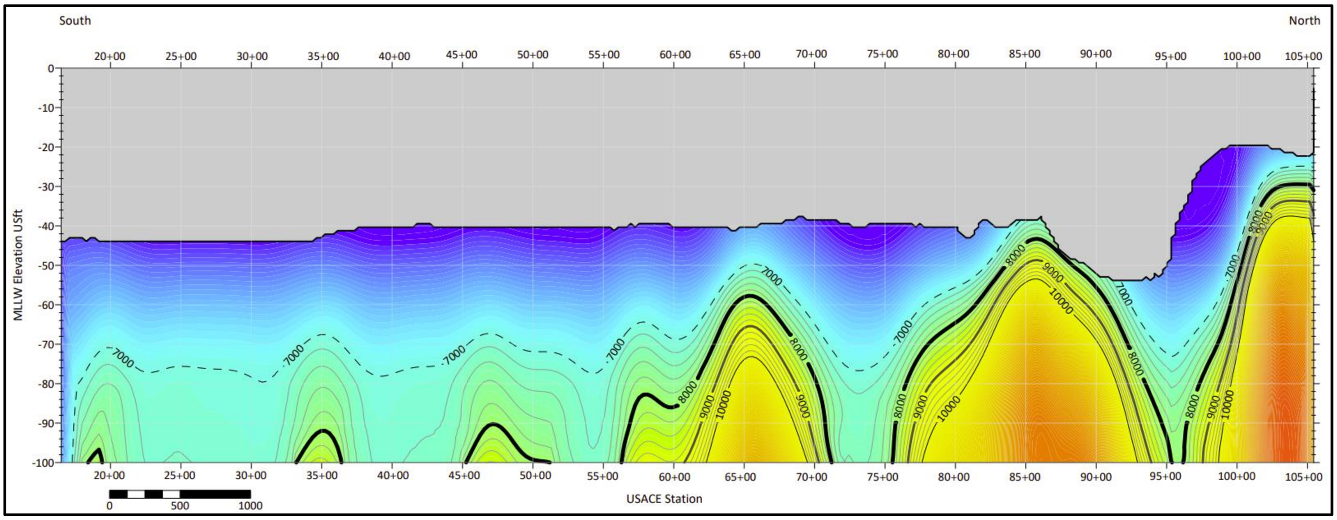

Figure 78. Example refraction profile along the approximate centerline of the channel template. P-wave velocity contours are reported in ft/sec.

6.3.2 Rock Area of Interest (Station 65+00 to 113+25)

6.3.2.1 Surface Results

The seabed of the outer harbor between stations 65+00 and 120+00 contains two seabed sediment units: Marine Sands (MS) that have been moved into various, small scale bedforms (ripples, small sand waves, etc.), and Organic Sediment (OS) that appear to be accreting on top of the Marine Sands unit. This span of channel is both inside and outside the breakwaters, with that division being approximately 85+00.

Outside the breakwaters, the seabed is unprotected from the dynamics of Long Island Sound. The surface units found in the borings taken in this area are Poorly Graded Sand with Silt with the silt content being less than 9% and the sand being sized medium to coarse. This is consistent with the high energy environment outside the breakwaters.

Inside the breakwaters, the seabed remains sand until a clearly defined boundary that curves across the channel, striking approximately NW/SE and running between station 95+00 and 115+00. Between these stations a transition occurs from the Marine Sands dominated surface sediments from Long Island Sound and the Organic Sediment from the New Haven Estuary. Between these stations the surface and shallow subsurface sediments will contain varying amounts of MS and OS. This is visually represented in Figure 81 below where the orange S-shaped line denotes a relative boundary for this accretion of organic sediments. Generally, between these stations the OS sediments are found in lower stations where the water is shallow, up on the channel shoulders, and MS sediments remain where water is deepest. From station 115+00 and northward, the surface is more consistently OS with some notable MS outcroppings in the deeper parts of the maintained channel. Shallow areas of channel shoulders and higher up the slope, the surface sediment is consistently OS.

Backscatter data in this area depict a relatively high backscatter intensity when compared to the entire channel. Backscatter results between these stations are found below in Figure 79 to Figure 81. Most variation in this area are attributable to limitations in the frequencies used to image the backscatter and survey direction. Taken as an entire area (65+00 to 113+25) the data presents a homogenous and consistent seabed until station 95+00 where it begins to transition into lower reflectivity (Figure 81).

Figure 79. Acoustic backscatter mosaic depicting relative reflectivity of the seabed between stations 60+00 and 100+00

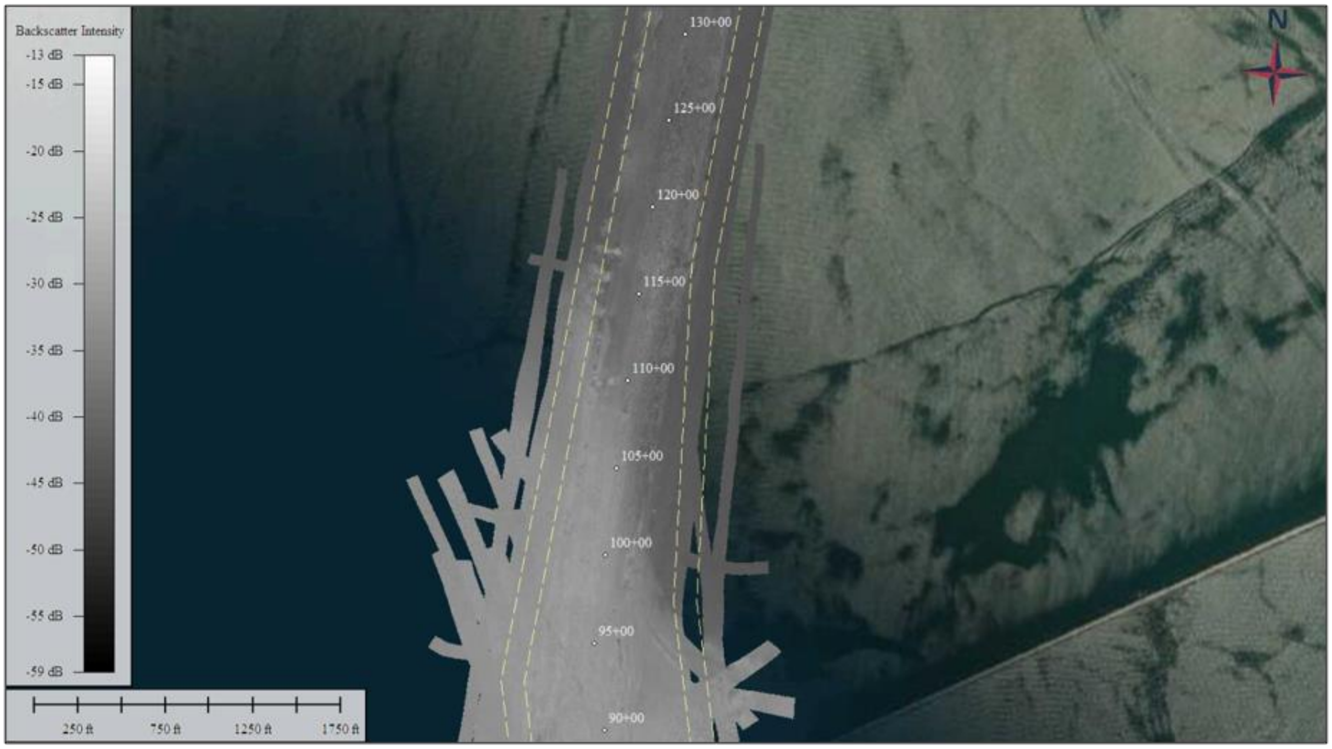

Figure 80. Acoustic backscatter mosaic depicting relative reflectivity of the seabed between stations 90+00 and 130+00

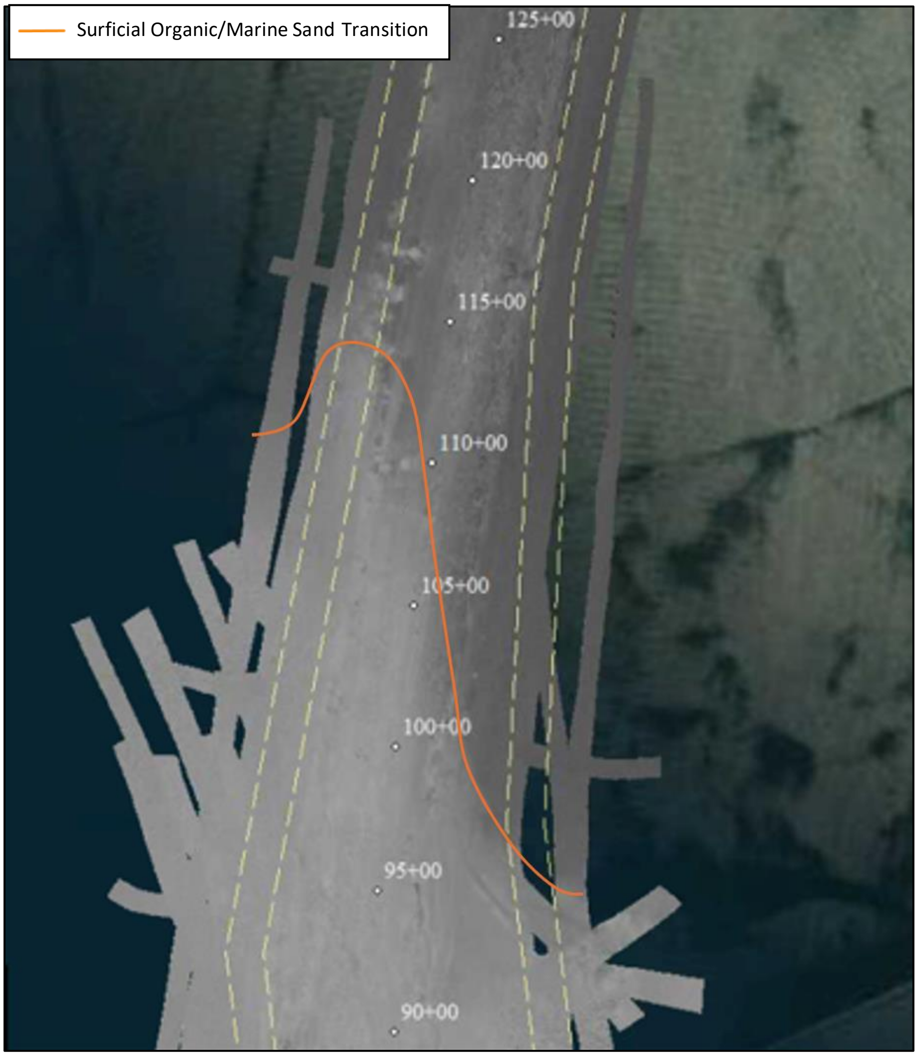

Figure 81. Acoustic backscatter mosaic depicting relative reflectivity of the seabed between stations 95+00 and 115+00, where surficial Marine Sands transition to Surficial Organic Sediments.

6.3.2.2 Subsurface Results

The subsurface between stations 65+00 and 113+25 is a complicated area filled with sharp undulations of extremely hard, altered granite schists that outcrop at the surface, and then dive to over -100 ft in some areas. Laboratory results show that this rock is extremely hard and with UCS values above 8,000 psi with a plurality of specimens reporting over 16,000 psi values. Most of the rock is found between 80+00 and 110+00 with two smaller but significant outcroppings found at station 65+00 and 75+00. In the images below, Figure 82 through Figure 84, examples of the recovered rock from different cores in the rock area are presented. These are for illustrative purposes and are not comprehensive.

Figure 82. Photo of Bedrock Recovered from FD24-RC-01 in vicinity of outcrop at Station 65+00

Figure 83. Photo of Bedrock Encountered at FD24-RC-06, Station 77+57

Figure 84. Photo of Bedrock encountered at FD24-RC-04, Station 92+07

The surface sediment unit is Marine Sands (MS), and it extends all the way to the top of rock. No significant gravel or glacial till deposits were encountered throughout the area but it is possible and expected that some small, localized gravel will be found within the sand layers from outwashing events. It is also possible that thin lenses of Glacial Till deposits may be encountered on top of the rock in localized areas since Glacial Till was encountered at borings FD24-RC-02 and FD24-RC-03. Previous research from Bjerklie et al. (2012). suggested that Glacial Till should be encountered at the crests and troughs of undulating bedrock and the findings in borings FD24-RC-02 and FD24-RC-03 are consistent with this previous work. An example of the Glacial Till as recovered in FD24-RC-03 is shown below in Figure 85.

Figure 85. Marine Sand overlying a thin lens of Glacial Till above Top of Rock at FD24-RC-03

Seismic reflection data collected in this area was successful in defining the top of bedrock and its complicated setting throughout these stations. The bedrock can be found outcropping at the surface in some areas and at depths over -100ft MLLW in others. Figure 86, Figure 87, and Figure 88 depict the 2D seismic profiles across stations 87+00, 93+00, and 99+00, respectively. The highly variable top of rock surface is shown in black. In these figures you will see the bedrock outcropping at the surface, and sufficiently deep all within a very short span of channel. Due to this complicated environment, the results of the 3D, 2D, geotechnical and refraction datasets were combined into a single Top of Rock (TOR) surface to guide the expectations of rock locations.

The accompanying charts depict the TOR surface as contours as well as polygon areas where the rock is found at depths within consideration for the dredging design. Please refer to the drawing sets in Appendix D for a comprehensive understanding of the rock locations and top of rock depth distribution throughout the area.

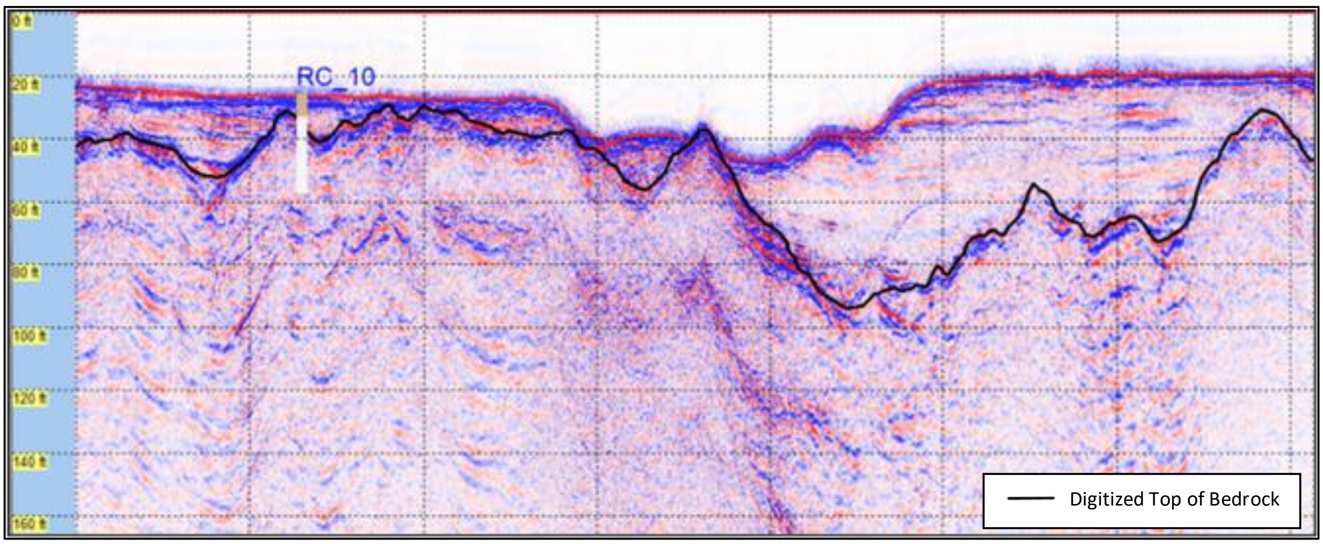

Figure 86. 2D seismic profile across station 87+00. Top of Rock is digitized in black, and FD24-RC-10 is shown for reference.

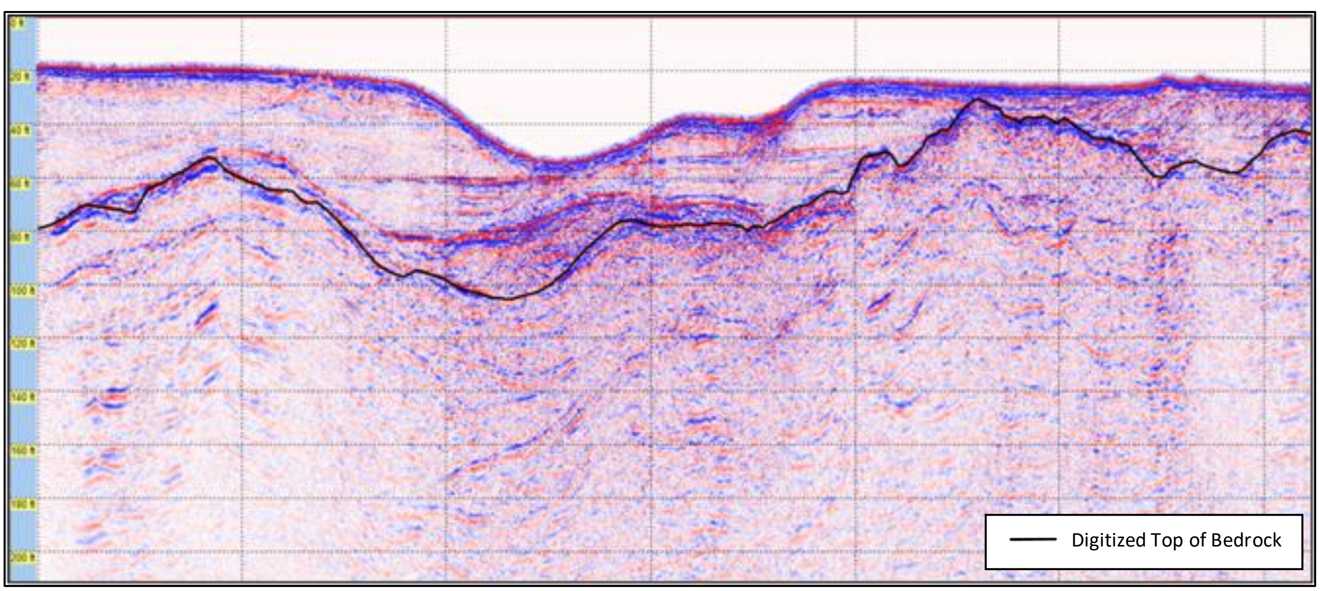

Figure 87. 2D seismic profile across station 93+00. Top of Rock is digitized in black.

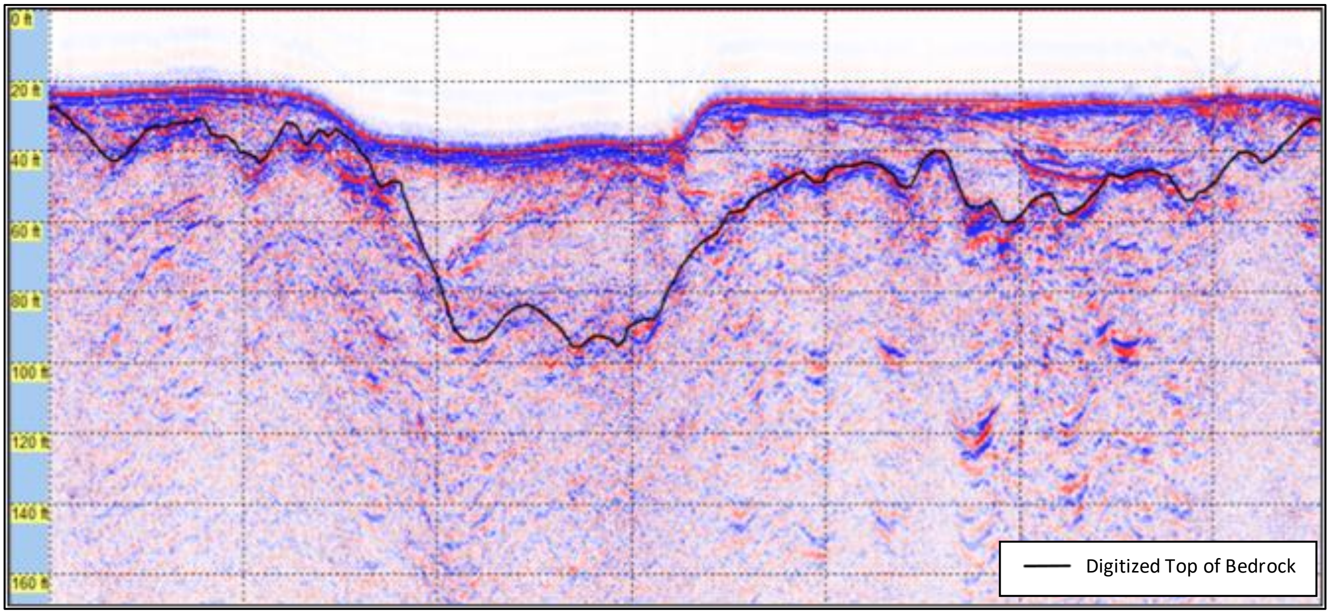

Figure 88. 2D seismic profile across station 97+00. Top of Rock is digitized in black.

Seismic refraction data was collected along all stations in the Outer Harbor. Refraction data collected in this area shows a complex, highly dynamic environment containing everything from saturated sediment to solid crystalline rock. Velocities encountered ranged from less than 5,000 ft/sec (interpreted to be saturated, unconsolidated sediment) to more than 18,000 ft/sec (interpreted to be competent, granite schist). An example detail of a refraction profile is provided below in Figure 89.

The refraction data is particularly useful for understanding the northern boundary of the rock area, nominally station 113+25. Based on geologic maps and the steepness of the bedrock dip, this boundary was interpreted to be an expression of the Eastern Boundary Fault (Rodgers, 1985). Between stations 95+00 and station 113+25, the bedrock dips steeply to the north. This is entirely consistent with the results of the seismic reflection surveys and rock core results.

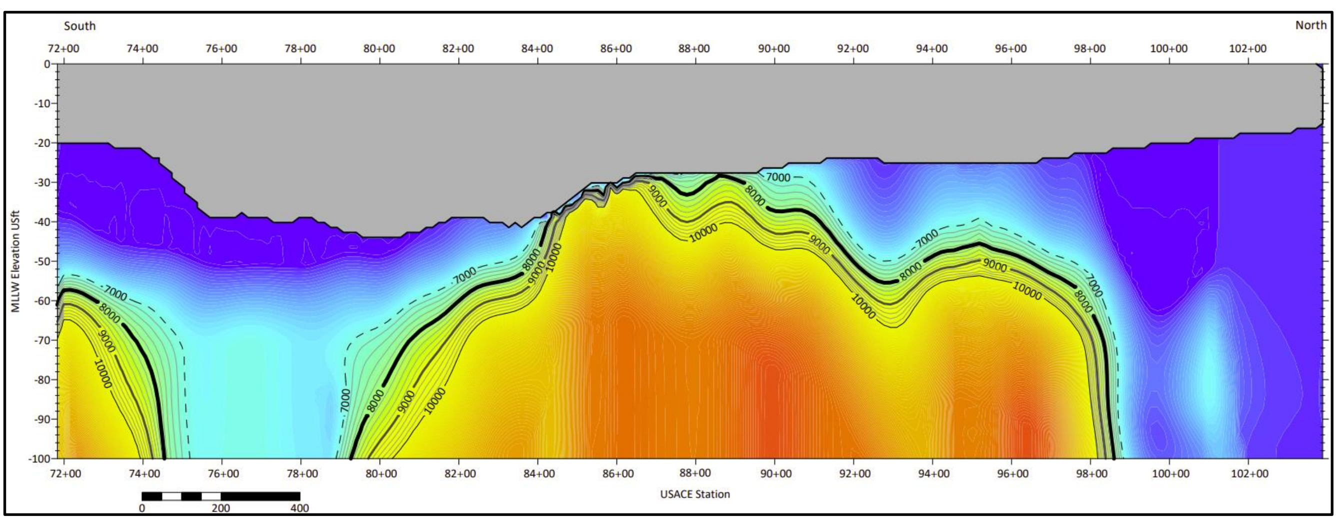

Figure 89. Detail of 2D seismic refraction contour profile for trackline R3001_A. Contours represent P-wave velocity in ft/sec.

Below in Figure 90 the upthrown side of the Eastern boundary fault can be seen at approximately 109+00 where the velocity drops precipitously with increasing station. By station 110+00, the bedrock is found well over -100 ft MLLW, where it remains for most of the Inner Harbor and CAD Cell areas. The variation in velocity across the profile from station 74+00 to 122+00 demonstrates the complexity of the underlying bedrock.

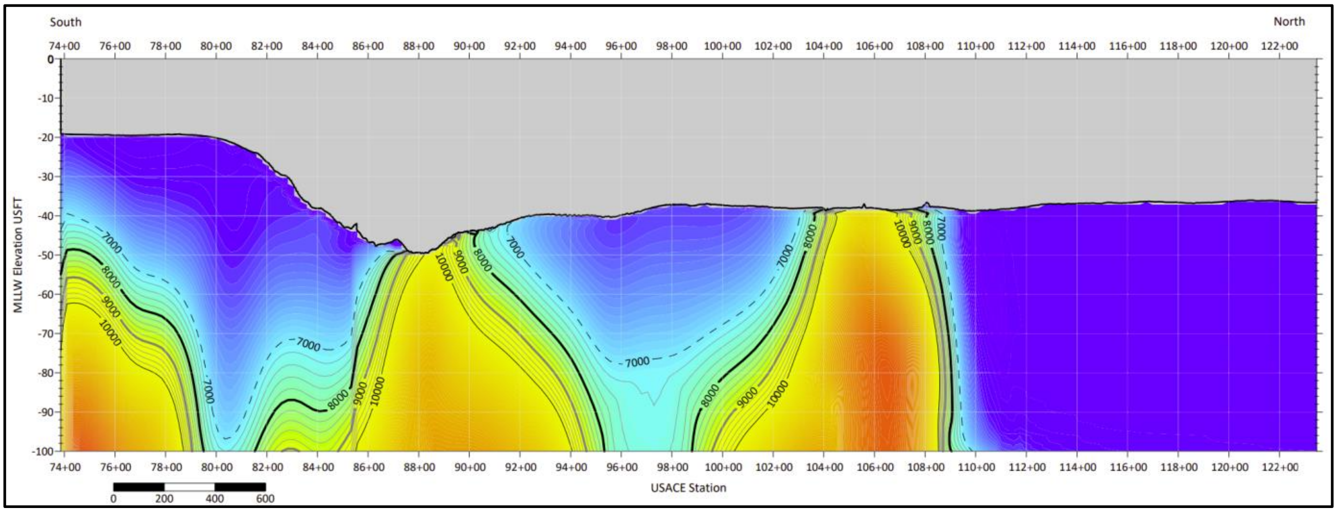

Figure 90. Detail of 2D Seismic refraction profile for track line R3003, approximately along the channel centerline from 90+00 through 122+00. Contours represent P-wave velocity in ft/sec.

6.3.3 CAD Cell

Six (6) geotechnical Borings were collected within the CAD Cell boundaries achieving an elevation termination depth of approximately -100 ft MLLW. Due to the shallow water depths and gas-laden surficial Organic Sediment (OS), the seismic reflection data collected in the area is not of sufficient quality to identify the geologic units found in the 6 cores. Seismic refraction data was able to show that the bedrock is sufficiently deep (>200 ft below surface) as to not impede material removal within the CAD template.

Subsurface results from the CAD Cell, therefore, are based almost entirely on the geotechnical borings performed with prefix CAD (FD24-CAD-01 Through FD24-CAD-06). Seabed analysis and surficial material were imaged and analyzed with a combination of the borings and backscatter/MBES data to determine the extents of the Marine Sands (MS) layer found near the modern breakwaters and to identify a potential man-made hazard (pipeline) near the surface of the northern CAD Cell area.

In the accompanying profile drawing provided in Appendix D, the CAD Cell template is depicted along with these identified geologic units. The Geologic units are a combination of as-found results from the 6 geotechnical borings, and direct interpolation between those borings. As with any interpolation, uncertainties of the precise shape and elevation of the interface are modeled, and not directly observed. CAD cell cross sections containing the actual geotechnical cores should be viewed as less uncertain than those that only contain interpolated data.

6.3.3.1 Surface Results

Water depths within the CAD cell vary from approximately 3.5 to 11.5 ft with the shoalest areas being proximal to the existing breakwaters. The water depth gently increases toward the main channel to the East (Figure 91). The shoalest, high-energy areas near the breakwaters are correlated with a surface unit of Marine Sand (MS). This unit is observed in Borings FD24-CAD-01 and FD24-CAD-03. In the areas covered by the remaining CAD borings the surface unit is

Organic Sediment (OS). Because of the correlation between the dynamic environment around the breakwater and occurrence of the MS unit in soil borings, it is likely that the MS layer follows an approximate depth contour, yet unknown. MBES surface texture suggests this contour is roughly 5 ft, MLLW water depth.

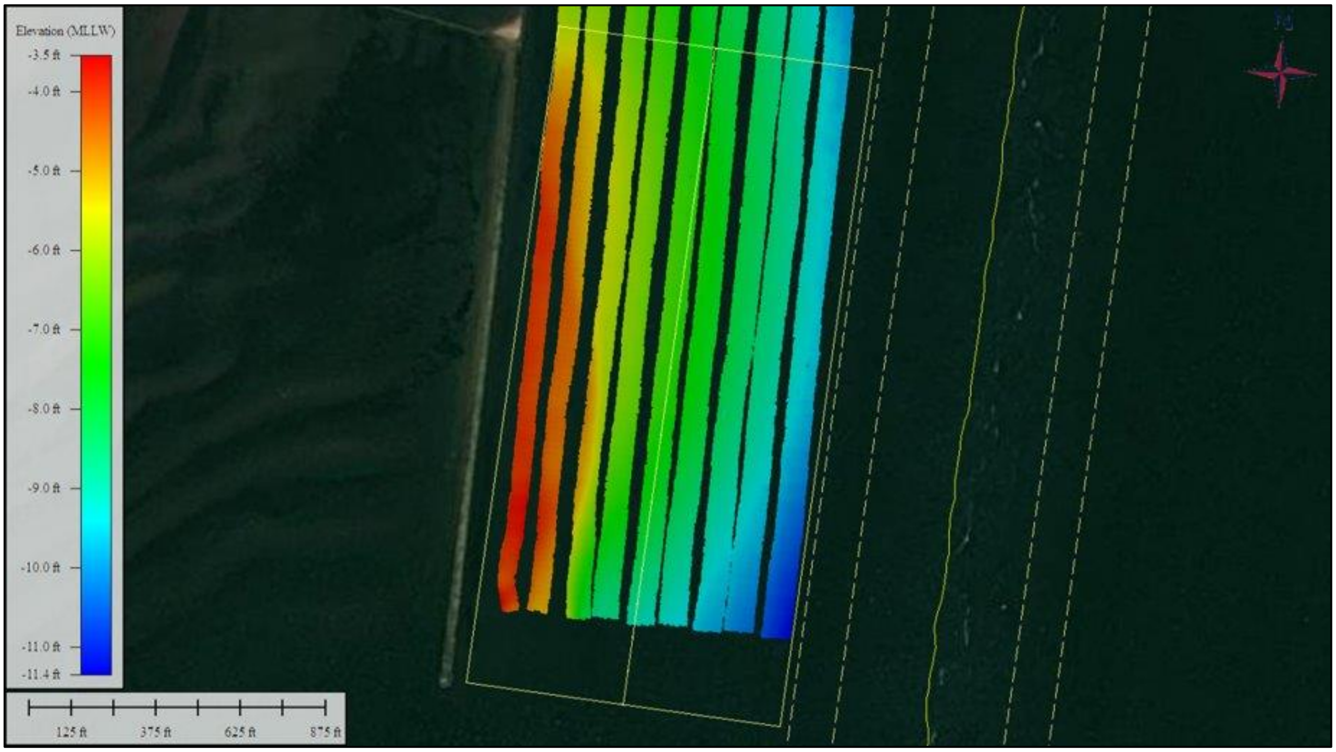

Figure 91. Color coded bathymetry shown with CAD Cell boundary (solid yellow rectangles)

Acoustic Backscatter data indicates the CAD cell is homogenous with small patches of higher reflectivity in the southwestern portion of the mosaic (Figure 92). Correlating the backscatter to the soil borings, most of the surface area is interpreted to be Organic Sediment (OS), and the small patches of higher reflectivity are interpreted to be larger grains, likely Marine Sands (MS). Due to water depth constraints, acoustic backscatter is not available near the modern breakwaters where a layer of Marine Sand (MS) is found to be present in the upper 3 ft. It is reasonable to infer from data collected that the MS layer is found primarily in the Southwest quarter of the CAD Cell and the remaining area is OS with negligible sand.

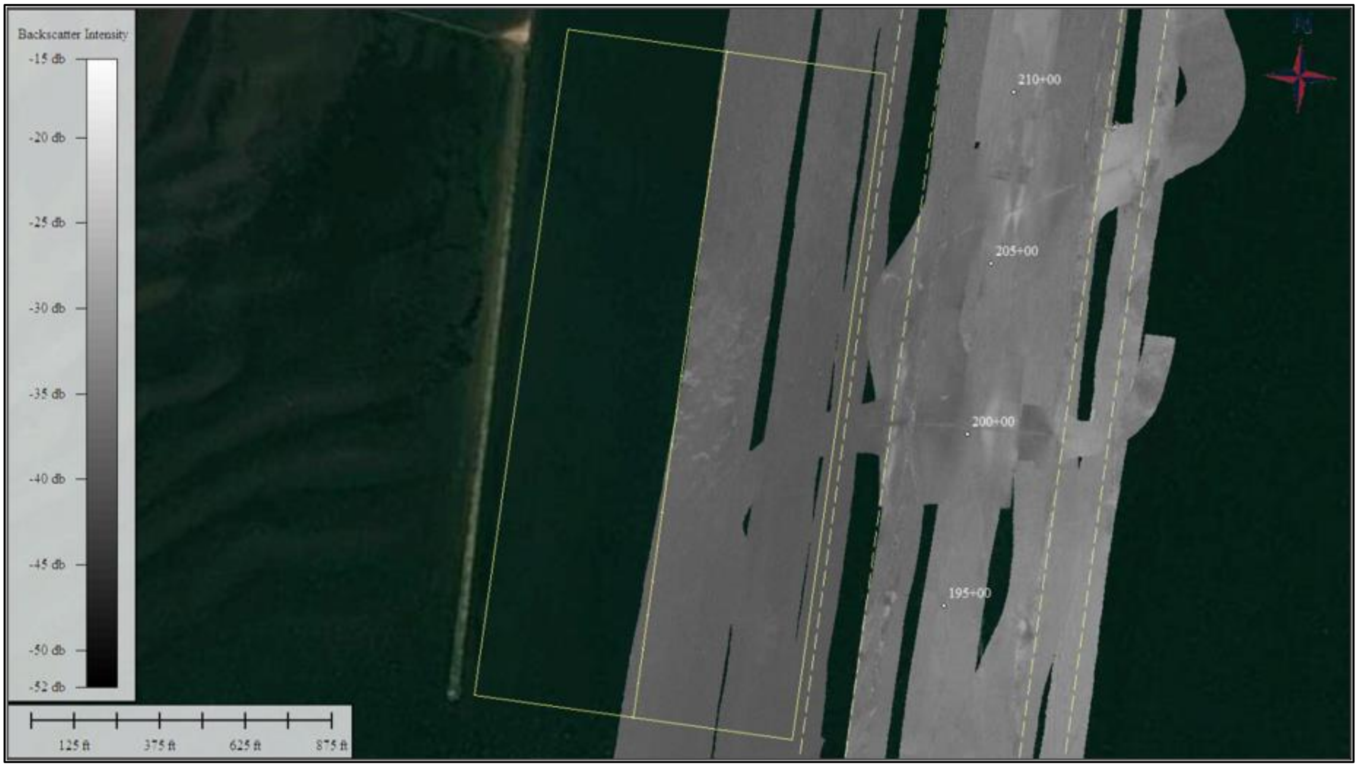

Figure 92. Acoustic Backscatter mosaic with the CAD Cell boundary (solid yellow lines).

6.3.3.2 Subsurface Results

CAD Cell borings reached an elevation depth of -100 ft MLLW. The six borings within the boundary provide us with the deepest, and potentially the oldest sediment units collected in the Inner Harbor area. An example boring log from the CAD cell is shown below in Figure 93. The sediment units encountered throughout the CAD cell area are substantially consistent in sequence: Organic Sediments (OS), Marine Sand (MS), Glacio-Marine Silt (GM), Glacio-Marine Sand (GS). Near the breakwaters there is a thin layer of modern Marine Sand (MS) up to about 3 ft thick on top of the Organic Sediment.

The uppermost units in the CAD cell are both Organic Sediment and Marine Sand. Organic sediment begins at the seafloor on the East side of the CAD cell area, away from the breakwaters. As one moves West, toward the breakwater the surface unit gradually becomes Marine Sand until this unit is about 3 ft thick.

The interface between Organic Sediment and Marine Sands is found between -30 ft and -35 ft. This substantial sand unit is about 15 ft thick and is underlain by Glacio-Marine Silt (GM). The interface is found between -50 ft and -75 ft and is visually obvious with grey Marine Sands turning to red, lensed silt.

Below the Glacio-Marine Silt (GM) is a layer of Glacio-Marine Sand (GS). The top of this GS unit dips quite steeply to the southwest. At the shallowest point sampled, the GS layer is found about -73 ft MLLW at FD24-CAD-06, and beyond the bottom of the borehole (-100 ft) at FD24-CAD-01. An example of this interpreted sequence is found in Figure 94.

Due to shallow water, gaseous surface sediment and depth of interfaces, the seismic data within the CAD cell is not sufficient to define these above-mentioned interfaces. Nearby seismic data shows that the bedrock is at least 50 ft below the bottom of the planned CAD cell, -150 ft MLLW.

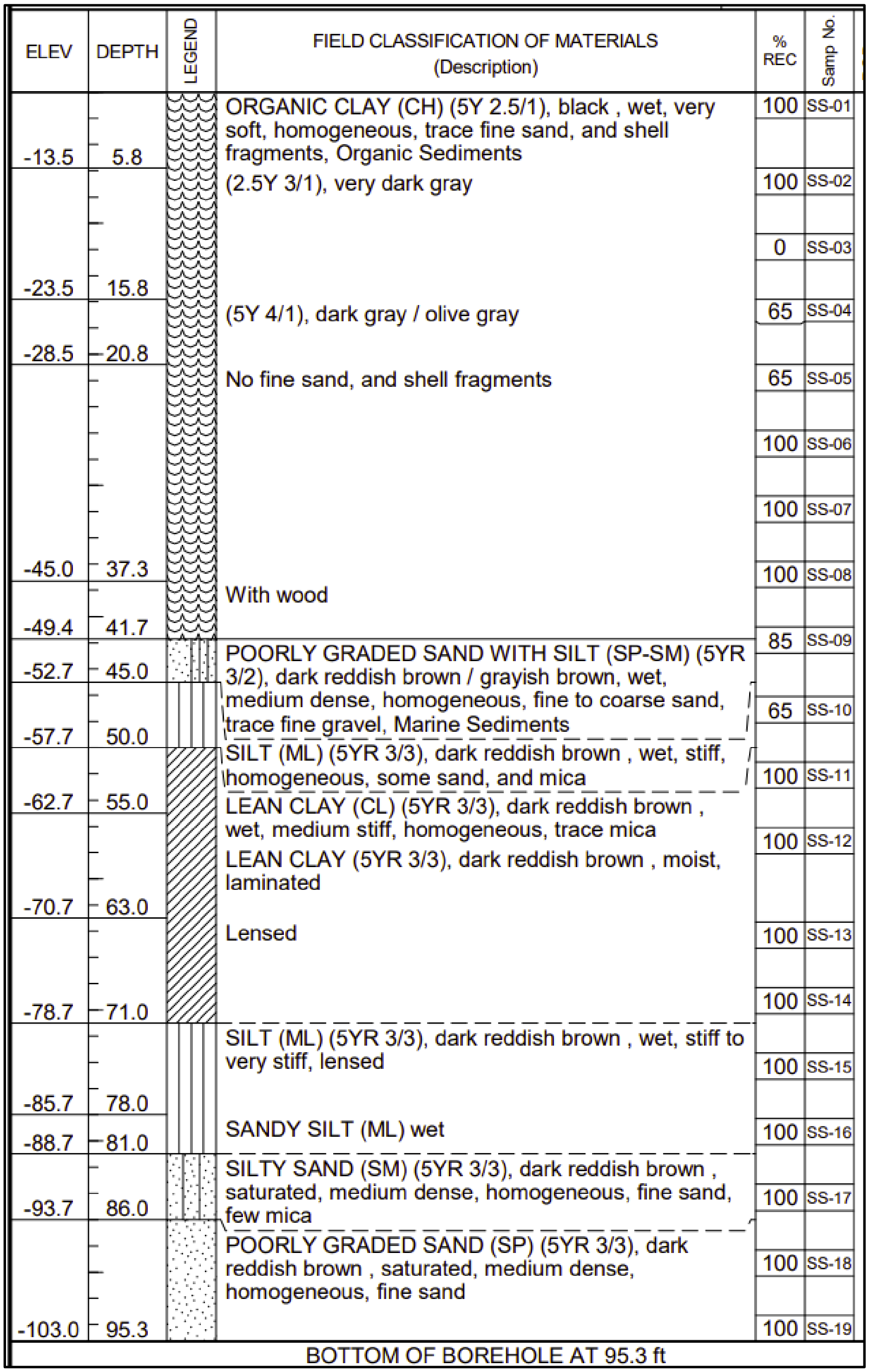

Figure 93. Example of Typical CAD Cell sediment sequence from Boring FD24-CAD-03

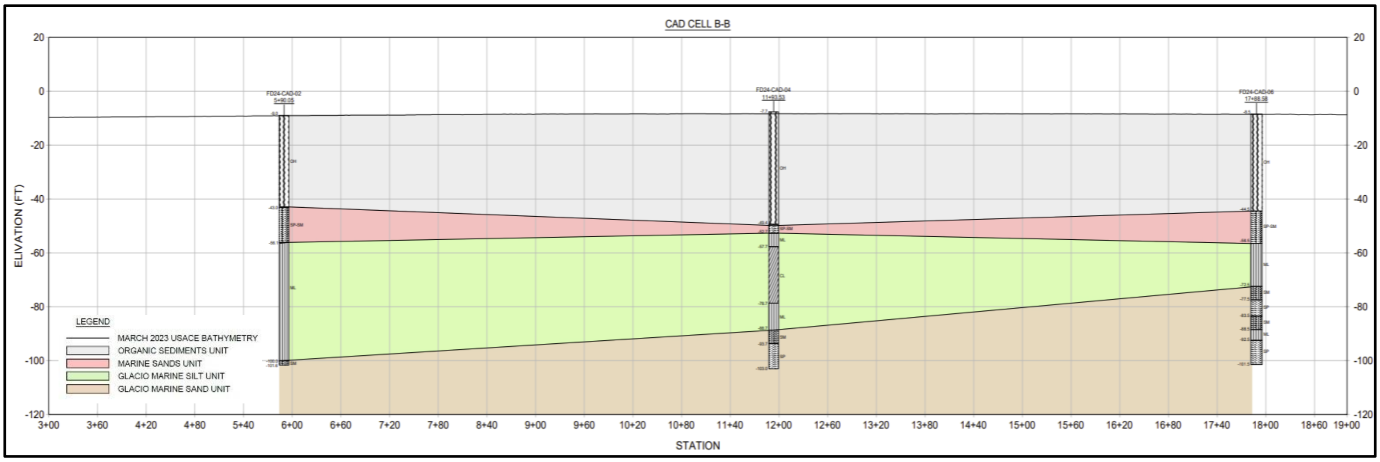

Figure 94. Example CAD Cell geologic interpretation

6.3.4 Inner Harbor (Sta. 113+215 to 324+50)

6.3.4.1 Surface Results

Surface units recovered in geotechnical borings within the Inner Harbor consistently show a surface and upper sediment unit of Organic Sediment (OS), the primary constituent is Organic Silt with some varying amounts of secondary sand. Multibeam bathymetry shows a highly disturbed bottom especially in water depths shallower than 35 ft (Figure 96). This is consistent with an active port setting. These disturbances create a mottled texture in the Backscatter (Figure 97 - Figure 102). Areas where the acoustic intensity is highest are potentially areas where the Marine Sands layer is outcropping above the Organic Sediments. For example, the eastern half of the channel between station 265+00 and 280+00 has a higher reflectivity than the surrounding seabed.

The modeled surface units created from all geotechnical borings does depict areas where the Marine Sands Unit is the surface unit. For example, Station 286+00 shows both Organic Sediment and Marine Sands as the surface unit (Figure 95). Each station in the Inner Harbor should be viewed considering the modeled surface and backscatter imagery to assist in understanding the volume differences between the amounts of OS and MS encountered in the Inner Harbor.

The marine sands unit is geologically older and is the second sediment unit. Where the modern Organic Sediment has been removed to a certain depth, the Marine Sands are exposed. In general, the Marine Sands are found at shallower depths in the North and deeper in the South.

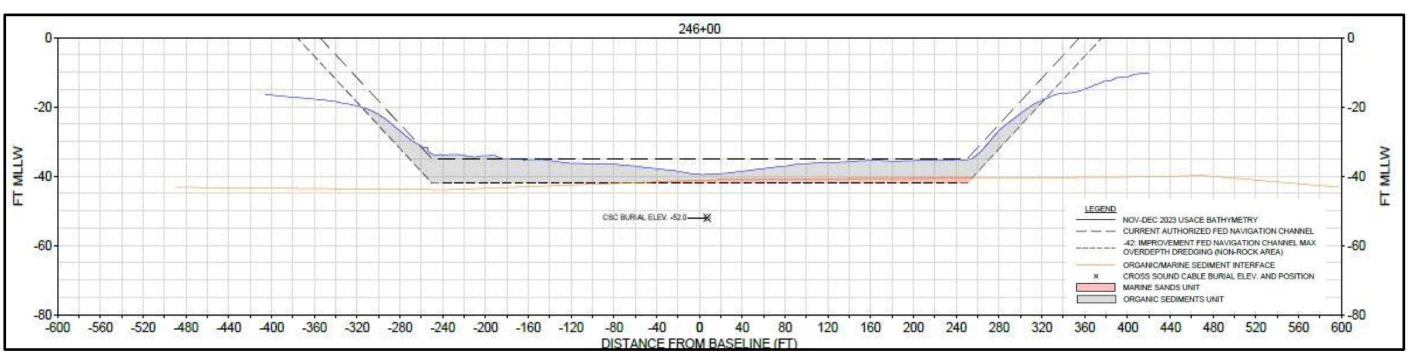

Figure 95. Example geologic interpretation profile of station 246+00 showing Marine Sands (salmon color) and Organic Sediment (gray color) as the surface unit

GBA ENGINEERS ★ SURVEYORS EST. 1974
S. T. HUDSON ENGINEERS, INC.
PROFESSIONAL ENGINEERS & CONSULTANTS

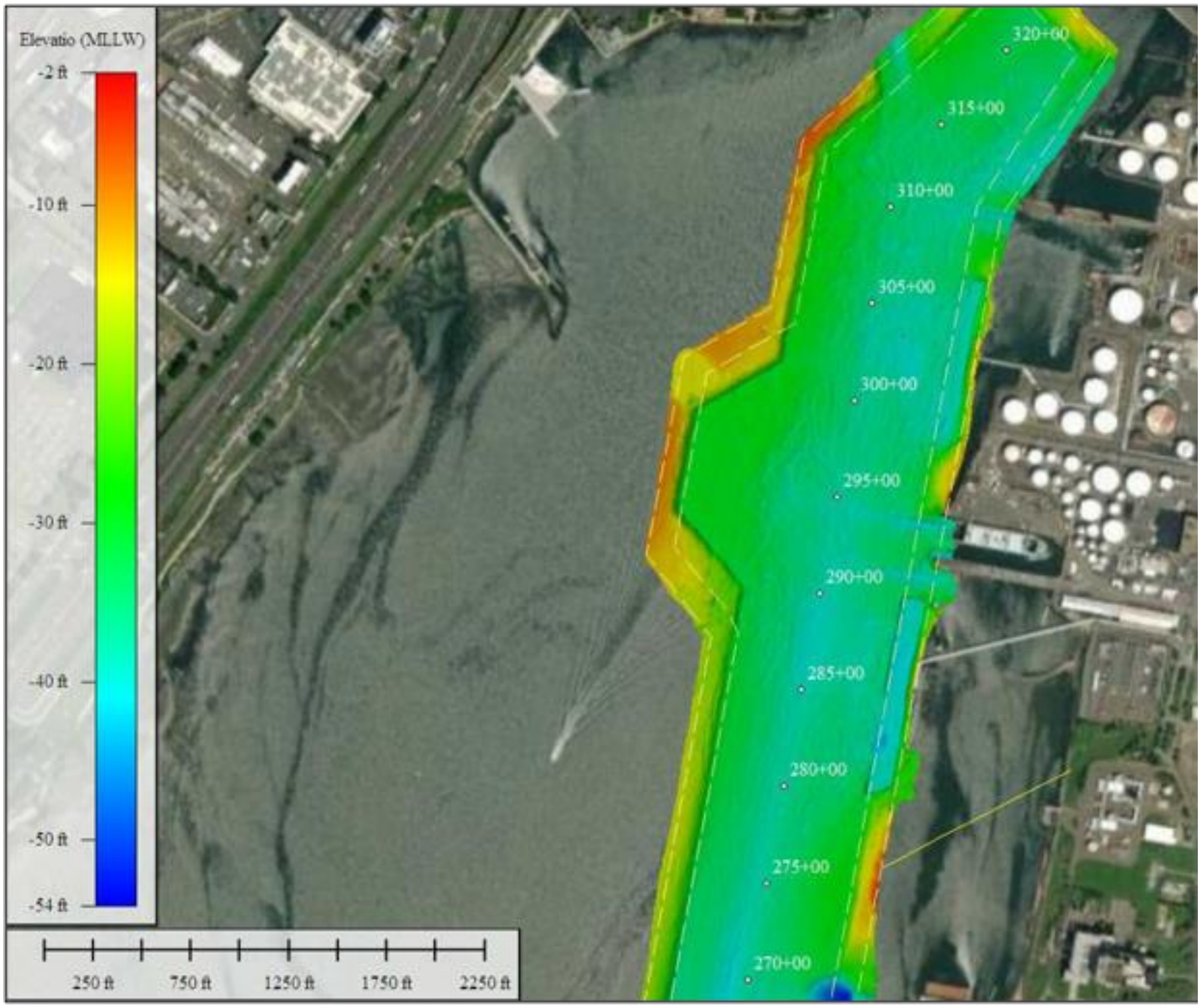

Figure 96. USACE Provided Multibeam bathymetry depicting typical surface texture of the Inner Harbor

Figure 97 through Figure 102 below show the Backscatter mosaic referenced to the channel template. The surface variations of texture and reflectivity (mottled appearance) can be seen throughout the Inner Harbor. Based on surface samples taken, the variations of acoustic reflectivity do not corelate to a meaningful change in sediment grain size. They are most likely linked to bottom roughness texture and small veneers of increased secondary sand.

Figure 97. Backscatter mosaic of acoustic intensity shown with channel stationing and channel boundaries

Figure 98. Backscatter mosaic of acoustic intensity shown with stationing and channel boundaries

Figure 99. Backscatter mosaic of acoustic intensity shown channel stationing and channel boundaries

Figure 100. Backscatter mosaic of acoustic intensity shown with stationing and channel boundaries

Figure 101. Backscatter mosaic of acoustic intensity shown with stationing and channel boundaries

Figure 102. Backscatter mosaic of acoustic intensity shown with stationing and channel boundaries

A significant submerged object was found and imaged during the survey of the Inner Harbor and CAD Cell. This linear feature is found at station 217+00, just north of the CAD Cell and runs East/West beginning just inside the western channel shoulder (Figure 103 and Figure 104). A small section can be seen inside the boundary of the boundary of the channel template (yellow dashed line). The total length is unknown as the feature extends outside the collected data. Based on historical data, it is likely that this feature is associated with the City of West Haven combined sewer outfall (CSO). Any bottom disturbance or anchor placement near this feature should avoid working near it without a new survey at that time to re-confirm its location at that time.

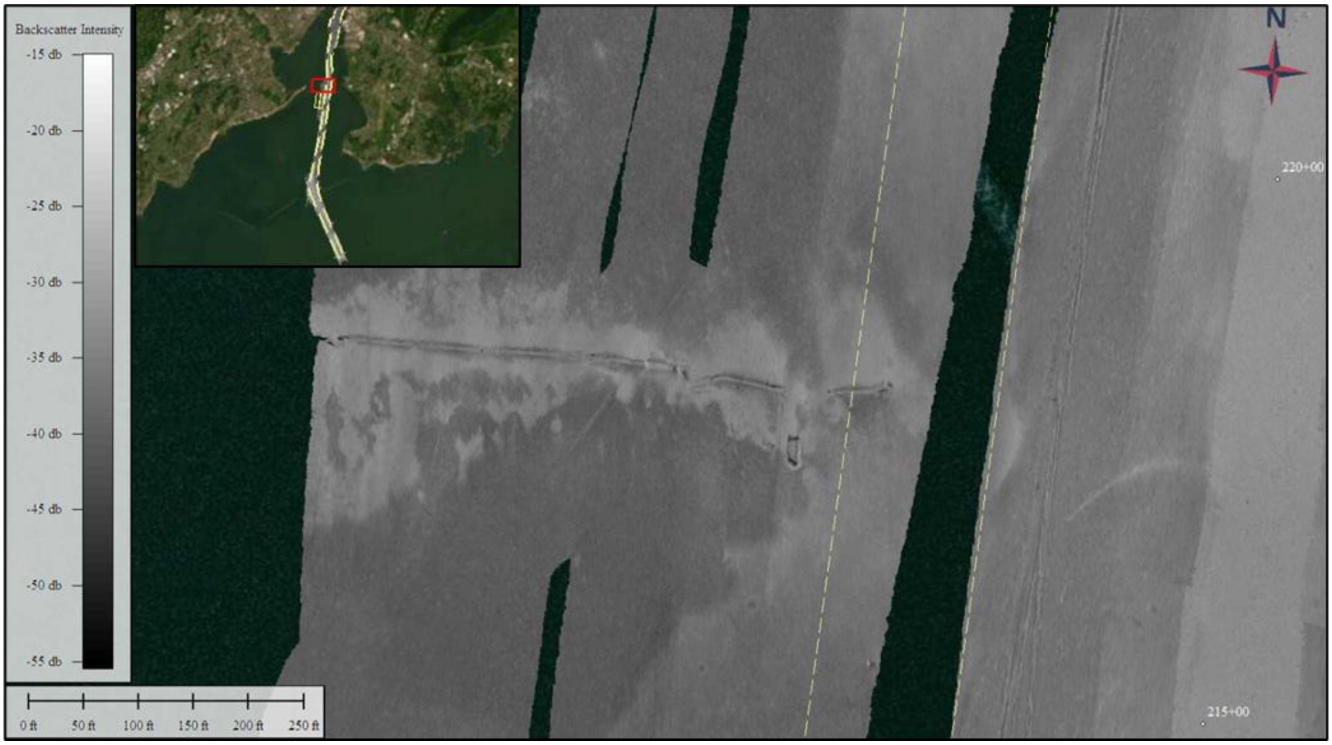

Figure 103. Acoustic Backscatter showing the submerged City of West Haven CSO at station 217+00

S. T. HUDSON ENGINEERS, INC.
PROFESSIONAL ENGINEERS & CONSULTANTS

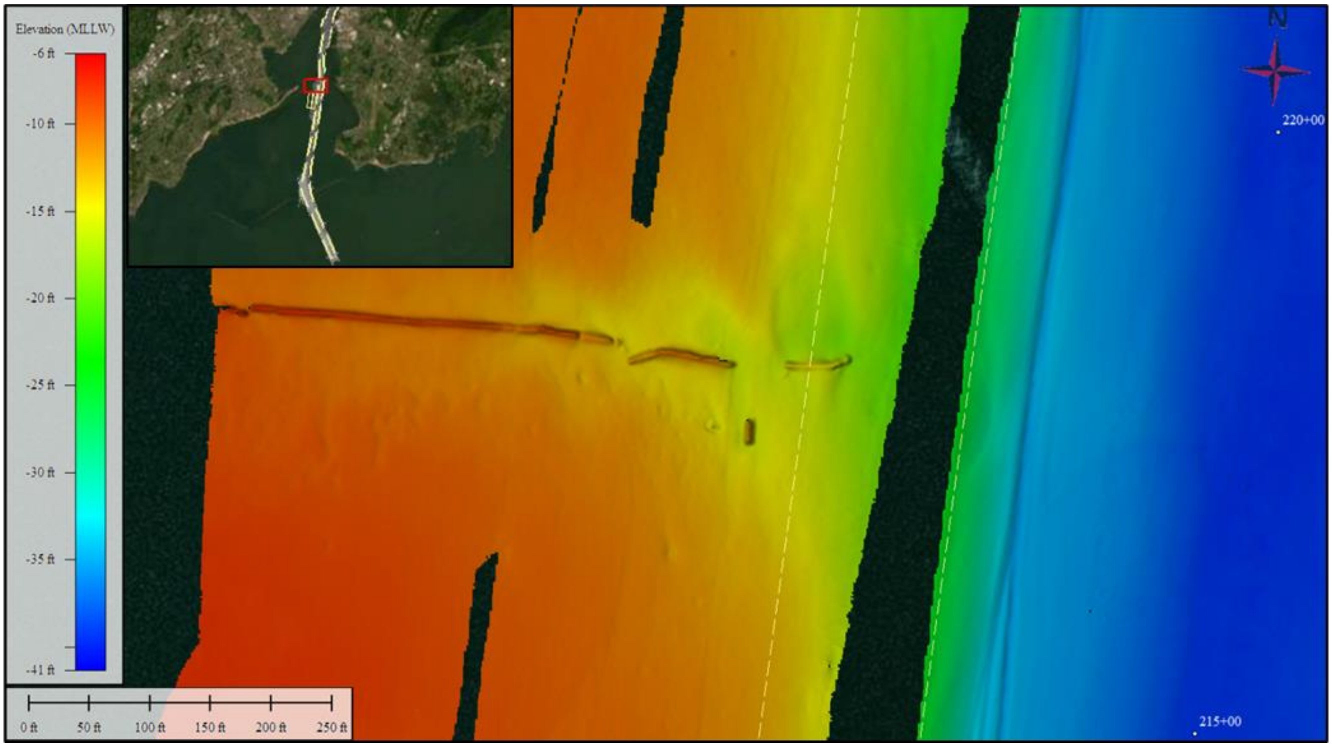

Figure 104. Multibeam Bathymetry collected by GBA in April 2024 showing the submerged City of West Haven CSO.

6.3.4.2 Subsurface Results

Combined geologic and geophysical results of the Inner Harbor show only moderate variations in subsurface material within the dredging template. The Organic Sediment (OS) unit is the most relevant sediment unit, and it is found beginning at the seabed (Figure 105). This layer is underlain by Marine Sands (MS) which periodically is found within the dredge template. Between stations 301+50 and 308+00 there is a significant surficial outcropping of the MS layer in the deeper parts of the channel where no surface OS layer is present. No rock is expected within the template between stations 115+00 and 325+00.

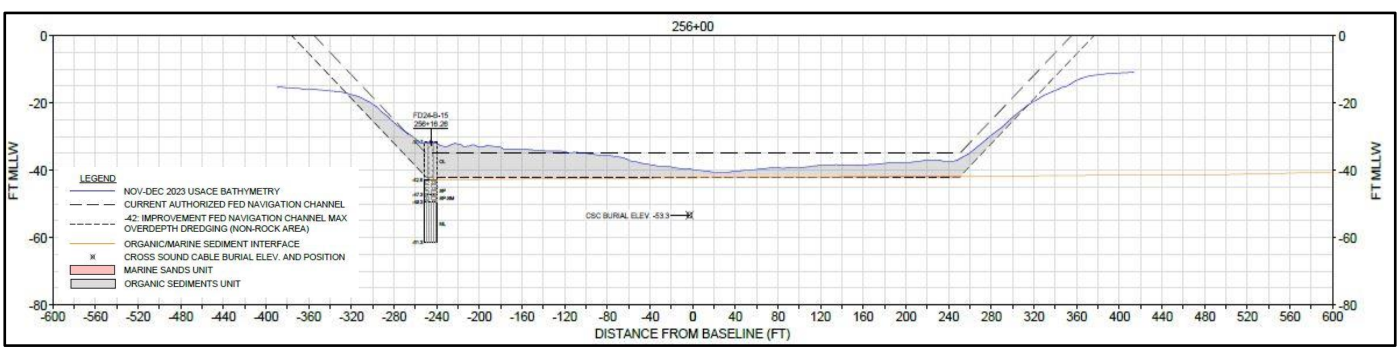

Figure 105. Example Profile at station 256+00 showing the typical setting of the Inner Harbor. Organic Sediment (OS) is shown in gray and the interface between OS and MS shown in Yellow.

Borings FD24-B-05 through FD24-B-20 were collected throughout the Inner Harbor. Boring FD24-B-17 is shown below as an example (Figure 106). The borings consistently show that the most relevant layers for dredging consideration are Organic Sediment (OS) immediately underlain by a unit of Marine Sands (MS). Glacio-marine Silt is encountered in some borings but at depths beyond consideration for the dredging template (>60 ft MLLW). A gravel deposit was found within FD24-B-08 between approximately -39.2 and -41.2 ft MLLW. Small, episodic gravel deposits may be encountered throughout the Inner Harbor within the MS unit. The range of sizes of these deposits are not known but based on sampling they are not expected to be common within the dredge template nor be of any significant volume.

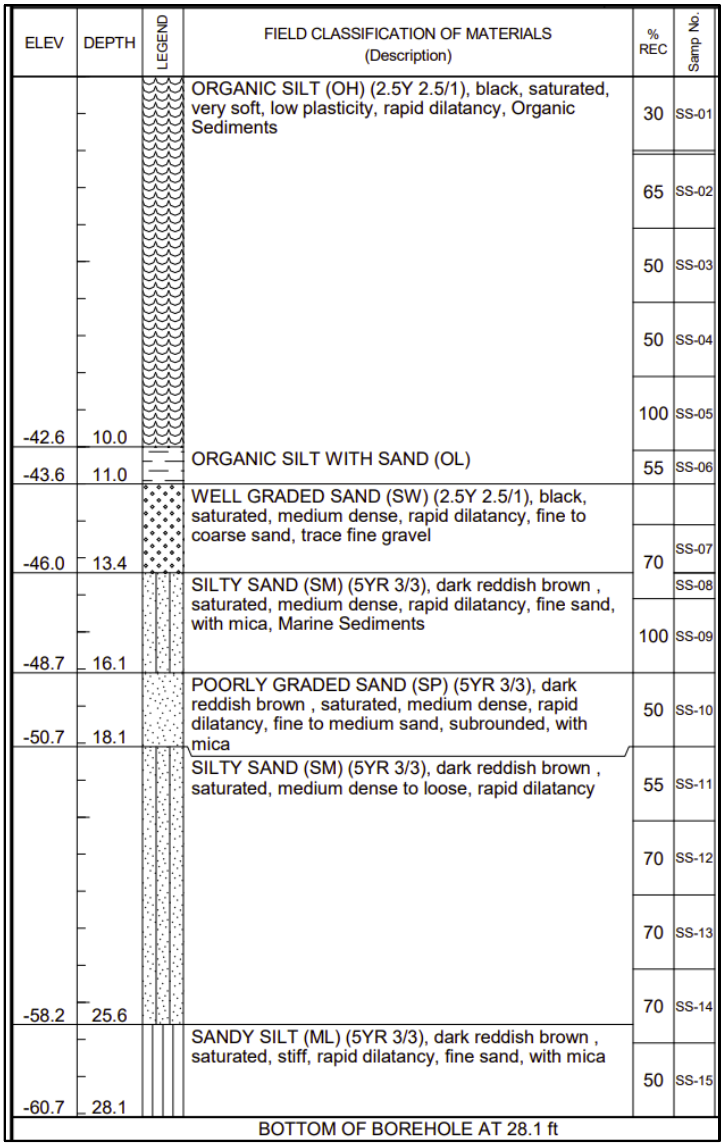

Figure 106. Boring FD24-B-17 Geologic Classifications to 60.7ft MLLW showing Organic Sediment (OS) to-43.6ft followed by Marine Sands (MS) to -58.2ft MLLW and Glacio-marine Silt (GM) from there to the bottom of the Borehole.

Seismic reflection data in the Inner Harbor shows a near homogenous shallow subsurface. Reflection data is strongly suggestive of gaseous sediment masking the imaging of any interfaces below the first sediment unit. Sporadically, reflection data can resolve the bedrock in the Inner Harbor well below the gaseous layer (Figure 107). The bedrock is found greater than -150 ft MLLW in these intermittent windows apart from the vicinity of station 202+00 where the bedrock rises to about -62 ft MLLW.

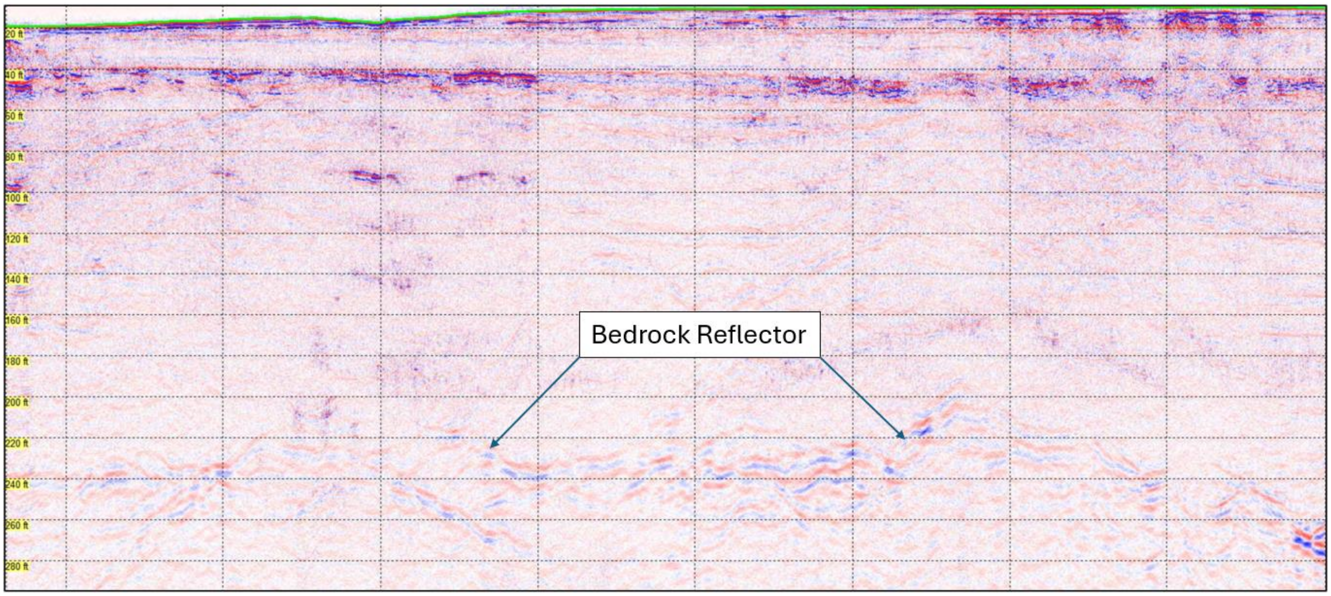

Figure 107. Seismic profile taken near station 200+00. Bedrock is seen at approximately -220ft MLLW.

The interface between Organic Sediment and Marine Sands does not appear as a reliable, consistent seismic horizon in the data collected throughout the Inner Harbor. Seismic reflections rely on differences in acoustic impedance to provide robust and repeatable reflectors. It is likely the case that there is simply not enough of a difference between the acoustic impedance of the Organic Sediment and Marine Sands in this area. Additionally, the presence of shallow gas throughout the Inner Harbor reduces the overall effectiveness of seismic imaging (Figure 108).

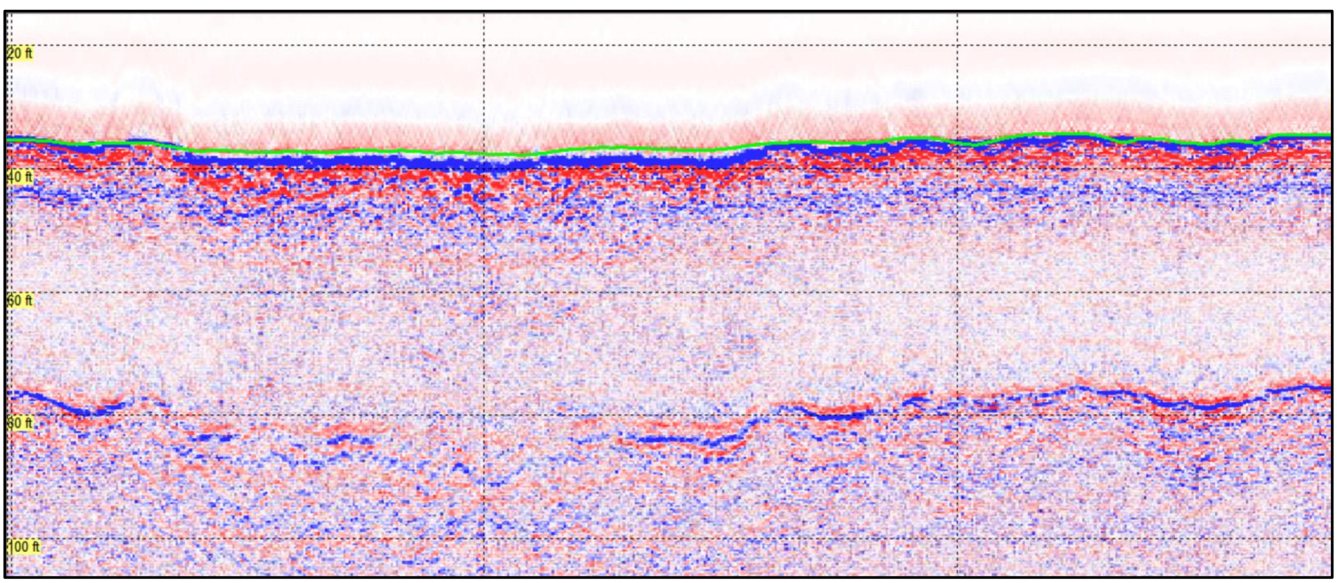

Figure 108. Seismic profile taken near station 270+00 showing an acoustically transparent shallow subsurface. No meaningful reflectors are seen in the data.

The modeled surface for the interface between the Organic Sediment and Marine Sand in the Inner Harbor was created using the geotechnical borings alone. Interpolations between borings are performed to assist in visualizing this interface throughout the Inner Harbor.

Seismic refraction data was collected along all stations within the Inner Harbor. Refraction data collected in this area did not detect any meaningful seismic velocity changes within the upper 50 ft of sediment below the seabed with one notable exception near station 200+00. Since the saturated, organic sediment and unconsolidated marine sands dominate the upper 50 ft, the P-wave velocity is nominally the same as the water column above it. In these areas, because no contrast was imaged, no profiles are provided.

Along refraction track 3001A between stations 197+00 and 207+00 there is a notable velocity anomaly that coincides positionally with the bedrock imaged in the seismic reflection profiles (Figure 109 and Figure 110). Based on the maximum velocities encountered at this station (~10,500 ft/sec) this rock is notably different than the bedrock encountered seaward of 110+00. The velocities are slower at this anomaly across from the CAD cell, but still well above the minimums to suggest solid, competent bedrock.

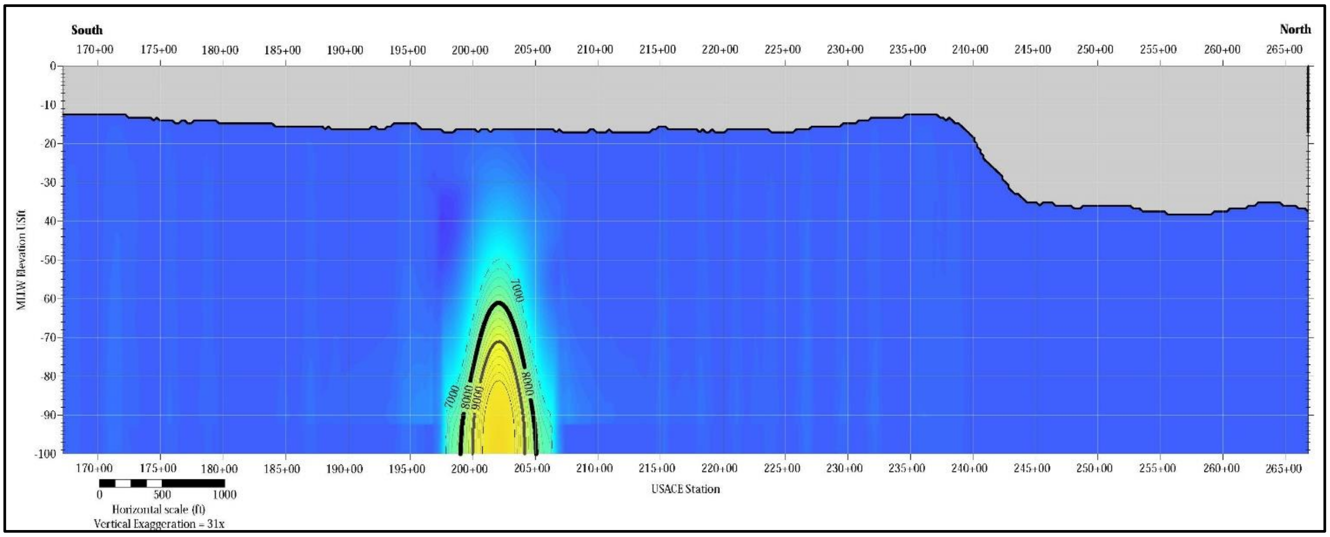

Figure 109. Modeled P-wave velocity profile depicting the anomaly between station 197+00 and 207+00

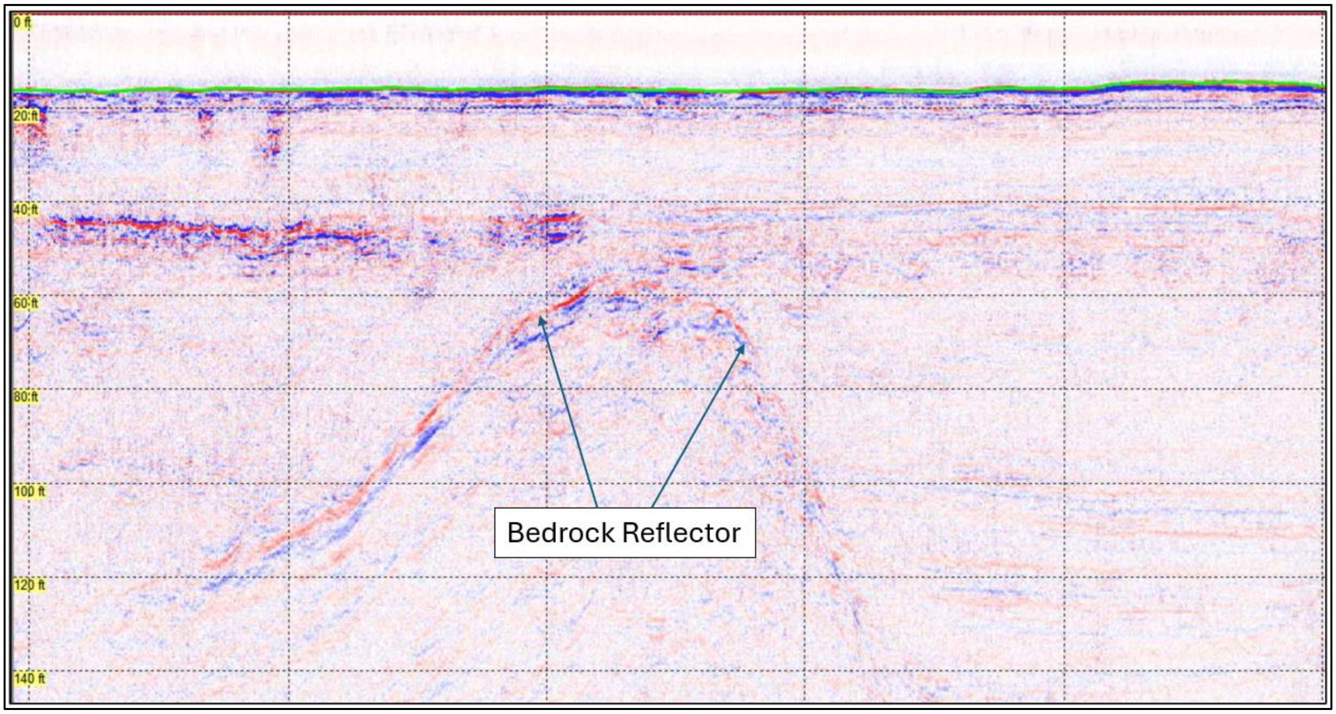

Figure 110. 2D reflection profile depicting the bedrock anomaly rising to about -62ft MLLW

Originally, a rock core was planned to sample the velocity anomaly across from the CAD cell. The boring was terminated at -60 ft MLLW with no rock encountered at that depth. This boring is recorded as FD24-B-10. The rock body is reasonably assumed to be outside consideration for this dredging task. However, should any further deepening or expansion be undertaken beyond the -40 ft authorized depth and planned 4 ft of additional Over Dredge Depth in areas of rock (-44ft MLLW total), it is recommended that a sampling campaign be undertaken to physically locate the top of this rock body.

Due to the distance between successfully sampled bedrock and this anomaly, similar petrology should not be assumed. Based on the surrounding, known bedrock this anomaly may be Arkose, Diabase (Dolerite), or Granite Schist. P-wave velocities suggest that, of the three, Arkose is most likely.

In the accompanying CAD cross sections this anomaly can be seen in sheets S-126 through S-128 in Appendix D.

7 Rock Dredging Opinions

The scope of work called for recommendations regarding the means and methods of removal of the rock. This section provides rock dredging insights and dredging engineering opinions associated with rock removal methods and the field data collected and analyzed during this investigation. It is expected that pre-treatment will be performed on the bedrock, and then a mechanical dredge will excavate the rock and place it into hopper barges for transport and disposal. Pre-treatment methods, described below, will be necessary to break up and create rock pieces of a size that is not too cumbersome for a mechanical dredge to efficiently excavate.

Historical data provided from previous site investigations was reviewed, compared, and discussed below. This report and the associated data will help inform the future design to be performed by the New England District (NAE). The actual means and methods used by the dredging industry may vary and will depend on the final design and the preferences of the successful bidder. Historically, rock dredging means and methods performed by the US dredging industry have varied and will be discussed below.

7.1 TOR Source Data

The TOR X, Y, Z source data provided to NAE was derived from seismic reflection data, seismic refraction data, and 9 rock core borings collected between May and August 2024. The TOR data included data points for all bedrock identified throughout the project area. Please note there were some areas where overlying fine grained organic material and gas prevented a clear definition of TOR when using seismic reflection. The NAE designers and others may use the TOR source data points to create interpretative Triangular Irregular Network (TIN) surfaces in various manners. This report provides an example plan view that presents one interpretive TOR TIN surface, which is discussed below.

7.1.1 Rock Characteristics

As described in Sections 6.2.1.5 and 6.3.2, the rock to be dredged was high strength granite, with high UCS values and higher RQD data. Weathered rock overlying the competent bedrock was not identified in the rock cores.

7.1.2 Rock Footprint Analysis

The example TOR TIN surface described above provides one estimate of the rock footprint (above -44 MLLW) and is displayed in Figure 111 and Figure 112.

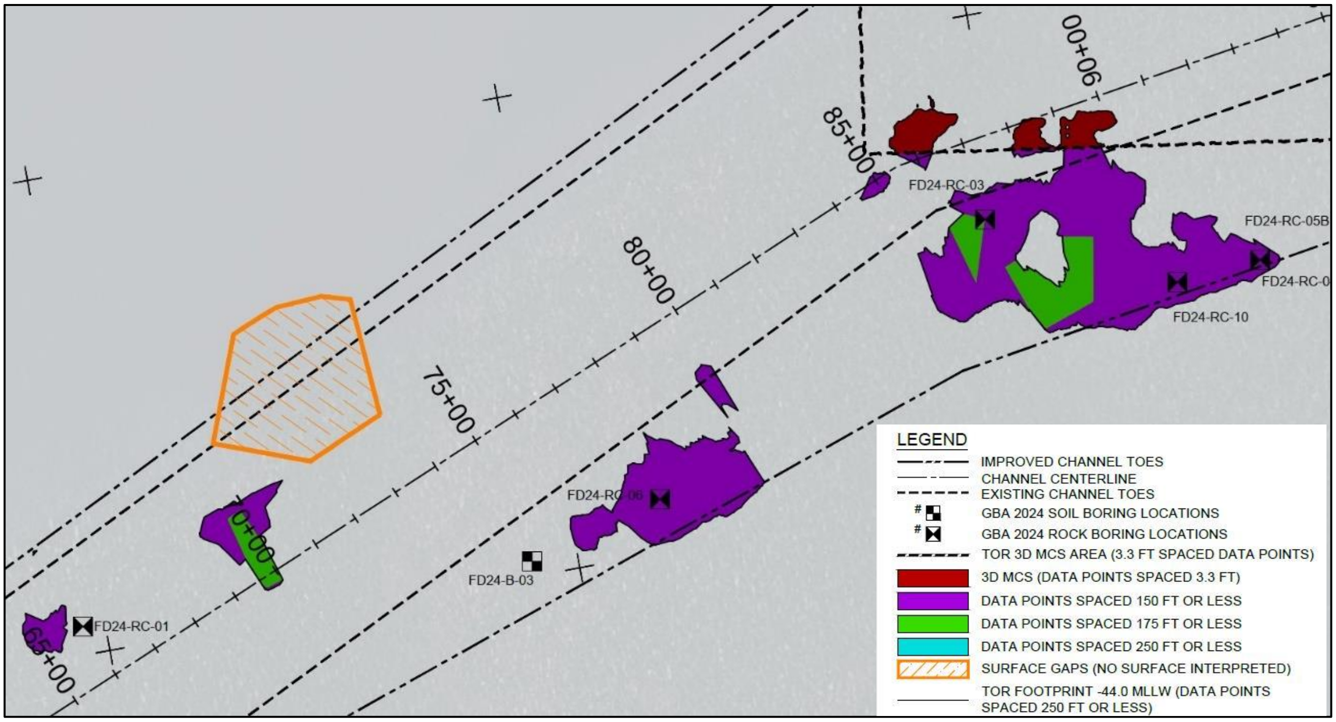

Figure 111. Plan View of TOR footprint within widener area, Stations 65+00 to 90+00

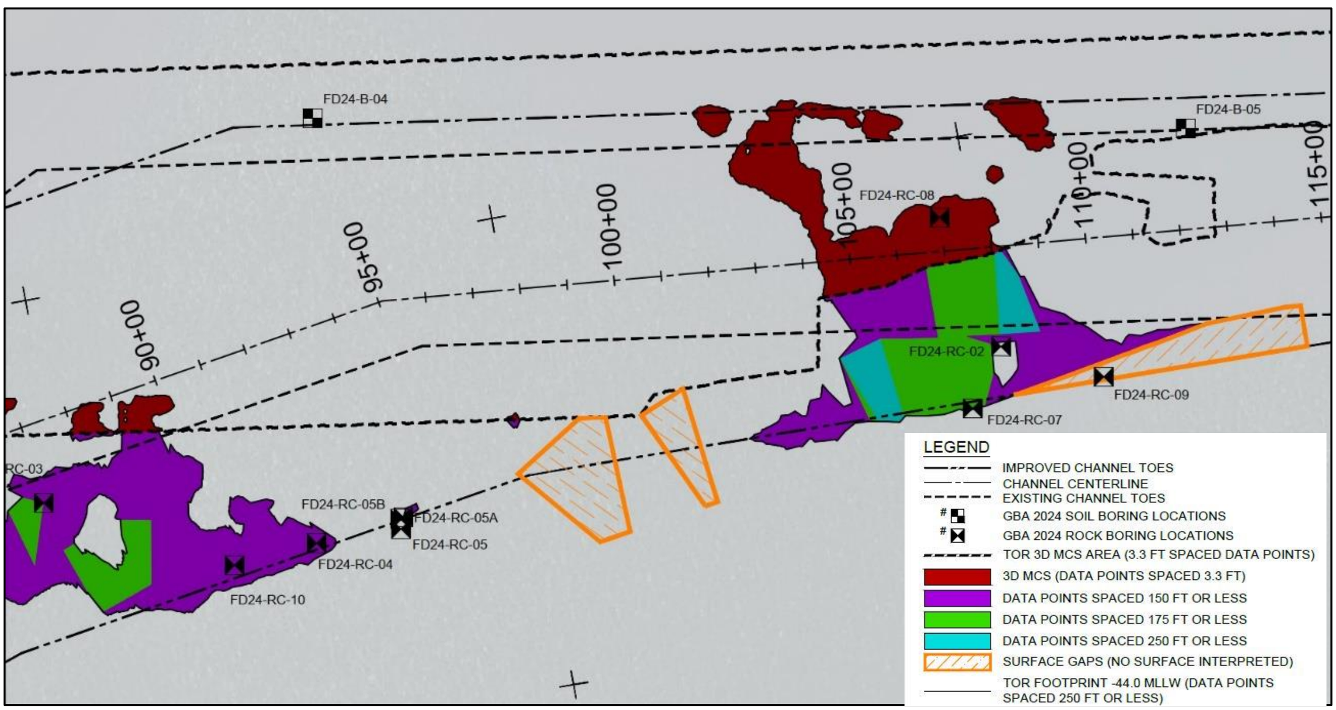

Figure 112. Plan View of TOR footprint within widener area, Stations 90+00 to 115+00

The two figures above are presented with legends, notes, and additional details in Appendix D. The survey vessel track lines where seismic data was collected are also displayed in Appendix D.

The red/brown rock footprint is where 3D Multi Channel seismic data was collected with a source data spacing of about 3.3 ft. The 3D data was collected from stations 95+00 to 115+00, generally on the western half of the improved channel (see dashed line polygon). This data was the most plentiful and reliable seismic data from the investigation. Because of budget constraints, 3D data collection did not occur throughout the entire project area. The purple, green, and blue rock footprint data was not as dense, with source data spacing less than 150 ft, 175 ft, and 250 ft, respectively. Therefore, the example rock footprint displayed for these three areas is, to some degree, less confident than the red/brown 3D seismic area. The surface gaps shown in orange hatch had source data spacing greater than 250 ft and were not included in the example rock footprint due to the large distance between data points.

Of particular interest was the orange hatch area from station 108+50 to 115+00 along the eastern channel toe line. Because of limited seismic source data and the fact that rock core RC-09 showed no rock near the dredging template, this area was not included in the example rock footprint. However, the seismic data (track line R4006 and S4006) just west of this area showed rock in the dredging template. Therefore, the rock footprint design should consider some rock in this orange hatch area.

The geometry of the rock footprint was very irregular in some areas, and there were scattered “islands of rock” in other areas. These geometries will influence the pre-treatment (drilling and blasting) production rate, which is discussed below.

7.2 TOR Cross Sections

Cross sections have been developed throughout the project area. The cross sections are presented in Appendix D with the data from this investigation and other historical data sets, legends, notes, and other detailed information. The TOR cross section data is the focus of this section.

The TOR example TIN surface, described in section 7.1 above and presented in the cross sections, was created by the 9 rock cores and the seismic data; it correlates very well with most of the historical data provided by NAE and Cross Sound Cable, LLC. The historical data sets were utilized to assist with confirmation of the TOR surface; however, they were not integrated into the model used to generate the surface. Figure 113 and Figure 114 are good examples of repeatability between the rock data sets. The seismic data had very good repeatability with rock data sets provided by others at this cross section and throughout most of the rock footprint.

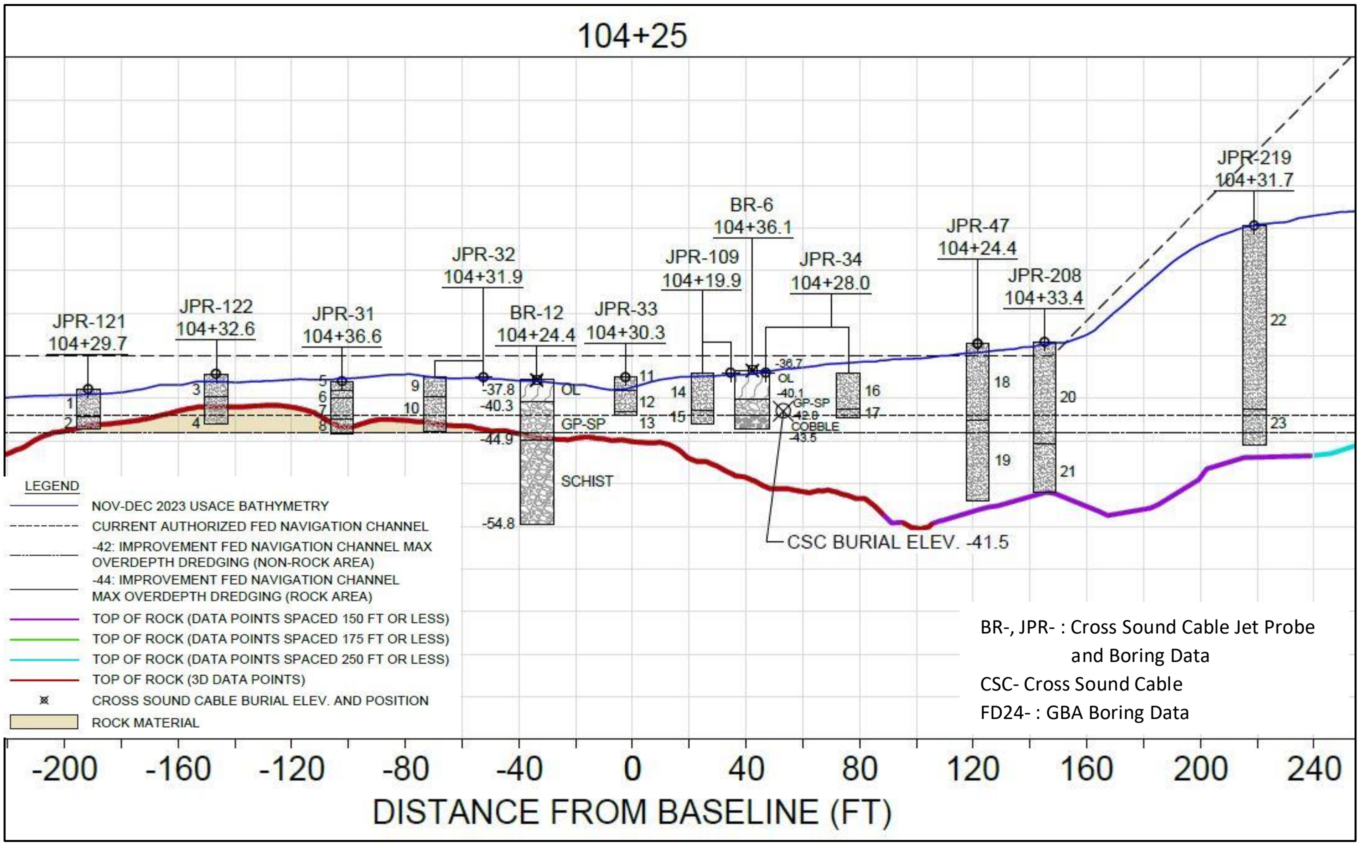

Figure 113. Cross Section at Station 104+25

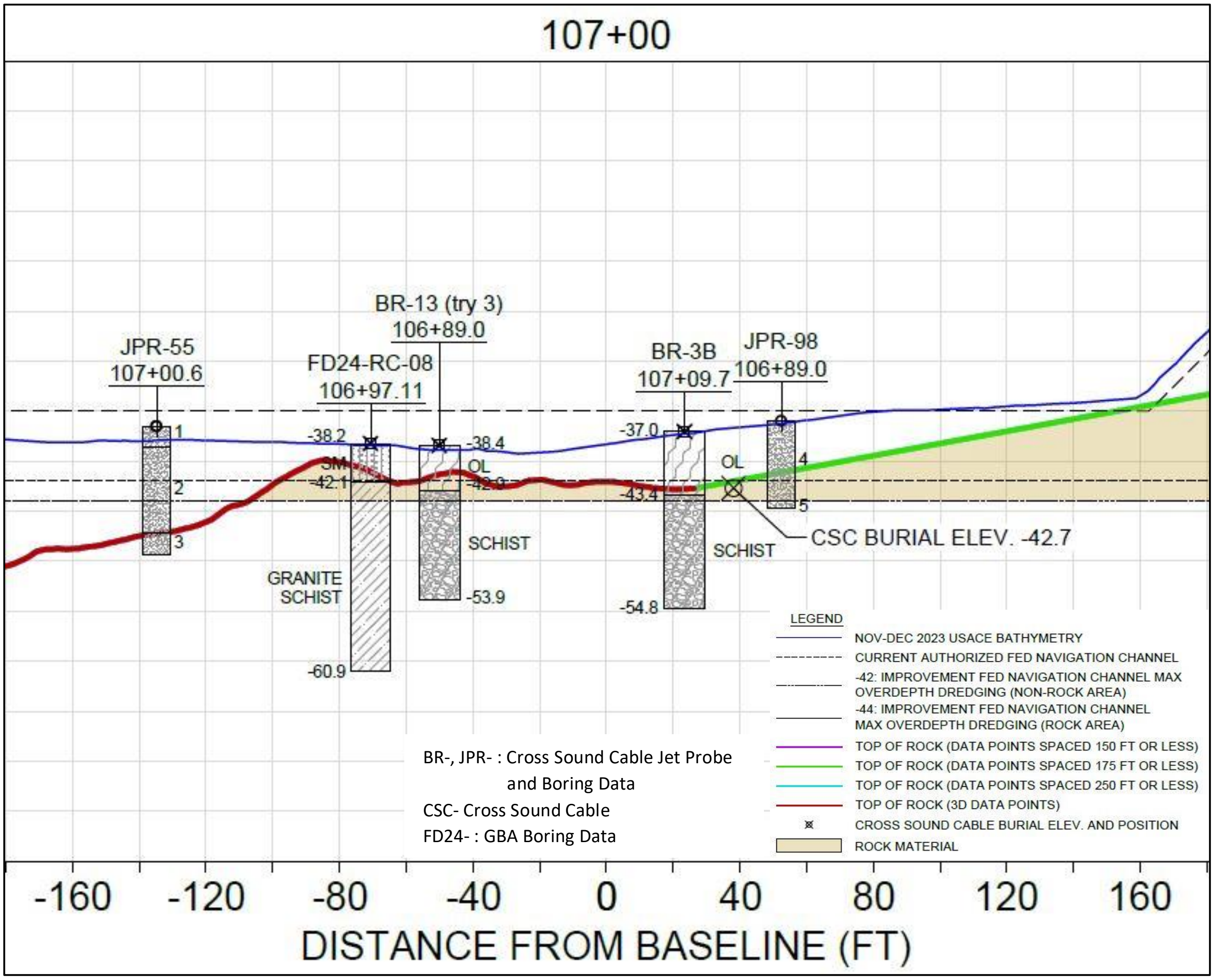

Figure 114. Cross Section at Station 107+00

There were several observations that may influence how well the various rock data sets compare to each other. These observations should be considered when comparing rock data sets:

1. The TOR surface undulated significantly with pinnacle slopes that were steeper than 1v on 1h in some areas. Data sets that were just a few feet horizontally apart from each other also had elevation differences that were a few feet. Therefore, when the historic data sets are compared to the seismic data, this should be considered along with distances between source seismic data points.
2. The seismic data vessel track lines, outside of the 3D data area, were at times up to and greater than 200 feet apart. Therefore, some of the undulating rock surfaces and steep sloped pinnacles were very challenging to document.
3. In some areas, gas pockets in the fine-grained organic material hindered the collection of plentiful seismic reflection survey data, especially on the east side of the improved channel between stations 100+00 to 115+00.
4. When comparing seismic data to the Jet Probes (JPR), it is possible that JPR refusal on dense sand, gravel or other hard materials may be mis-labeled as top of bedrock.

In some cases, there were inconsistencies between data sets which should be closely reviewed and studied by the rock design team and bidders. For example, a review of the cross sections between stations 105+00 and 110+00 showed some inconsistencies between TOR data sets. It is important to review the TOR surface presented in this area compared to the historical data sets, especially the jet probes. One data set compared to the other data set may either overstate or understate the footprint and volume of rock to be dredged.

The Jet Probes were provided by the Cross Sound Cable, LLC The accuracy of these jet probe surveys can vary depending on several factors including the type of probe used, the sediment conditions being investigated, the survey design, and the operator's skill. Generally, jet probes are moderately accurate for identifying sediment layer types and thicknesses, with potential limitations in precise depth measurements particularly in complex or highly variable sediment environments. Jet probes are more effective in soft, unconsolidated sediments and may struggle to accurately penetrate dense or hard layers like rocks, gravel, cobbles, or dense sand.

The project designer and contract bidders are advised to take the above into consideration when comparing various rock data sets.

7.3 Rock Pre-Treatment Means and Methods

The US Dredging Industry has employed several methods of rock pre-treatment on deepening and widening projects in the New England District and other ports along the East Coast. The following sections present descriptions of pre-treatment means and methods employed.

7.3.1 Ripper Attachment on Backhoe Dredge

Similar to a bulldozer ripper attachment, the ripper is attached to the lower stick of a hydraulic backhoe dredge (Figure 115).

Figure 115. Backhoe with Ripper on Land

The pre-treatment method is productive and economic in weathered rock, which was minimal to non-existent for this project. The ripper method may be feasible to pre-treat rock above overdepth in some isolated areas, thus eliminating the need for a drill barge to perform very unproductive work. However, in areas where rippable rock overlies non-rippable high strength rock within the dredging template, pre-treatment with a ripper is not feasible. In most of the rock footprint, there is high strength, minimally weathered rock which would be challenging for this method.

7.3.2 Milling Cutter

The Milling Cutter technique involves a specially designed cutter head weighing over 25 tons configured with 8 to 9 cutter arms and over 100 pick point teeth (note a standard cutter head utilizes 5 or 6 cutter arms). The milling cutter employs closely spaced rock pick point cutter teeth (Figure 116).

This technique is employed in areas of low face, hard rock. The cutter swings slowly over the rock pinnacle with the head turning at high RPMs, essentially milling down the very hard rock. Multiple passes are required to lower the rock elevation to below grade level.

Figure 116. Milling Cutter Head

7.3.3 Hydro Hammer

A Hydro Hammer is a percussion tool used with a backhoe dredge or on a drill frame to fracture very hard rock (Figure 117 through Figure 120). A typical pattern involves hammering 5-inch holes on a 5ft-by-5ft diamond pattern. Penetration depth is approximately 4 ft.

This method is effective in hard rock but limited by the number of faces that can be broken. In higher face, multiple passes of fracturing and dredging are necessary which increases cost. This method is most suitable in low face (vertical thickness) rock areas.

Figure 117. Hydro Hammer

Figure 118. Great Lakes Dredge and Dock (GLDD) Backhoe Dredge employing Hydro Hammer

Figure 119. Cashman Backhoe employing Hydro Hammer

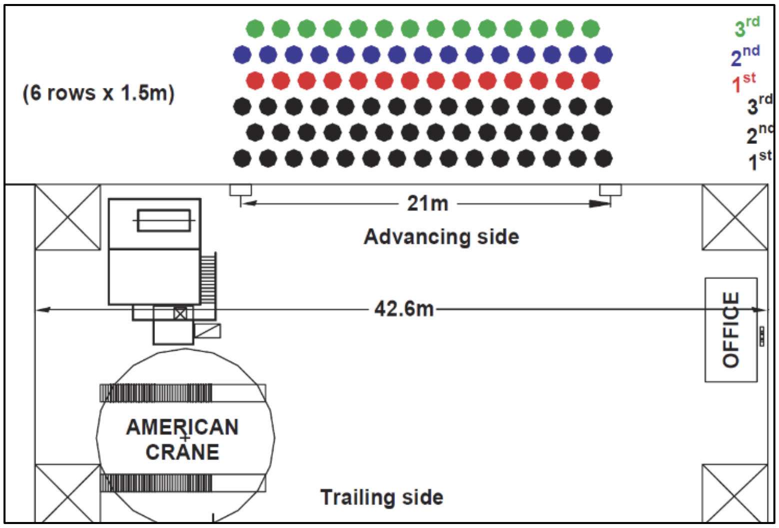

Figure 120. Typical Hydro Hammer Fracture Pattern

7.3.4 Drilling and Blasting

Cashman, Dutra, Great Lakes, and Weeks Marine have employed special built drilling and blasting barges for deepening projects in Boston, New York, Philadelphia, and Wilmington NC (Figure 121 and Figure 122). A typical drill and blast barge employs three drill frames and is configured for high production blasting covering large areas. This tool is cost effective in large, high face, hard rock areas. Layers of soft overburden can be penetrated by the drill frame.

The New Haven irregular rock footprint areas and “rock island” areas will influence pre-treatment production. When drill barges are employed over smaller, isolated rock outcrops, drill production efficiency drops. At times, one or two drill frames are utilized, lowering production area coverage and increasing costs.

Figure 121. Bean/Cashman Drill Barge 301

Figure 122. GLDD Drill Barge Apache

7.4 Recommendations for Rock Removal

7.4.1 Pre-Treatment Method

Rock engineering properties, example rock footprint areas, and cross sections with 2024 rock data overlaid on previous rock data sets by others helped identify the most probable pre-treatment method. This data indicated the rock was high strength, minimally weathered, with higher RQD's and SCR's, and predominantly larger area TOR footprints with some smaller "rock islands".

The four pre-treatment methods considered and discussed above include ripper, milling cutter dredge, hydro hammer, and conventional drilling & blasting barge.

The ripper method was not considered viable because of the high strength, minimally weathered rock, which would be challenging and likely unsuccessful.

The milling cutter dredge is a feasible method to pre-treat the high strength, low face rock. However, the high overall cost of employing this method is likely not cost effective. There are some isolated "rock islands" where this method may be effective; however, the mobilization and operation of a large cutter dredge would yield a high unit cost compared to a conventional drill barge and bucket dredge.

The hydro hammer method is feasible for fracturing high strength, low face rock outcrops (rock islands) but not to complete the larger rock footprint areas. Also, there is significant cost outfitting the backhoe dredge and time required to convert from chiseling to dredging. A conventional drill barge will likely be the most cost-effective pre-treatment method for the New Haven project.

Therefore, the dredging engineering opinion of the probable pre-treatment rock removal method is to utilize a conventional drilling and blasting barge.

8 Works Cited

Bennett, M. M., & Glasser, N. F. (Eds.). (2011). Glacial geology: ice sheets and landforms. John Wiley & Sons.

Bird, D. E., Hall, S. A., Burke, K., Casey, J. F., & Sawyer, D. S. (2007). Early central Atlantic Ocean seafloor spreading history. Geosphere, 3(5), 282-298.

Bjerklie, D. M., Mullaney, J. R., Stone, J. R., Skinner, B. J., & Ramlow, M. A. (2012). Preliminary investigation of the effects of sea-level rise on groundwater levels in New Haven, Connecticut.

Boose, E. R., Chamberlin, K. E., & Foster, D. R. (2001). Landscape and regional impacts of hurricanes in New England. Ecological Monographs, 71(1), 27-48.

Clark, P. U., & Mix, A. C. (2002). Ice sheets and sea level of the Last Glacial Maximum. Quaternary Science Reviews, 21(1-3), 1-7.

Clark, P. U., Dyke, A. S., Shakun, J. D., Carlson, A. E., Clark, J., Wohlfarth, B. & McCabe, A. M. (2009). The last glacial maximum. science, 325(5941), 710-714.

Cornet, B., & Traverse, A. (1975). Palynological contributions to the chronology and stratigraphy of the Hartford Basin in Connecticut and Massachusetts. Geoscience and man, 11(1), 1-33.

Deasy, R. T., Wathen, B., & Wintsch, R. P. (2017). Bedrock geology of the Paleozoic rocks of western New Haven quadrangle, Connecticut. Journal of Maps, 13(2), 632-643.

Favre, P., & Stampfli, G. M. (1992). From rifting to passive margin: the examples of the Red Sea, Central Atlantic and Alpine Tethys. Tectonophysics, 215(1-2), 69-97.

Golonka, J. (2002) Plate-Tectonic Maps of the Phanerozoic. Institute of Geological Sciences, Jagiellonian University, Krakow, Poland.

Heani F.P. and Sanders J.E. (1974) Field Studies Map MF-557A.

Lewis, R. S., & DiGiacomo-Cohen, M. (2000). A review of the geologic framework of the Long Island Sound basin, with some observations relating to postglacial sedimentation. SJournal of Coastal Research, 522-532.

Lewis, R. S., & Stone, J. R. (1991). Late Quaternary stratigraphy and depositional history of the Long Island Sound basin: Connecticut and New York. Journal of Coastal Research, 1-23.

Mattei, J. H., Botton, M. L., Beekey, M. A., & Colón, C. P. (2015). Horseshoe crab research in urban estuaries: challenges and opportunities. Changing global perspectives on horseshoe crab biology, conservation and management, 537-555.

McHugh, C. M., & Olson, H. C. (2002). Pleistocene chronology of continental margin sedimentation: New insights into traditional models, New Jersey. Marine Geology, 186(3-4), 389-411.

McHugh, C. M., Hartin, C. A., Mountain, G. S., & Gould, H. M. (2010). The role of glacio-eustasy in sequence formation: Mid-Atlantic Continental Margin, USA. Marine Geology, 277(1-4), 31-47.

Miall, A. D., Balkwill, H. R., & McCracken, J. (2008). The Atlantic Margin Basins of North America. Sedimentary Basins of the World, 5, 473-504.

Mickelson, D. M., & Colgan, P. M. (2003). The southern Laurentide ice sheet. Developments in Quaternary Sciences, 1, 1-16.

Parker, C. A., & O'Reilly, J. E. (1991). Oxygen depletion in Long Island Sound: A historical perspective. Estuaries, 14, 248-264.

Pillans, B., Chappell, J., & Naish, T. R. (1998). A review of the Milankovitch climatic beat: template for Plio–Pleistocene sea-level changes and sequence stratigraphy. Sedimentary geology, 122(1-4), 5-21.

Pisias, N. G., & Moore Jr, T. C. (1981). The evolution of Pleistocene climate: a time series approach. Earth and Planetary Science Letters, 52(2), 450-458.

Poppe, L. J., Robinson, A. C., Blackwood, D., Lewis, R. S., & DiGiacomo-Cohen, M. L. (1998). The distribution of surficial sediments in New Haven Harbor, Connecticut, and the New Haven Dumping Grounds, north-central Long Island Sound. US. Geological Survey Open-File Rep, 98-217.

Poppe, L. J. and US Geological Survey (2001). Sidescan sonar images, surficial geologic interpretations, and bathymetry of the Long Island Sound sea floor in New Haven Harbor and New Haven dumping ground, Connecticut. The Survey.

Poulos, H. M. (2010). Spatially explicit mapping of hurricane risk in New England, USA using ArcGIS. Natural hazards, 54, 1015-1023.

Rodgers, J. (1985) Bedrock Geological Map of Connecticut, Sheet 1 and 2. Connecticut Geological and Natural History Survey.

Rozan, T. F., & Benoit, G. (2001). Mass balance of heavy metals in New Haven Harbor, Connecticut: Predominance of nonpoint sources. Limnology and Oceanography, 46(8), 2032-2049.

Sanders, J. E. (2010). Buried, Anomalously Deep V-Shaped Valley in Bedrock Surface, New Haven Harbor, Connecticut.

Stone, J. R., Schafer, J. P., London, E. H., & Thompson, W. B. (1992). Surficial materials map of Connecticut. US Geological Survey.

Uchupi, E., Driscoll, N., Ballard, R. D., & Bolmer, S. T. (2001). Drainage of late Wisconsin glacial lakes and the morphology and late quaternary stratigraphy of the New Jersey–southern New England continental shelf and slope. Marine Geology, 172(1-2), 117-145.

Ullman, D. S., Ginis, I., Huang, W., Nowakowski, C., Chen, X., & Stempel, P. (2019). Assessing the multiple impacts of extreme hurricanes in southern New England, USA. Geosciences, 9(6), 265.

Upson, J. E., & Spencer, C. W. (1964). Bedrock valleys of the New England coast as related to fluctuations of sea level. Washington, DC: US Government Printing Office.

www.usgs.gov

www.noaa.gov

Wu, T., & Barrett, J. (2022). Coastal land use management methodologies under pressure from climate change and population growth. Environmental Management, 70(5), 827-839.

Williams, S. J. (1976). Geomorphology, shallow subbottom structure and sediments of the Atlantic inner continental shelf off Long Island, New York. US Army Coastal Engineering Research Center.

Zecchin, M., Catuneanu, O., & Rebesco, M. (2015). High-resolution sequence stratigraphy of clastic shelves IV: high-latitude settings. Marine and Petroleum Geology, 68, 427-437.

9 APPENDICES

Appendix	Title
A	Daily Progress Reports
B	Geotechnical Boring Logs
C	Laboratory Results
D	Plan View Drawings and Geologic Cross Sections
E	Refraction Velocity Profiles
F	SPT Overburden and Rock Core Photo Logs
G	NGS OPUS Shared Solutions Control Sheets
H	On-site SPT Drill Rig Auto Hammer Calibrations
I	Cross Sound Cable Jet Probe Investigation 2024
J	Historical Geotechnical Investigations
K	New Haven Harbor Improvement Performance Work Statement (PWS)
L	New Haven Harbor Improvement Workplan
M	New Haven Harbor Improvement Accident Prevention Plan (APP)